INFORMATION TO USERS

This manuscript has been reproduced from the microfilm master. UMI films the text directly from the original or copy submitted. Thus, some thesis and dissertation copies are in typewriter face, while others may be from any type of computer printer.

The quality of this reproduction is dependent upon the quality of the copy submitted. Broken or indistinct print, colored or poor quality illustrations and photographs, print bleedthrough, substandard margins, and improper alignment can adversely affect reproduction.

In the unlikely event that the author did not send UMI a complete manuscript and there are missing pages, these will be noted. Also, if unauthorized copyright material had to be removed, a note will indicate the deletion.

Oversize materials (e.g., maps, drawings, charts) are reproduced by sectioning the original, beginning at the upper left-hand corner and continuing from left to right in equal sections with small overlaps. Each original is also photographed in one exposure and is included in reduced form at the back of the book.

Photographs included in the original manuscript have been reproduced xerographically in this copy. Higher quality 6" x 9" black and white photographic prints are available for any photographs or illustrations appearing in this copy for an additional charge. Contact UMI directly to order.

UMI

A Bell & Howell Information Company
300 North Zeeb Road, Ann Arbor MI 48106-1346 USA
313/761-4700 800/521-0600

MOLECULAR ANALYSIS OF THE DOMAINS OF MYELIN BASIC PROTEIN INVOLVED IN MYELIN COMPACTION

by

David Rickman

A dissertation submitted to the Graduate Faculty in Biomedical Sciences in fulfillment of the requirements for the degree of Doctor of Philosophy, City University of New York

1997

This manuscript has been read and accepted for the Graduate Faculty in Biomedical Sciences in satisfaction of the dissertation requirement for the degree of Doctor of Philosophy.

September 23, 1997

Robert A. Lazzarini, Ph. D.
Chair of the Examination Committee

September 23, 1997

Terry A. Krulwich, Ph. D.
Executive Officer

David Colman, Ph. D.
Francesco Rameriz, Ph. D.
Mariann Blum, Ph. D.
Steve Pfeiffer, Ph. D.

Supervisory Committee

THE CITY UNIVERSITY OF NEW YORK

ABSTRACT

MOLECULAR ANALYSIS OF THE DOMAINS OF MYELIN BASIC PROTEIN INVOLVED IN MYELIN COMPACTION

by

David Rickman

Advisor: Professor Robert A. Lazzarini

The myelin basic proteins (MBP) constitute a family of proteins that is found in the compact myelin around axons in the central and peripheral nervous systems (CNS and PNS, respectively). These different proteins result from an alternatively spliced message from a single 32 kb gene, and in mice, have molecular weights ranging from 14 kDa to 21 kDa. They are essential for the formation of compact myelin which is derived from elaborated processes of oligodendroglial cells (CNS) and Schwann cells (PNS), and when absent, as in the naturally occurring null mutant, the shiverer mouse, CNS myelination is blocked. The effects of this mutation have been rescued by expressing, transgenically, either the whole *mbp* gene (21) or the smallest isoform (8). To determine the domains of MBP that are involved in the compaction of myelin, I have made two truncated, nonnatural MBP cDNAs to be expressed in shiverer mice using an expression vector that is specific oligodendrocytes (44). These cDNAs, one expressing two exons (D2), the other expressing four exons (D4) of *mbp* were expressed in wild type (wt) mice for initial characterization. A short eleven amino acid tag sequence was appended to the carboxy terminal of each of the proteins, providing an epitope distinguishing them from endogenous MBP. The transgenes were genetically crossed onto the shiverer background, the D4 mini-MBP was able to facilitate myelin compaction and to partially rescue the dysmyelinating phenotype. D2, on the other hand, was unable to facilitate compaction despite robust expression levels and appropriate localization to the sheaths surrounding the axons. A cDNA encoding the endogenous isoform used in the above rescue experiment (8) with the

appended tag sequence was employed as a control. Interestingly, one representative transgenic mouse line (on the wt background) for each cDNA developed a dysmyelinating pathology. This dissertation shows that a protein encoded by exons one, three, four and seven of *mbp* can facilitate the compaction of CNS myelin, while a protein encoded by a subset of these exons (exons one and seven of *mbp*) cannot. Therefore, the endogenous isoforms of MBP contain information that is not necessary in the compaction of CNS myelin, and thus may be important in other functions of MBP in the oligodendrocyte.

ACKNOWLEDGMENTS

I would first like to acknowledge the faculty and staff of the Brookdale Center for Molecular Biology at Mt. Sinai School of Medicine for their support and scientific insights which aided in my development as a student. I would especially like to thank the administrative staff for their patience and unlimited help while I passed through the different stages of my studentship. I would also like to thank the people in the laboratory of Dr. Robert A. Lazzarini, without their help my tenure as a student would have been much longer. I would especially thank Eugenia Basyuk for her constant patience, her sense of humor, and her fortitude while sharing an office with me.

I am indebted to Dr. Robert A. Lazzarini, my advisor, for his scientific guidance and opprotunity to work in his laboratory. He provided an excellent scientific environment and offered me a challenging, insightful project for my thesis. He was also very helpful, engaging and through his constant perseverance, taught me how to think more scientifically.

I would also like to thank Dr. Victor Friedrich for his countless nuggets of wisdom for which I will be forever grateful. He provided much support, both scientifically and emotionally. He was reassuring and invaluable throughout my entire studentship. I will always be indebted to him for the role he served in my growth as a student.

Lastly, but most importantly, I would like to thank my friends and especially my family. They will always hold a special place in my heart, for without them, none of this would have been possible. Most notably, my mother, Jane Sparks and my brother, Dr. Richard Rickman provided immeasurable emotional support, that I hope one day can be repaid.

TABLE OF CONTENTS

CHAPTER 1: *AN INTRODUCTION TO MYELIN*

A. General Morphology and Function of Myelin

There are two distinct regions of an adult brain often referred to as the gray and white matter, with the latter getting its distinctive color from a lipid rich material called myelin. First described by Virchow in 1854, myelin is specialized multilamellar sheathing that surrounds many axons and is an essential component of the nervous system. The rest of the neuron (i.e. the cell body and most of its dendrites) remains unensheathed in the gray matter region. Myelin comprises 50-60% of the total mass of white matter and is present throughout the nervous system. This accounts for 20-25% of the dry weight of an adult rat brain and 35% dry weight of a human brain which has a higher white matter to gray matter ratio.

Myelin functions as a protective cushion for the axon and as an insulator which increases the speed of signal propagation down its length. The myelin ensheathment is segmental (Fig. 1) and each unit, or internode, is separated from its neighbor by a very short unmyelinated space called the node of Ranvier, named after the 19th century scientist Louis-Antoine Ranvier. These nodes are highly specialized regions of the axon that are endowed with a high density of sodium channels and thus have the highest electrical activity along the axon (39).

Once a signal or action potential is generated in neurons, it propagates itself, via depolarizing and opening voltage-gated sodium (Na^+) channels located on the axon plasma membrane (axolemma), from the cell body progressively down the axon towards the synapse. When voltage-gated channels open, ions pass through the membrane of the axon along a concentration gradient. For Na^+, ions move from the outside (higher Na^+ concentration) to the inside of the axoplasm (lower Na^+). Voltage-gated chloride (Cl^-) channels also open allowing the Cl^- ions to move across the axolemma to the inside. The resulting current (movement of ions) changes the membrane potential or voltage which

depolarizes a proximal voltage-gated potassium (K) channel. K^+ ions cross in the reverse direction also along a gradient established by the high concentration of K^+ inside and low K^+ outside the axon. This results in a net accumulation of positive charges inside the axoplasm and negative charges outside (due to higher Na^+ influx vs. K^+ efflux). This change in membrane potential depolarizes the next proximal group of voltage-sensitive Na^+ channels and eventually propagates the signal along the axon.

Figure 1. Structural schematic of CNS myelin, shown in modified form. Oligodendrocyte and attached processes showing the multiple myelinated axons by this one cell soma with labeled regions characteristic of CNS myelin. Picture adapted from reference 28.

Since myelin has very low electrical conductivity and very high resistance, continuous conduction along the length of the internode is extremely difficult. However, due to the high density of Na channels at the nodes and the high resistance along the myelinated stretches, an action potential is generated of such magnitude that the next proximal node is excited. Therefore, at each node, the impulse is regenerated and sent down the axon, almost jumping from node to node in what is commonly referred to as saltatory conduction (from the Latin *saltare* , to leap, ref. 39). In the case of an unmyelinated axon, this process occurs along the entire length of the axon requiring a

greater energy expenditure. After the action potential peaks, the gated Na channels close followed by the closing of the K channels, resulting in the observed down slope of the action potential. The Na/K pump activated by ATP expenditure eventually restores the equilibrium of charge concentration, which regenerates the resting membrane potential for both ions (76). The regeneration of the membrane's resting and action potential create an energy debt that must be repaid.

Saltation of conduction is advantageous for several reasons. To begin with, this sort of conductivity is energy cost efficient. The energy needed to propagate and regenerate an action potential continuously down an unmyelinated fiber is less than if this process took place at regularly spaced intervals. Secondly, myelinated axons conduct a signal faster that unmyelinated axons. The time it takes for an action potential to "jump" from one node to the next, down the length of a myelinated nerve fiber, is approximately one tenth that necessary to conduct down an identical sized unmyelinated axon. Since speed of propagation is also proportional to cross sectional area, the axon would have to be ten times larger to achieve the same rate of transmission (76). Third, myelin assists in preserving signal coherence and eliminating "cross-talk" between nerve fibers (28). Therefore, myelin allows for saltatory conduction that transmits a nerve signal more rapidly and with greater coherence.

Myelin, therefore, is very abundant and necessary for efficient neural signalling, and any disruption of the myelin sheath leads to serious ramifications. The destruction of the sheath or its failure to develop properly results in severe disease and, in most cases, early death. The most common human myelin disease is multiple sclerosis (MS), which affects 200,000 to 250,000 in the United States alone. This disease is characterized by numerous demyelinated regions in the CNS of affected individuals which increase in number and in severity with age. This breakdown of myelin ultimately can lead to deficiencies in sensory, motor and cognitive functions (73).

The neuron is the major electrically active cell in the CNS but the myelin sheaths that insulate its axon are actually synthesized by a second cell type, the oligodendrocyte. Oligodendrocyte progenitors arise from the highly proliferative ependymal zone or subventricular zone (SVZ) of the perinatal brain. After they proliferate and migrate away from the SVZ, the precursor cells differentiate into mature glia, send out processes and initiate ensheathment of axons having diameters of at least one micron (3). These cellular processes elaborate and create semi-flattened membranous sheets which begin to wrap around the axon many times systematically extruding the cytoplasm toward the cell body, compacting the inner leaflets of the lipid bilayer. During this compaction, the outer leaflets of the oligodendrocyte's plasma membrane between adjacent wraps also come into close contact. So, every wrap of the oligodendrocyte membrane around the axon compacts and produces another lamella of the multilamellar myelin sheath (Fig. 3).

B. The molecular organization of the myelin sheath

A cross-sectional view of compact myelin seen through an electron microscope reveals a periodicity that results from the two different apposed membrane leaflets (Fig. 2). The thicker electron dense band, termed the major dense line (MDL), is a small aqueous space created by the apposition of the cytoplasmic surfaces of the bilayer and the distance between two of these MDLs defines the periodic distance of compact myelin. The periodicity of CNS myelin is around 10.5 nanometers (nm) varying slightly depending on the hydration state of the compact myelin during tissue preparation, procedural differences of preparation, the varying bilayer thickness in different animals and age of the animal (70). The other or minor electron dense band arises from the apposition of the extracellular leaflets of the lipid bilayer and is referred to as the intraperiod line. The dimensions of the MDL and the intraperiod line are very small, measuring 3-4 nm and 3-5 nm, respectively, as small as the separation in a gap junction (74). Interspersed within the internode of the compacted myelin are structural specializations known as radial components which run

perpendicular to the direction of the MDL and the intraperiod line. These regional scaffold- or lattice-like complexes were first described in 1961 by Peters (62) and are thought to have a stabilizing effect in the developing myelin (63).

There are also noncompact veins of cytoplasm running through the otherwise compact sheaths which contain mitochondria and other cellular factors (Fig. 1). They serve as conduits supplying the myelin with a metabolic reservoir and add flexibility to the myelin sheath. The lateral channels which form the paranodal loops lie juxtaposed to the axolemma. These channels also extend longitudinally, either as clefts in the compact region of the myelin (Schmidt-Lanterman incisures) or as complete channels that extend from one paranodal loop to another (longitudinal incisures, ref. 75).

Figure 2. Electron micrograph (66K X magnification) of CNS myelin. Cross section view of a myelinated axon (*). Note the periodic electron dense lines in the compact myelin (arrow).

A closer look at a single period of myelin reveals a highly organized architecture consisting of lipids and proteins (Fig. 3). The myelin sheath contains a variety of lipids which are segregated asymmetrically between the two leaflets in different proportions (74).

The reason for this asymmetry is unknown, however, one can speculate that the distribution of one lipid over the next in a given leaflet of the myelin lipid bilayer may serve a specific function in its structural uniqueness. For instance, cholesterol has a high molar content in the myelin membrane with a greater proportion located in the external leaflet of the lipid bilayer (74) and is thought to suppress thermal transitions within a lipid bilayer (28). Therefore, cholesterol could possibly have a rigidifying effect on the myelin membrane resulting in the pseudo-crystalline-like state of the myelin membrane (28). This is purely hypothetical, as functional data pertaining to the role of the asymmetry of a particular lipid in myelin formation has yet to be provided.

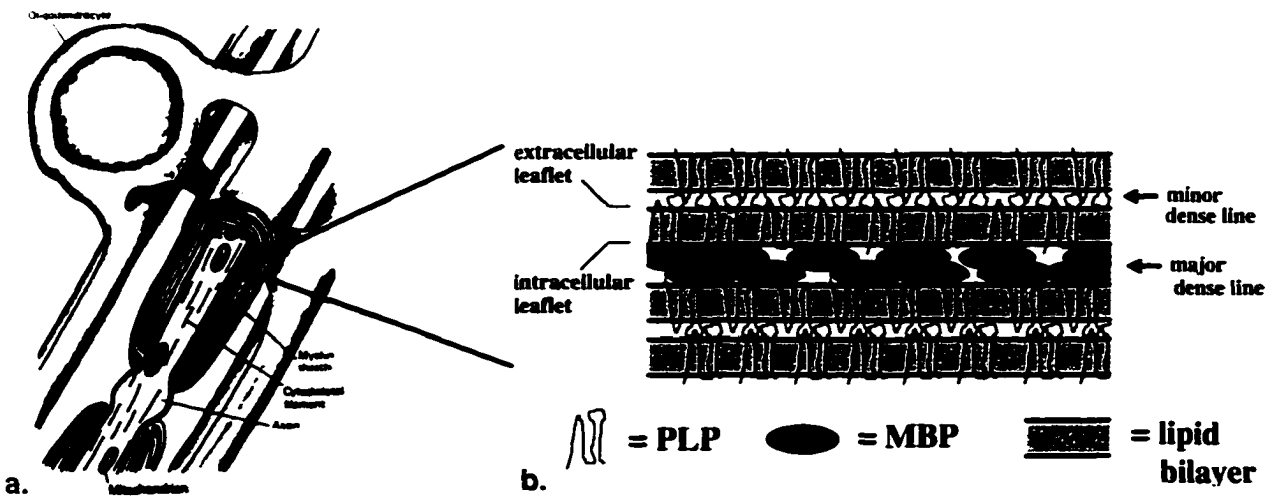

Figure 3. Representation of a multilamellar myelin sheath around an axon of the CNS showing a cross section and longitudinal view of the compact myelin (A, taken from ref. 39, adapted from ref. 109); and a cartoon of the molecular organization of the two major structural proteins, MBP (blue) and PLP (red, black) in the lipid bilayer of the compact myelin (B). For clarity, the relative dimensions of compact myelin are not preserved in panel B. The major dense line of compact myelin is formed by the extrusion of cytoplasm from an oligodendrocyte process and the apposition of the intracellular leaflets of the lipid bilayer formed by its association with MBP. The apposition of the extracellular leaflets form the minor dense line, where extracellular domains of PLP are located (PLP from one of the oligodendrocyte's wraps is represented in red).

Proteins comprise thirty percent of the dry weight of myelin. Eighty percent of the total protein content of compact myelin is composed of three structural proteins, proteolipid proteins (PLP and DM-20) and MBP. Minor protein components of CNS myelin include 2',3'-cyclic nucleotide 3'-phosphodiesterase (CNP) and three glycoproteins: myelin-associated glycoprotein (MAG), myelin-oligodendrocyte glycoprotein (MOG) and oligodendrocyte-myelin glycoprotein (OMgp) which are briefly described below and summarized in Table 1.

The proteolipid proteins account for 50% of the total protein content in compacted CNS myelin. PLP and DM-20 are generated by an alternatively spliced transcript from a single *plp* gene (23). DM-20 shares the same amino acid sequence with PLP except for the absence of 35 amino acids (numbers 116-150 of the PLP polypeptide), which is derived from a deletion in exon three of *plp* . Independent studies have shown that these polypeptides are composed of a series of alternating hydrophobic and hydrophilic domains that weave in and out of the oligodendrocyte's plasma membrane (42, 66, 81). Developmentally, these two isoforms appear to be regulated as expression of mRNA in mice peaks at 21-22 days postpartum and remains relatively high throughout life (23). DM-20 is the predominant form in premyelinating oligodendrocytes while PLP is proportionately more abundant in adult compact myelin (23, 109). The PLPs are localized exclusively in the CNS and thought to primarily function as an adhesive component that holds the extracellular faces of adjacent myelin wraps in tight register (10, 12, 13).

The other major structural myelin peptide is MBP, which comprises 30-40% of the total protein content found in CNS compact myelin, and 5-15% of total protein in the PNS compact myelin (27, 28). The protein contains a significant proportion of the basic amino acids lysine, arginine, and histidine and as a result, has a high isoelectric point (pI>10, Fig. 4, refs. 5, 28). MBP was originally purified from homogenized CNS tissue by delipidation with chloroform-methanol followed by acid extraction, and was found to be soluble in an aqueous phase at low pH (around pH 3, ref. 28, 31). MBP has been

immunocytochemically localized to the major dense line and is thought to play a role in forming the tight apposition of the membranes in compact myelin (37). Whether MBP is just neutralizing the negatively charged phospholipid headgroups or has a specific interaction with proteins/lipids dictated by its amino acid sequence remains unclear. Microtitre well-binding assays and ligand-blot overlay suggest that PLP can reversibly dimerize with MBP in aqueous solutions (36), but any homo- or hetero-protein/protein interaction with MBP and PLP has yet to be verified in myelin. The role MBP plays in myelin formation will be discussed extensively in the Chapter 2.

CNP comprises 4% of the total myelin proteins, is expressed prior to the two structural proteins of CNS myelin and thus considered by some to be a marker for early myelinogenesis (53). It is an acylated, amidated and phosphorylated protein that has two isoforms (48 and 46 kDa, ref. 53). CNP possesses two domains that are homologous to peptide regions believed to participate in GTP binding. However, these domains are unrelated to the catalytic domain responsible for the phosphodiesterase activity (28). CNP has been visualized immunocytochemically in the cytoplasm of noncompact myelin, however the function of the protein has not been elucidated (86). Overexpressing the protein interferes with compaction of the major dense line suggesting an interaction between CNP and MBP and thus may play a putative role in the compaction of the myelin sheath (52). These experiments will be discussed further in Chapter 6.

MAG is an integral membrane protein that is a member of the immunoglobulin superfamily by virtue of its five extracellular variable-like immunoglobulin-related domains and comprises 1% of the total myelin protein content. Immunolocalization and biochemical studies demonstrates that MAG is found at the periaxonal regions and may be involved in the initial attachment of the glial process to the neurite by virtue of the HNK-1 carbohydrate on its extracellular domain (12, 13). It has been suggested that MAG can act as an inhibitor of axonal regeneration (55); and later with a MAG knockout experiment, it

was shown to be necessary in the PNS to enhance or optimize axonal regrowth following nerve injury (54).

TABLE 1: THE DIFFERENT MYELIN PROTEINS OF THE OLIGODENDROCYTE

protein	oligodendrocyte localization	expression level*	possible function	ref.
PLP	compact myelin: minor dense line	50%	-adhesion of extracellular leaflets of bilayer	10, 12, 23
MBP	compact myelin: major dense line	30%	- adhesion of intracellular leaflets of bilayer	1, 2, 4, 8, 21,
CNP	noncompact myelin: cytoplasm of perikaryon	4%	-unknown	12, 13, 28, 52
MAG	noncompact myelin: inner mesaxon	1%	-unknown	12, 13, 54, 55
MOG	noncompact myelin: outer mesaxon, oligo process	0.05%	-unknown	16, 49
Omgp	noncompact myelin	minor**	-unknown	24, 25
OSP	oligodendrocytes myelin fraction	unknown	-unknown	87

* level of expression refers to the individual amount of each protein relative to the total myelin protein content from Western blot analysis.
** minor component of the CNS, percentages of total myelin protein content not given.

MOG is a 26-28 kDa protein localized to the oligodendrocyte process and the external surface of the myelin sheath, being excluded from the compact myelin and representing roughly 0.05% of the total myelin protein content (16). It contains a single Ig-like variable region domain, spans the lipid bilayer twice and is thought to function in the maintenance and the completion of the ensheathment. MOG is also a major antigenic target for the dysmyelinating disease, experimental allergic encephelomyelitis (EAE), which is an autoimmune disease in mice (49).

Another myelin glycoprotein that may be involved in glial cell adhesion is the oligodendrocyte-myelin glycoprotein (OMgp). This glycosylated protein is anchored to the membrane via a glycosylphosphatidylinositol (GPI) anchor (25). Recent results mapped the gene for this 46 kDa protein to one of the introns in the neurofibromatosis (NF) type 1 gene, and is thus implicated in playing a role in the heritable condition NF-1 (24). OMgp also contains the HNK-1 carbohydrate, which has been shown to mediate cell-cell contact again, supporting its putative role in adhesion. It has been localized, with immunoblots, to both the white and gray matter of mouse CNS, and in purified but not compact myelin. There is high homology between the mouse and human primary sequence which provides clues to its putative function, however, there is little direct evidence elucidating its role in myelination. (24, 25).

Oligodendrocyte-Specific Protein (OSP) is another component of myelin. Recently cloned and sequenced (87), OSP was immunocytochemically localized to the plasma membrane around the oligodendrocytes and to the myelin fraction from the CNS in mice. It is a 22.1 kDa transmembrane protein that shares sequence homology to the peripheral myelin protein, PMP-22. OSP is first detected in spinal cord at P2 and peaks at P10. Although it appears slightly before PLP, OSP follows a similar developmental expression time course (87). The function of the protein is unknown at this time, however, due to its effects in transfected cultured cells, it has been suggested that it functions, like PMP-22, in regulating oligodendrocyte proliferation (87).

C. The Evolution of Myelin and its Major Proteins

Myelination does not arise throughout the nervous system simultaneously commencing in the PNS a few days before CNS myelinogenesis (28). In rodents, myelination of the CNS is initiated first at the most rostral areas of the spinal cord spreading bidirectionally, caudally towards the tip of the spinal cord and rostrally to the telencephelon (45). Additionally, myelination begins and peaks at different times in

different species which may account for the relative differences among animals in motor coordination at the time of birth. For example, primates and most ungulates myelinate their axons much sooner in development than most laboratory animals such as rodents. At birth, humans are almost fully myelinated, whereas the peak of myelination in mice approximately occurs during the third week postnatal (75). Though the timing of myelination differs among species, myelin has been well conserved morphologically. Mouse CNS myelin is very similar to human CNS myelin, with respect to its molecular and morphological organization. The postnatal myelination in rodents makes them an attractive model for studying myelin assembly.

Although only vertebrates have compact myelin, invertebrates contain a substantial glial population functioning in a semi-insulatory and nutritive fashion, similar to myelin (11). In terms of evolution, the most distant organisms from humans that are similarly myelinated, are the chondrichthyes (sharks and rays). Primates and chondrichthyes diverged approximately 200 million years ago, however, it is believed that the first shark-like myelinated organism employed much of the same structural proteins. It has been demonstrated that MBP and DM-20, for instance, must have evolved earlier, around 440 million years ago (51, 60). Today, the availability of the chondrichthyes has proved helpful for studying the evolutionary as well as the functional aspects of the myelin proteins.

The amino acid sequences of the major proteins of compact myelin, PLP and MBP, have remained well conserved throughout great periods of evolution (61). The high degree of conservation in both myelin morphology and in peptide sequence of myelin proteins suggests that myelination is an extremely organized and controlled event, and is sensitive to the slightest perturbation. In the case of the PLP, single amino acid mutations result in severe dysmyelination (59). MBP has been observed to be one of the first constituents of CNS myelin, as demonstrated by its presence, though in small amounts, in the myelin of sharks and rays (51). The other major CNS myelin protein, PLP, however,

is thought to have evolved later (110), replacing protein zero (P0), a transmembrane protein which is the primary constituent in the myelin of shark CNS as well as mammalian PNS (11). Recently though, it was shown that PLP is present in amphibians and DM-20 is present in both bony and cartilaginous fish coincident with P0. Since this demonstrated that PLP and DM-20 were found in organisms earlier in evolution than previously thought (61), it was concluded that P0 and PLP evolved in parallel in myelinating cells of vertebrate species (60).

CHAPTER 2: *MYELIN BASIC PROTEIN GENE AND ITS PRODUCTS*

A. The molecular organization, expression and regulation of the MBP gene

The *mbp* gene is over 30 kb long (Fig. 4) and has been mapped to the distal end of chromosome 18 in the mouse (19, 22). It is composed of seven exons that encode five isoforms (21.5, 18.5, 17.2, 17.0 and 14 kDa) of the protein in mouse and four isoforms (21.5, 20, 18.5, and 17 kDa) in human as a result of alternative splicing of a transcript from a single gene (5, 6, 32).

In rodents, the developmental expression of *mbp* follows a time course which closely parallels the pattern of myelin formation (43). The expression of the *mbp* gene can first be detected at birth, peaking at 16 to 20 days postnatal (1, 2). All of the isoforms are found in adult compact myelin but are also developmentally regulated. In general, it seems that exon-2 containing isoforms (21.5, and 17 kDa in mice) are proportionately higher in early brain development, while the other isoforms are proportionately enriched in adult brain. It has been shown that the 14 kDa or smallest isoform expression increases with age and is the most abundant form of MBP in the adult mouse (1, 2). Similarly, exon-2 containing isoforms are more highly expressed early in the developing human CNS myelin (6). These developmental changes appear to be regionally controlled and only occur in the brain, since immunoblots of the spinal cord from 2-25 day old mice do not show any similar variation in the MBP isoforms (34).

Analysis of transcriptional activity of various 5'-upstream regions indicate three major regulatory domains that confer differential transcriptional activities in glial and non glial cells (15, 29, 30). Studies have shown that the level of MBP is determined by events other than alternative splicing of the primary transcript, including mRNA translocation, translation, and posttranslational modifications. Glucocorticoids, for instance, are known to stimulate the translation of the MBP mRNAs (14); posttranslationally, MBP is phosphorylated, methylated and glycosylated. It has been speculated that phosphorylation

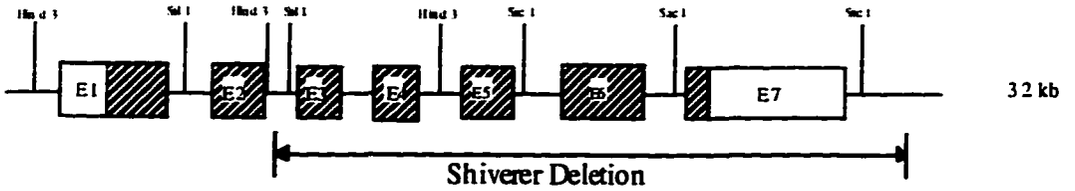

Isoforms	mRNA size (kb)	Protein size (kDa)	pI
1. exons 1, 2, 3, 4, 5, 6, and 7	2.1	21.5	11.8
2. exons 1, 3, 4, 5, 6, and 7	2.0	18.5	11.2
3. exons 1, 3, 4, 6 and 7*	2.0	17.0	12.3
4. exons 1, 2, 3, 4, and 7	1.8	17.0	10.9
5. exons 1, 3, 4, 5, and 7	1.8	14.0	12.2

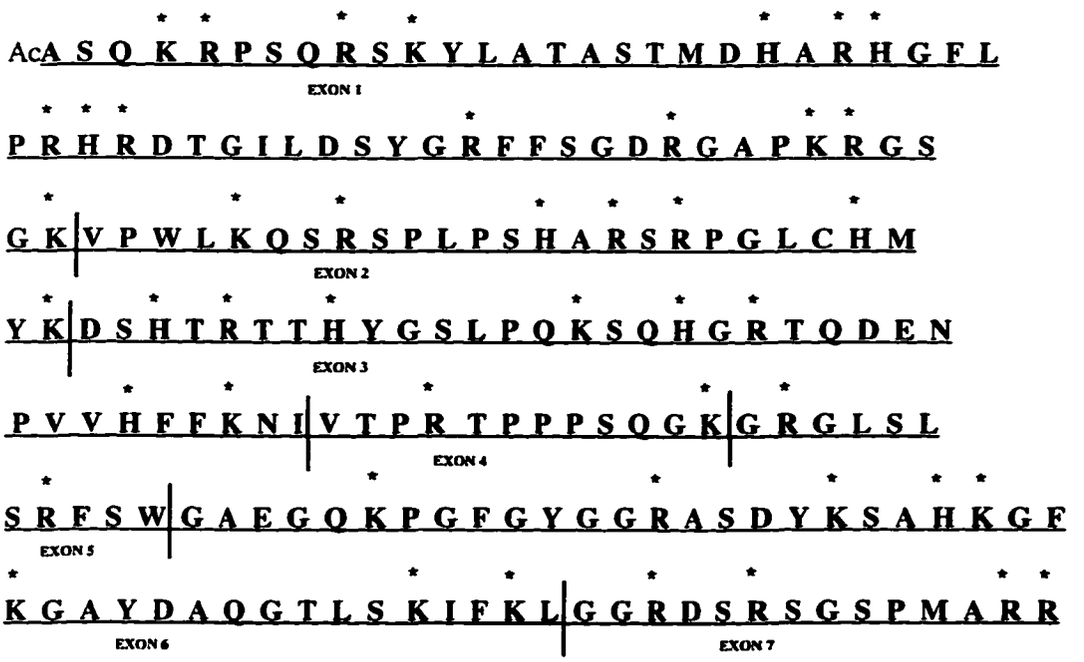

Figure 4. A schematic of the genomic *mbp* gene in rodents, shows the seven exons that compose the 5 different isoforms (stippled regions indicate peptide coding region). The shiverer mutation is a deletion starting in the middle of intron 2 and extending throughout the rest of the gene. The sizes of the mRNA and protein isoforms are indicated below the gene, along with the composition of each isoform with respect to exons, as well as isoelectric point (pI). This isoform (*) is described as a minor constituent of the MBP family of proteins in mice (32). Below is the amino acid sequence of the mouse MBP 21.5 kDa isoform which includes delineation of the peptides encoded by the seven exons. The basic amino acids (* above the single letter code for the amino acids) are uniformly distributed throughout the entire peptide sequence.

of MBP is necessary for the early sheath formation, while methylation may play a role in compaction of the inner leaflets of the lipid bilayer (28). MBP also contains sequence motifs that are homologous to sequences in *tau* protein (tubulin binding protein). Sequences in the peptides encoded by exon 2 and exon 6 of MBP have homology to the *tau's* tubulin binding domain and the regions containing phosphorylation sites, respectively (20). These sites are highly conserved in the MBPs of other vertebrates and have been implicated in modulating a putative interaction between MBP and the oligodendrocyte cytoskeleton (71).

B. MBP's role in the molecular architecture of myelin: the current dogma

The exact function of MBP in myelin compaction has yet to be defined, but the properties of the protein have led to certain speculations. MBP is an extremely basic protein with a high isoelectric point (pI>10), more basic than the DNA binding histone proteins (Fig. 4). It is known that MBP has a high affinity for acidic phospholipids, which are the primary class of phospholipids in the myelin membrane (28, 40). It seems likely therefore, that MBP could function by neutralizing the phospholipid headgroups of the cytoplasmic leaflets of the lipid bilayer, allowing for their close apposition in compact myelin. MBP has a higher affinity for anionic lipids than other types of lipids (41) and thus may interact highly with other organelles in a nonspecific manner (33, 56). To overcome this problem, MBP message is translocated to the glial processes, translated on "free" polysomes, and then incorporated into the myelin membrane (4, 14 and 31). The localization of MBP's message in the myelin takes place in three stages: 1) assembly of MBP RNA-granules, which contain many components of the translational machinery, in the perikaryon of the oligodendrocyte (112); 2) transport of the MBP RNA-granules in the processes of the oligodendrocyte; and 3) localization of the granules in the myelin compartment (111). In cell culture experiments, it was demonstrated that the 3' UTR of

mbp contains signal sequences that specify the latter two stages. The mRNA of the translation coding region for the 14 kDa isoform of MBP, by itself, can form RNA-granules but is restricted to the perikaryon of the transfected oligodendrocyte (111).

To date, the only study addressing the "neutralizing" function of MBP has tested the ability of different basic proteins to cause spontaneous lamellar formation of the anionic lipid fraction from myelin in an aqueous mixture (40). MBP in an aqueous environment was able to form structured lamellae with the phospholipids that had a periodicity of 15.4 nm, close to the lamellar spacing measured in native CNS myelin. When other basic polypeptides such as cytochrome *c*, lysozyme protein, and poly-l-lysine, where mixed with the acidic fraction of lipids, ordered lamellae were also observed creating a periodicity of 8.0 nm. This suggests that MBP might simply be neutralizing the highly repulsive charged head groups of the lipid bilayer holding them together in close contact. If this is the case, then possibly any small, basic peripheral membrane protein may function in the compaction of myelin.

The shiverer mouse mutant has provided an excellent cell biological, biochemical, and molecular tool to study the function of MBP. These mice have an autosomal recessive mutation which is a deletion in chromosome 18, removing most of the coding region of the *mbp* gene (Fig. 4, ref. 22, 77). Affected mice have no compact myelin in their CNS while the PNS is normally myelinated (35). Nuclear run-on experiments have confirmed that neither the rate of *mbp* gene transcription nor the developmental regulation is affected in shiverer mice. The reduction of MBP message observed is the result of the instability of the truncated mRNA (18). Further evidence supporting the notion that the shiverer phenotype is a direct result of the absence of MBP, comes from a transgenic study which expressed an antisense message of MBP in oligodendrocytes. A cDNA antisense of the smallest isoform (14 kDa), expressed in wild type mouse, recapitulated the shivering phenotype (7), further supporting the idea that MBP is essential in the compaction of myelin in the CNS.

Using a similar approach, two separate groups have been able to rescue the shiverer phenotype by introducing transgenes encoding different forms of MBP (8, 21). In one case, transgenic mice expressing genomic MBP were generated and through a series of back-crossings, four transgenic shiverer mice that did not display the shiverer phenotype were obtained. The level of transgene expression was 25% of wild type *mbp* message in normal littermates (21). This provided definitive evidence for the following: 1) MBP is the sole agent that is required to alleviate the dysmyelinating phenotype in the shiverer mice, and 2) MBP is essential in the compaction of CNS myelin.

Kimura and colleagues expanded on these conclusions by showing that the 14 kDa MBP isoform cDNA expressed alone in shiverer oligodendrocytes can rescue the phenotype (8). In these studies, five transgenic-shi/shi mice expressed a range of transgene message (from 3-40% mRNA of MBP mRNA in wild type littermates), and were able to form compact myelin resulting in a nonshivering behavioral phenotype. This data argues that the other isoforms of MBP are not necessary for the formation of compact myelin in the CNS.

With the characterization of the shiverer mice, the role of MBP in the compaction of myelin has become well accepted. However, further experimentation is needed to determine if the individual MBP isoforms play individual roles in myelination. As vertebrates evolved, MBP became a predominant structural protein of the CNS. A common feature between the different isoforms during the speciation of *mbp* is the inclusion of the first, third, fourth and the last exons (Fig. 4) which are also the most highly conserved amino acids throughout evolution (51).

The expression of the different MBP isoforms is developmentally regulated, which are localized to specific regions within the oligodendrocyte. Immunolabeling of CNS myelin with anti-MBP exon 2 specific antibodies shows an enrichment of the 17 and 21.5 kDa isoforms in the radial components of CNS myelin (64). As mentioned before, the radial component is thought to stabilize myelin assembly and aid in compaction. Since

these two isoforms of MBP are also proportionally more abundant early in myelinogenesis, then perhaps exon-2 containing isoforms may play a structural role in early CNS myelination (2, 12, 13).

It was demonstrated that the MBP isoforms containing exon 2 (i.e. 17 and 21.5 kDa isoforms), when expressed in transfected nonglial cells (56) and in transfected cultured shiverer oligodendrocytes (113), localize differently than the localization of the other transfected isoforms (i.e. 18.5 and 14 kDa). These experiments show that exon-2 containing isoforms of MBP localize to the cytoplasm and the nucleus, whereas the exon-2-less MBP isoforms (18.5 and 14 kDa) associate with the plasma membrane (33, 56, 113). Hardy et al. reinforced these observations by reporting the presence of all of the MBP isoforms in the nucleus of pre-myelinating and early myelinating cells *in vivo* (17). These data together with later observations by Pedraza et al. (107) suggests that MBP might play an, albeit undefined, role in the nucleus, and that exon 2 containing isoforms may serve as a "carrier", shuttling an MBP-complex into the nucleus. The implications of these experiments suggest alternative roles for the MBP isoforms in the oligodendrocyte other than in the compaction of myelin; and is further discussed in Chapter 8.

The other possibility is that the different isoforms of MBP may have no distinct functions in myelin assembly. To begin with, the different isoforms share many internal homologies and repeated sequences and have approximately the same isoelectric point (Fig. 4, ref. 38). Over time, the *mbp* gene could have recombined several times with the multiplication of certain essential domains forming today's 32 kb gene. So the different isoforms of MBP could have been generated during evolution and have remained because every combination of exons in each isoform preserves the reading frame of the mRNA. Certainly in the case of the shiverer rescue experiment one could argue that the multiple isoforms are redundant since a single isoform is able to allow for the compaction of the oligodendrocyte's processes. However, as noted above, the multiplicity of MBP forms may relate to other functions besides facilitating compaction of the myelin membranes.

Kimura's experiments have not addressed the question of whether the facilitation of compaction requires specific domains or a specific conformation of MBP. Conceivably the simple neutralization of the phospholipid headgroups could be achieved by any small, extrinsic, basic protein. This dissertation describes my studies to resolve this question.

CHAPTER 3: *SPECIFIC AIMS AND OVERVIEW OF EXPERIMENTAL STRATEGY*

This dissertation addresses the issue of what domains and subsequently, what characteristics of MBP are important in the compaction of CNS myelin. Since the amino acid sequence of MBP has remained fairly the same throughout evolution, it is reasonable to suggest that there might be essential domains of the protein that are strictly needed for either myelin compaction or localization of the protein to the myelin compartment of the oligodendrocyte process.

The fundamental experimental paradigm of this project relies on the fact that the shiverer mouse can be rescued by transgenes expressing MBP in its oligodendrocytes (8, 21). I have used this paradigm to assess whether mini-MBP's containing amino acid sequences encoded by four conserved exons, or a subset of these exons, can support the compaction of myelin. I have designed several transgenes (tgs) to be expressed in oligodendrocytes of the mouse CNS, each of which encode either truncated versions of MBP that are not found naturally in mammalian CNS myelin, an endogenous form of MBP and other basic proteins that share no sequence homology with MBP. These mini-MBPs were first expressed in wild type mice to determined their behavior in the presence of endogenous MBP (i.e. expression levels and localization). Afterwards, they were introduced into the shiverer mouse by classical genetic means and the ability of each mini-MBP to support compaction by itself was determined.

I chose not to use cell culture or organotypic culture systems for this assessment because of the complexity of the questions being addresses. For instance, it is possible to culture shiverer oligodendrocytes (113), however, the efficiency of their transfection is very low. Organotypic myelination assay systems involve explant cultures using brain slices, which cannot be manipulated in culture, genetically. This type of systems has been used in the identification of growth factors and/or other agents that influence myelinogenesis. For example, Wood and Bunge have described *in vitro* myelination

assays with purified oligodendrocytes to study the factors and other supporting cells that govern the development and maintenance of the myelin sheath (91). Furthermore, several investigators have demonstrated that explant cultures of the CNS initiate myelinogenesis and even recapitulate some CNS myelin diseases (92, 93, 94). However, these studies have relied upon normal myelinating glial cells while testing the effects of different helper cells or effects of growth factors that can easily be added to the culture. This system does not lend itself to the experimental alteration of the oligodendrocyte that would allow the expression of the mini-*mbp* genes. Although establishing transgenic lines expressing these tg proteins is time consuming, it is the most efficient way to assay the functionality of the miniMBPs in the compaction of myelin.

Each MBP minigene was expressed in oligodendrocytes of the shiverer mouse to determine which can substitute functionally for MBP in the compaction of CNS myelin. I used the M'P vector (Fig. 5) which can express appended sequences specifically in mouse oligodendrocytes (44).

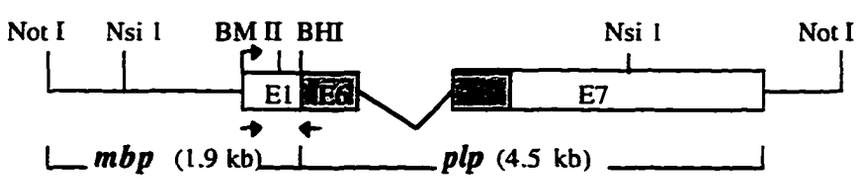

Figure 5. Cartoon of the M'P 6.7 kb expression cassette (44). Boxes represent mRNA with the hatching representing protein coding region. Each cDNA, containing its own translation stop codon, was cloned into the sites BspMII (BM II) and BamH1 (BH1) or into the BH1 site. The vector includes 1.9 kb of MBP 5'UTR or promoter sequence and 4.5 kb of PLP 3'UTR. The former includes a transcription start site (arrow) which transcribes, in frame, the appended sequence, and the initiation codon from exon 1 (E1) of *mbp*, while the latter contains part of exon 6, intron 6 and exon 7 of the *plp* gene, including splice donor and acceptor sites, and a ploy-A signal. This expression cassette, after being liberated with Not I enzyme, was used to express the different appended transgenes in oligodendrocytes of mice $MBP^{+/-}$. Arrows depict the primers (AG037 and DRP 25) used in the PCR screen for the tg mice, and the Nsi 1 sites were used in the Southern blot analyses.

Three mini-*mbp* encoding proteins (miniMBPs) and two viral gene encoding peripheral membrane proteins were tested. One of the transgenes, D2, contains

information from exons one and seven of *mbp*, encodes an 85 amino acid long polypeptide which is 9.4 kDa and has an isoelectric point (pI) of 12.4. The second, D4 contains information from exons one, three, four, and seven of *mbp*, produces a protein of 131 amino acids in length, which is 14.4 kDa and has a pI of 12.1. The third cDNA encodes a natural form of MBP (14 kDa isoform) containing information from exons one, three, four, five, and seven of *mbp*, and was used as a positive control. The resulting transgenic protein is 15.8 kDa with an isoelectric point of 12.2. To each miniMBP transgene a thirty three base nucleotide sequence encoding an epitope tag was appended, in frame, just before the stop codon of the cDNA. This "tag" sequence is an eleven amino acid polypeptide derived from a nucleocapsid protein of the T7 bacteriophage. A monoclonal antibody, which has been made available, can recognize this epitope providing a way to distinguish the miniMBPs in the presence of endogenous MBP.

The other two cDNAs encode the matrix (M) proteins from Measles or Vesicular Stomatitis Virus (VSV). They were included initially to test whether a completely heterologous, basic protein could function in myelin compaction. These proteins are small peripheral membrane proteins that are very basic with a high isoelectric point (98-102). However, transgenic mice expressing these proteins in oligodendrocytes were not obtained presumably because such expression may be lethal to the developing embryo. Consequently, further work on this aspect was not continued.

The first priority after the completion of the transgene constructions, was to generate a method to verify that the desired proteins encoded by the cDNAs were translated properly. This was accomplished by transfecting cultured fibroblasts with each of the MBP and viral cDNAs, and immunostaining the cells with an tag, and MBP antibodies in the case of the mini-MBPs, or with antibodies that are specific for the Measles or VSV M-proteins. The former antibodies recognize epitopes either at the NH_2-, and COOH-termini, respectively, and so immunostaining of both epitopes tests whether the entire encoded

protein was translated in frame. I have also compared the localization of a natural MBP isoform with the nonnatural MBP proteins by expressing the 18.5 kDa MBP isoform.

For these purposes, I subcloned the coding region of each minigene into an expression cassette that was transfected and expressed in Cos-7 cells. The expression vector, called pCMV-5, contained the cytomegalo virus (CMV) promoter, a polycloning site, into which the cDNAs were inserted, followed by the human growth hormone polyadenylation signal. Once these *in vitro* verifications of the minigenes were complete, I then assembled the cDNAs into the oligodendrocyte specific expression cassette diagrammed in Figure 5, and generated founder transgenic mice.

Quantitation of the message and protein levels of the transgenes relative to endogenous MBP were assessed to determine which transgenic lines would be used in the rescue experiments. RNase protection assays, Northern and Western blot analyses accompanied by phosphoimaging quantitation were carried out on all of the transgenic lines. To determine if the transgenic proteins were targeted to the correct compartment of the oligodendrocytes, I followed the localization of the miniMBPs with stained cryostat sections of tg mouse CNS using double labeling, immunofluorescent, confocal microscopy.

The test for the functionality of each miniMBP is its molecular behavior in myelin assembly in the absence of the natural MBP isoforms. To accomplish this, I crossed each of the transgenic minigenes (produced on a wild type background) onto the shiverer background and monitored whether the nonnatural forms of MBP can function compared to the natural isoforms in CNS myelin assembly.

Although confocal immunofluorescence microscopy can confirm the coincidence between the tagged protein and other myelin specific proteins, this type of microscopy cannot resolve the precise intracellular position of the miniMBPs. For example, the confocal microscope cannot distinguish compact from noncompact myelin. To address these questions, I used electron microscopy (EM) and immuno-EM to determine where the

tagged proteins are located ultrastructurally. I determined that exons one, three, four, and seven of *mbp* encode a protein sufficient to allow for the compaction of myelin, whereas the protein encoded by exons, one and seven only, does not suffice.

In the next chapters I discuss, in detail, the transgene construction and verification, the creation of the transgenic mice, examination of transgene expression in their CNS, and finally, the evaluation of the mini-MBP's ability to facilitate compaction of myelin in transgenic shiverer mice.

CHAPTER 4: *MATERIALS AND METHODS*

A. Transgene Construction

1. ***D2*** (MBP exons 1, 7 and tag)

This cDNA was constructed by using the specific polymerase chain reaction (PCR) primers to the plasmid pDRMG-3 (described below), DRP 18 (GGATCCAGGCCTCTTGCCAGAGCCCCGCTT) and AG037 (GGAGGACAACACCTTCAA-AGACAGG). DRP 18 contains the antisense sequence of the last 11 bases of exon 1 of *mbp* a Stu 1 restriction site, followed by a BamH1 restriction site, with AG037 (described below), amplifies a 270 base pair fragment was amplified which contains the upstream BspMII site in the *mbp* promoter, exon 1, a Stu1 site, and a BamH1 site. The fragment was digested with BspMII and Bam H1 and subcloned into the BspMII/BamH1 site of the plasmid WJHS2 (pWJHS2), which contains a 2 Kb HindIII/Sal1 fragment with exon 1 and 1.5 Kb of upstream MBP sequence. This plasmid was digested with BspMII and Stu 1 and the subsequent fragment subcloned into the same sites of the DRMG-3 plasmid (Fig. 6). This plasmid was digested with BspMII and BamH1 and the 240 base pair fragment that included exons 1 and 7 of *mbp* and the tag sequence was subcloned into the M'P vector (Fig. 5) resulting in a 9.2 kb plasmid (pD2).

2. ***D4*** (MBP exons 1, 3, 4, 7 and tag)

Plasmid pHF43 is a pUC 19 based vector that contains a 2.2 kb EcoRI cDNA fragment that contain exons 1, 3, 4, 5, 6 and 7 of *mbp* (95). An 84 base oligonucleotide flanked with StuI and BamHI restriction sites was ligated into the Stu1/Bam H1 restrictions sites of the pHF43 plasmid deleting exons 5 and 6 of *mbp* and appending the thirty three base pair tag sequence in front of the stop codon in exon 7. This plasmid, DRMG-3 (Fig. 6), was digested with BamHI and BspMII to generate a 495 base pair fragment (exons 1,

3, 4, 7 with the appended tag sequence), which was subcloned into the BspMII - BamHI site of the pM'P vector (Fig. 5) resulting in a plasmid (pD4) of 9.6 kb in size.

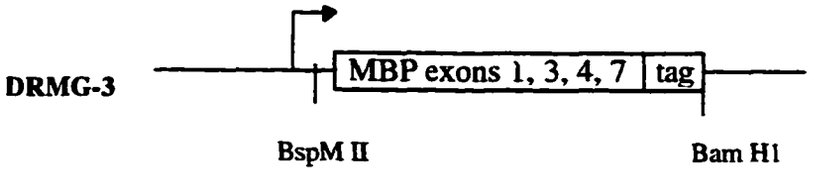

Figure 6. Schematic of the insert of the plasmid DRMG-3, which was constructed as an intermediate gene that was used in the construction of both pD2 and pD4. The BspmII/BamHl fragment (495 bp) was subsequently cloned into the M'P vector.

3. ***D5*** (MBP exons 1, 3, 4, 5, 7 and tag -- 14kDa MBP isoform plus the tag)

D5 was generated by amplifying a DNA product from DRMG-3 that will introduce the entire exon 5 of *mbp* into the cDNA of D4. This was done by using a PCR primer, DRP33 (GAGAGGCCTGTCCCTCAGCAGATTTAGCTGGGGAGGAAGAGACAGCCGCTCTGGAT) that includes the entire sequence of exons 5 (including the Stu 1 restriction site) and 7 of *mbp* (including a stop codon) and a BamHl site. This sense primer in combination with the DRP25 (CAACTCACCAGGGAAACCAGTGTAG, an antisense primer) amplified a157 base pair fragment with PCR, that was digested with Stu 1 and Bam Hl and ligated into these restriction sites of DRMG-3. Thus, this plasmid contains the same sequence as DRMG-3 with the addition of exon 5. Following a digestion with BspMII and Bam Hl the resulting 505 base pair (bp) fragment was subcloned into the M'P vector producing a 9.65 kb plasmid called pD5.

4. ***M'VP*** (vesicular stomatitis virus matrix protein)

The 800 bp temperature sensitive vesicular stomatitis virus (VSV) matrix (M) protein gene was obtained from Dr. Douglas Lyles (Bowman Gray Medical School ref. 96) and cloned into the BamHl site of the M'P vector. The mutation changed the methionine to an arginine in position 51 of the M protein. It translates into 230 amino acid peripheral

membrane protein, which is about 25 kDa in mass, and a pI > 9. Since the wild type protein has been shown to inhibit host cell transcription, the temperature sensitive mutant M protein of VSV, which has no effect on transcription, was used in these experiments.

2. ***M'MP*** (measles virus M protein)

The M protein gene from Philadelphia 26 strain of Measles kindly provided by Dr. William Bellini, Center for Disease Control, was subcloned into the M'P vector. The 1.4 kb M gene sequence produces a 335 amino acid polypeptide that has a molecular mass of 36 kDa. The gene was provided in a pBluescript based vector, which was removed as a 1.4kb Bam H1 to Kpn 1 fragment and ligated to a 8 oligonucleotide Kpn 1-Bam H1 linker, DRP 15 (5'-GATCGTAC-3') enabling the fragment to be flanked by the single restriction site Bam H1. This was then cloned into the Bam H1 site of pM'P

DNA Purification for Microinjection

The transgenes were liberated from vector sequences by digestion with the restriction enzyme Not 1, yielding DNA of 5.0 kb, 7.7 kb, and 7.0 kb for D2, D4 and D5, respectively. These mixtures were electrophoresed through a low-melting point gel, stained with ethidium bromide and the desired fragment excised. The agarose/DNA plug was melted at 65°C, and the DNA purified with a Magic DNA Cleanup Kit (Promega). The DNA fragments were dialyzed in 4 liters of 10mM Tris, .02 mM EDTA (microinjection buffer) for 48 hours at 4°C (3 changes of the dialyzing solution) (48). The concentration of the DNA was determined by gel electrophoreses and staining with ethidium using markers of known concentration and adjusted to 1-5 ng/ml with microinjection buffer. The samples were filtered twice through 0.2 micron filters (Nalgene), then given to the Transgenic Animal Facility (described below).

Production of Transgenic Mice

All manipulations were done at the Transgenic Animal Facility (Brookdale Center, Mt. Sinai Medical School) including the production and isolation of the fertilized eggs, pronuclear microinjection of the DNA, and reimplantation of the injected eggs into a host psuedopregnant mouse. The transgenes were injected into B6D2F1 fertilized eggs which were derived from the mating, C57BL x DBA2J mice. The host colony is made up of CD-1 random bred vasectomized males and sterile females.

Genotype Determination

Preparation of DNA from tail biopsies

The transgenic mice were identified from among their nontransgenic littermates by either PCR or Southern Blot analysis of tail DNA. A 1-2 cm of tail was cut and placed in a solution of 100mM EDTA, 50 mM Tris (pH 8), 0.5% SDS and 0.5 mg/ml Proteinase K (48). This solution was incubated at 55°C overnight to allow for complete digestion. After extracting with phenol, then phenol/chloroform and then chloroform, the DNA was precipitated with 0.1 X 3M sodium acetate (pH 5.2) and cold 100% ethanol (NaAOC/ETOH). The pellet was resuspended in 10mM Tris (pH 7.4), 1mM EDTA (pH8.0) or TE, (46) and the concentration determined by absorbance at 260nm.

PCR

2-3 micrograms of purified tail-DNA added to a tube with 2 mM $MgCl_2$, Taq polymerase (Promega), and 10X Taq polymerase buffer and primers (200ng/100µl rxn.). Each cycle of the Stratagene thermocycler was as follows: denature, 94°C one minute; anneal, 55°C one minute; elongation, 72°C one minute; for 35 cycles; followed by ten minutes at 72°C; 1 cycle. Primers which will specifically amplify a fragment from either the transgenes, or the *mbp* locus (wild type and shiverer alleles) were used in a PCR screen to determine the genotypes of mouse pups carrying either the transgene or the

shiverer allele. For the former, DRP25 and AG037 which are shown in Figure 5, and for the wild type and shiverer alleles, DRP31/DRP32 (TGTGGACGTACACCAGACCAGAACT and ATGTGCATCTTGTGTGTGCCTGCAT, respectively) and DRP31 with DRP40 (CTGTGCCTTGGAAATCTTGTGAACA) were used, respectively (Fig. 14).

Southern Blot Analysis

Southern blots were carried out following the protocol described in the Schleicher and Schuell Product Guide and Methods Book. Briefly, 10 µg of tail-DNA was digested with Nsi 1 overnight, precipitated, and electrophoresed through a 0.8% agarose gel for 3-4 hrs at 100 volts or until the dye front was 1-2 cm. from the bottom of the gel. The DNA was denatured by incubating the gel in a denaturation solution of 1.0M NaCl, 0.5M NaOH for 30 minutes at room temperature (rt), changing the solution twice. The gel was then placed in a neutralization buffer of 1.5 m NaCl, 0.5M Tris (pH 7.4). The DNA was transferred to a Nytran membrane (Schleicher and Schuell) overnight by capillary action in 20xSSC (17.5% NaCl and 8.8% sodium citrate, pH 7.0). ^{32}P-incorporated cDNAs were generated by random priming with hexamers as described by New England Biolab (NEB) and used to probe the blots for the desired DNA fragments. The membrane was washed stringently in 0.1% SDS, 2.0XSSC at room temperature for 15 minutes, twice, then at 0.1%SDS, 0. 2XSSC at 42^{0}C for 15 minutes, and lastly, in 0.5% SDS, 0.2xSSC at 59^{0}C

Cell Transfection assay

Cos-7 cells were transfected with the 20 micrograms of CMV-minigenes by the calcium phosphate co-precipitation method described elsewhere (47). Briefly, cells were trypsinized and seeded onto into 100-mm dishes the day before transfection at a cell density of 30-40% of total confluence. On the day of the transfection, the medium was changed and the cells were given 9 ml of fresh complete medium of CellGro™ Dulbecco's Modified Eagles Medium supplemented with 10% fetal bovine serum, 4mM L-glutamine, and 1%

penicillin-streptomycin (cDMEM). The 1ml DNA/CaPO4 precipitate solution was distributed evenly over the dish of cells and mixed with mild agitation. After 16 hours of incubation (37°C, 5% CO_2), the cells were washed with fresh, pre-heated, PBS and incubated with 10 ml of fresh cDMEM overnight (37°C, 5% CO_2). After 3 days, the cells were diluted 1 to 15 and seeded onto fresh dishes to be fixed and immunostained (described below).

RNA Purification

Mouse CNS RNA purification

The method for total RNA extraction has been described (50). Transgenic or wild type mice were sacrificed by cervical dislocation. The brains removed were quickly placed in a 15 ml polypropylene tube and emersed in liquid nitrogen. They were homogenized in a solution of 4M guanadinium isothyocyanate, 10mM Tris buffer, 1% sodium laurel sarcosine and 1% beta-mercaptoethanol for 1 minute and overlaid on a cushion of 0.75 mL of 2.4 M cesium chloride (CsCl) and 3 mL of 5.7M CsCl. After centrifugation at 35,000 RPM for 24 hours the supernatant was aspirated and the pellet was resuspended in 10mM Tris buffer, 5mM EDTA and 0.5% SDS. This solution was then extracted with 4:1 chloroform/n-butanol, and the RNA was precipitated with sodium acetate and ethanol. The pellet was resuspended in TE, and the concentration of the RNA was determined from the absorbance of 260 nm.

Northern Blot analysis

10-15 ug of total dried RNA pellet was resuspended in 20 ul of a solution consisting of 50% formamide, 1xMOPS buffer, 7% formaldehyde, 5% glycerol, and bromophenol blue, heat denatured at 65°C for five minutes, and electrophoresed through a 1% agarose MOPS/formaldehyde gel. The RNA was transferred overnight to a Nytran membrane via capillary transfer in 10x SSC (8% sodium chloride and 4% sodium citrate).

The membrane was then placed in pre-hybridization solution of 5x Denhardt's reagent (104), 10x SSC, 71% formamide, 2% salmon sperm, 4% SDS, 70mM sodium phosphate for at least 2 hours at 42 degrees, then hybridized with a ^{32}P-dCTP-labeled DNA probe overnight. The purified probe was denatured, and added to the pre-hybridization mixture and left to hybridize overnight at 42^{0}C. The membrane was stringently washed (as described above) and exposed to autoradiographic film, and developed. Phosphoimaging analysis (Molecular Dynamics) quantitated the amount of message normalized to control mRNA levels. To prepare the labeled probe, 25ng of the cDNA was heated in a boiling bath for 5 min followed by emersion in an ice bath. In a separate tube was combined 50uC of ^{32}P-dCTP, 5 units of the Klenow DNA polymerase, labeling buffer (random hexamers for random prime labeling from NEB) and was incubated at 37 degrees for one hour. The probe mixture was then purified by passing it over a G-50 Sephadex column, the fractions (100µl were collected, and the radioactivity for each fraction determined (Cerenkov counting).

RNase protection assays

DNA Template Preparation

RNase protection assays were carried out as described in Current Protocols (47) with a few modifications. Briefly, The cDNA of D2, D4, and D5 from the pCMV-tg plasmids were subcloned by digesting with EcoR1 and BamH1, into these restriction sites of a pBluescript II KS (+/-) vector (pBS) generating pBS-tg plasmids (pBluescript with the appended transgene). These plasmids were employed to generate sense and anitsense transcript probes from the T3 and T7 RNA polymerase sites that flank the cDNA inserts. 10 µg pBS-tg was linearized with either EcoR1 or BamH1 and purified by the following means: digested DNA (100µl reaction) was incubated with 5 µl of proteinase K (1mg/ml) and digested for 0.5 hour at 37^{0}C. The reaction was extracted twice with Tris (pH 8)

equilibrated phenol/chloroform, then once with chloroform (1:24 iso-amyl alcohol:chloroform). An aliquot (1 µl) was electrophoresed through a 1% agarose gel and stained with ethidium bromide to determine the concentration of the DNA mixture. The DNA was precipitated with NaAOC/ETOH (described above). The DNA pellets were resuspended in RNase free water to a concentration of 5-10 µg/ µl.

Preparation of the Sense and Antisense Transcript Probes

In vitro sense and antisense transcripts were generated to protect the mRNA in the RNase protection assays. The method used here followed the method described by Current Protocols (47). An in vitro transcription kit from Promega was used to transcribe the template DNA with incorporated ^{32}P-rUTP. 2 µl of template DNA was added to the mixture of RNA polymerase reaction buffer (Promega), 1 µl Rnasin, 3 µl α–^{32}P rUTP (800 Ci/mmol), 2 µl of 100 mM DTT, 2 µl of rNTP (equal molar ratio, 3mM of each, rCTP, rGTP, rATP) final concentration of 0.3 mM of each of the three ribonucleotides, 7 µl of 0.28 µM cold rUTP, and 1 µl of T3 or T7 RNA Polymerase. Reaction was incubated at 37^{0}C for 45 minutes. Afterwards, the reaction was digested with RQ1 Dnase (Promega) for 15 minutes at 37^{0}C. Transfer RNA (tRNA) was added (2 µl of 10mg/ml) to each tube to aid in the precipitation step below, and the reaction was brought to 50 µl with RNase free water. This mixture was extracted with phenol as described above, and then passed over a RNase free G-50 Sephadex column (obtained from Boehringer). The 50µl probe was precipitated with 200 µl 2.5M ammonium acetate, and 750 µl cold ETOH. The radioactivity of 1 µl was determined, while the rest was stored at -20^{0}C. An aliquot of the probe was electrophoresed through a 6% polyacrylamide denaturing gel (stock solution:

19% acrylamide/1% bis-acrylamide, 7M urea, in 1xTBE or Tris pH8.3, boric acid, EDTA) in 1xTBE to verify its size.

RNA Hybrid Protection Assay

Total RNA (1 µg) was dried and resuspended in 30 µl of hybridization buffer (4 parts formamide and 1 part of 5x stock buffer of 200mM PIPES (pH 6.4), 2M NaCl, % mM EDTA) containing $1x10^5$ cpm of probe RNA. The RNA/probe solution was incubated for 5 minutes at 85°C, and allowed to cool overnight. To the hybridization reaction, 350 µl of ribonuclease digestion buffer (10mM Tris, pH 7.5, 5 mM EDTA, pH8, 300mM NaCl) containing 40 µg/ml of ribonuclease A and 2 µg/ml ribonuclease T1 was added and placed in a 30°C water bath for 45 minutes. 10 µl of 20% SDS and 2.5 µl of 20mg/ml of proteinase K were added and incubated for 15 minutes at 37°C. The mixture was extracted once with phenol/chloroform/isoamyl alcohol, and 1 µl of 10mg/ml of tRNA was added. The RNA hybrids were passed over a RNase free G-50 Sephadex column (Boerhinger Mannheim) and precipitated with 1/2 volume (about 200 µl) of 7.5 ammonium acetate and 900 µl of cold ETOH. The pellet was resuspended in 20 µl RNase free TE and electrophoresed through a 8% nondenaturing acrylamide gel (3.75 ml of 10x TBE, 23.75 ml of water, and 10 ml of acrylamide stock solution 29% acrylamide and 1% bis-acrylamide). The gel was exposed to autoradiographic film (Kodak), and developed. The amount of hybridization was quantitated with phosphoimaging analysis.

Protein analysis

Purification of myelin

Mice were decapitated and each brain homogenized in 5 ml of 0.32M sucrose. Homegenate aliquots were set aside for protein concentration determination, while the rest

was layered on top of a 0.88M and 1.2M sucrose cushion and centrifuged (Beckman L7-65 ultracentrifuge) at 20K RPM overnight at 4°C. The myelin extract was purified as described in reference 103, by extracting the 0.32M/0.88M sucrose interface. The concentration of both myelin and brain extracts were determined with a Pierce micro BCA protein assay reagent kit.

Western Blotting

Equal amounts of protein (10 μg) were electrophoresed through a 16% (from a 49.5% acrylamide/3% bis-acrylamide stock solution in 1.0M Tris/HCL pH8.45) SDS-PAGE (SDS-polyacrylamide gel electrophoreses) gradient gel. The samples were equilibrated in loading buffer of 0.125M Tris (pH 6.8), 10% glycerol, BPP and Coomassie G (dyes), 1% SDS, 1% BME (added fresh), and loaded in wells of a 4% stacking gel, which was layered on top of a 10% spacing gel. Samples were electrophoresed at 15mA, overnight in a BIO-RAD protein gel system, with a 0.1M Tris pH 8.45, 0.1M tricine, 0.1% SDS as the upper buffer, and 0.2M Tris, pH 8.8, as the lower buffer. The next day, the separating/spacing (16%/10%) gel with the protein samples was cut from the 4% stacking gel and equilibrated, along with an appropriately sized Immobilon-P membrane (Millipore) in transfer buffer made up of 25mM Tris (pH 8.3), 192M glycine, 20% methanol, 0.01% SDS. Proteins were transferred onto the Immobilon-P membrane at 100V for 3 hours. The equilibration and transfer were done at 4°C. The membrane was incubated in blocking solution (5% milk, 1% bovine serum albumin (BSA), 0.05% Tween-20, and 0.02% sodium azide (NaAzide)) for 3 hours at room temperature (rt). Membranes were then incubated in either antibodies against MBP or tag (below) overnight at 4°C in 10% blocking solution. Afterwards, they were placed in an alkaline phosphatase (AP) conjugated secondary antibody (Jackson) for 1 hour, then treated with either a 1:500 NBT/1:500 BCIP substrate solution or an enzymatic chemiluminescence (ECL) system to react with the AP revealing the specifically stained epitopes.

Immunostaining

Transgenic or wild type mice were perfused with 2% paraformaldehyde/0.1M phosphate buffer (PB), left overnight at 4° C, and the brain and spinal cord were dissected out and placed in equilibrated with 20% sucrose/PB. The tissue were quick frozen in O.C.T. freezing compound (Miles Inc.) and sectioned with a cryostat micotome (15-75 microns). Sections were frozen, onto slides (Fischer), and stored at -20°C. Slides containing sections were postfixed in 4% paraformaldehyde and permeabilized with 100% methanol at 4°C for five minutes. The sections were then incubated in blocking solution consisting of 0.1% gelatin, 1% BSA, 0.05% NaAzide, made in PBS (PGBA) with 10% goat serum (gs). The sections were incubated with primary antibodies in PGBA+10% gs overnight, followed by 1 hour incubation with secondary and sometimes, tertiary conjugates. All of the immunofluorescent staining assays were analyzed with a Leica confocal microscope, equipped for three color simultaneous fluorescence detection. Two channels (green and red) were used to collect images stained using fluorescein or Texas Red conjugated antibodies, respectively, and were obtained from Amersham, Molecular Probes and Southern Biotech.

Primary Antibodies

For staining against MBP: mouse (ms) monoclonal MBP antibody obtained from Dr. Robert Fritz (Emory University, ref. 67), a rabbit polyclonal MBP antibody was obtained from Dr. David Colman (Mt. Sinai). The tag antibody is a mouse monoclonal against the peptide: **Met, Ala, Ser, Met, Thr, Gly, Gly, Gln, Met, Gly, Arg** from the T7 nucleocapsid protein, and purified from hybridoma cells generated by Dr. Tom Moran (Mt. Sinai). The PLP antibody was obtained from Dr. J. Benjamins (clone 81-11) described in ref. 66.

Electron Microscopy

Standard Electron Microscopy

Mice were perfused with 2% paraformaldehyde/ 0.5% glutaraldehyde, and brain, spinal cord and optic nerves were dissected 24hr later (half of the tissue was then processed for immuno-electron microscopy described below) and cut into 500μm sections. They were then incubated in a 2% osmium tetroxide in 0.1M phosphate-8% glucose buffer (PB/glucose), washed in a 0.1M NaAcetate/glucose buffer (NaOAC buf.), and then treated with 2% uranyl acetate/NaOAC buffer (UA). The tissue was then dehydrated with ETOH and treated with propylene oxide, and embedded in Epon. Semithin sections (1μm) were cut, stained with Toluidine Blue and mounted on glass slides and analyzed with light microscopy. Thin sections (60-100nm) were cut for standard electron microscopy (JEOL 100cX and Zeiss EM10 which were graciously provided by the departments of Pathology and Neurobiology at Mt. Sinai Medical School).

Immuno-Electron Microscopy

Tissue was prepared following the protocol described above (for standard EM), to the dissection of the tissue. After dissection, the tissue was cut into 100 μm sections with a vibratome and placed in a 0.1M maleate buffer overnight. They were then treated with 1% tannic acid, then incubated in 0.1% calcium chloride/maleate buffer solution. They were then treated with 1% UA followed by 0.5% platinum chloride. The tissue was dehydrated in ETOH treated with 1% PPD (para-phenylenediamine dihydrochloride) in 70% ETOH. After an additional UA treatment, the tissue was further dehydrated in 100% ETOH, incubated in propylene oxide, and embedded in epon. Sections were gold-labeled by incubated with a rabbit MBP antibodies (1:250 or 1:500) and then treating with anti-rabbit IgG-gold or with anti-rabbit IgG-biotin, followed by streptavidin-gold (12nm). The secondary and tertiary antibody conjugated with the gold particles were obtained from Jackson Immuno-Research Laboratories INC.

CHAPTER 5: *CREATION & TESTING OF THE TRANSGENES*

A. Synthesis of the transgenes

The minigene cDNAs that were used as transgenes in the pCMV or pM'P expression cassettes, diagrammed in Figure 7, were synthesized as described in Chapter 4 The exons in the larger mini-*mbp* transgene, D4, were chosen due to their presence in all of the isoforms of MBP and the high degree of conservation among different species. D2 differs from D4 for the absence of exons three and four, and was also used to determine if a smaller protein with the same pI can substitute for MBP in the function of compaction. Sequence from exon one of *mbp* is included in the miniMBP cDNA constructions to preserve the original transcription start site and 5' UTR region.

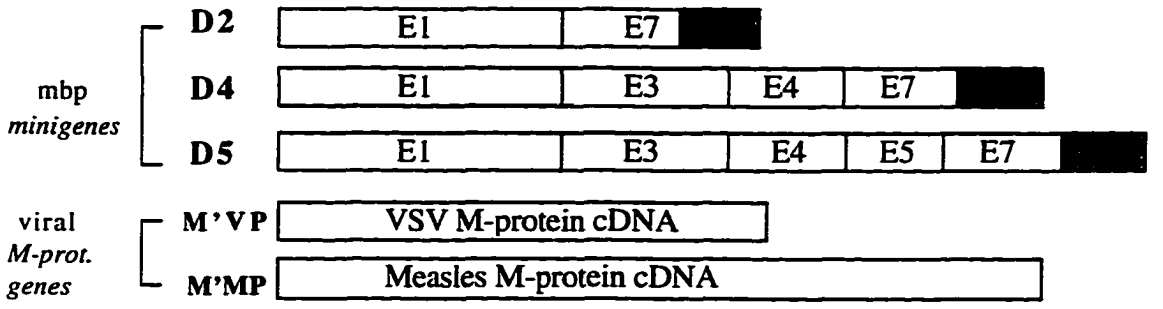

Figure 7. A schematic of the different cDNA transgenes used to be expressed both on a wild type and the mutant shiverer background. The top three minigenes are versions of the *mbp* gene drawn to scale, relatively. The 260 bp D2 cDNA contains exons (E) 1 and 7 of MBP. The 399 bp D4 cDNA contains exons 1, 3, 4, and 7 of MBP. The 432 bp cDNA D5 encodes the 14 kDa isoform of MBP which includes exons 1, 3, 4, 5, and 7. The stippled box at the end of each coding segment represents the 11 amino acid "tag" sequence which provides an epitope to interact with a specific monoclonal antibody. The bottom two cDNAs are the matrix (M) protein gene from either the measles or the VSV viruses, respectively. These two were drawn to scale relative to each other, with the M-protein gene from Measles virus 1,005 bp in length and the M-protein from VSV is 689 bp in length.

Changes in this sequence may effect the level and timing of tg expression relative to the endogenous *mbp* promoter. It was demonstrated that transcription of the truncated *mbp* gene in shiverer mice has the same efficiency and oligodendrocyte specificity as the endogenous gene (18, 22). Gow et al. delineated an enhancer region in the DNA sequence

of the mouse *mbp* gene between -1907 bp and +36 bp (the promoter used in the present experiments) that ensured efficient and specific expression of an appended heterologous transgene in oligodendrocytes following the same timing and pattern of expression as *mbp* (44). Therefore, in consideration of these studies, the DNA sequence in exon one of *mbp* that ensures the correct expression of appended sequences was included in the cDNAs to be expressed in shiverer oligodendrocytes. D5, which is the 14 kDa isoform of MBP plus the appended tag sequence, serves as a control in these experiments. Since it is known that the protein from this cDNA can rescue the shiverer mutant, D5 tg/wt mice enabled me to test if the tag acts as innocuously as predicted.

As another control, two MBP-like proteins were chosen to be expressed in the shiverer mice to test if MBP is functioning by simply neutralizing the anionic phospholipid headgroups of the lipid bilayer in compact myelin. The proteins chosen for these purposes were viral matrix (M) proteins from both the Measles and the VSV viruses. They are peripheral membrane proteins, that are 21-25 kDa in size, have a pI>9, and are known to interact with negatively charged phospholipid headgroups and nucleic acids. The M-proteins of these viruses function by interacting with the nucleocapsid and the viral genome causing them to form coiled structures, aid in virion formation and bind to the host cell membranes during the viral budding process (96-102).

B. Expression studies

Cultured cells were transfected with the different cDNAs and stained with MBP and tag antibodies to confirm the correct translation of the entire expected proteins. The cDNAs were subcloned into a cytomeglavirus (CMV) promoter expression cassette obtained from Mark Stinsky (University of Iowa). Appended to the 800 bp CMV promoter is a polycloning site and about 1 kb of 3' UTR sequence including a poly-adenylation site from the human growth hormone gene.

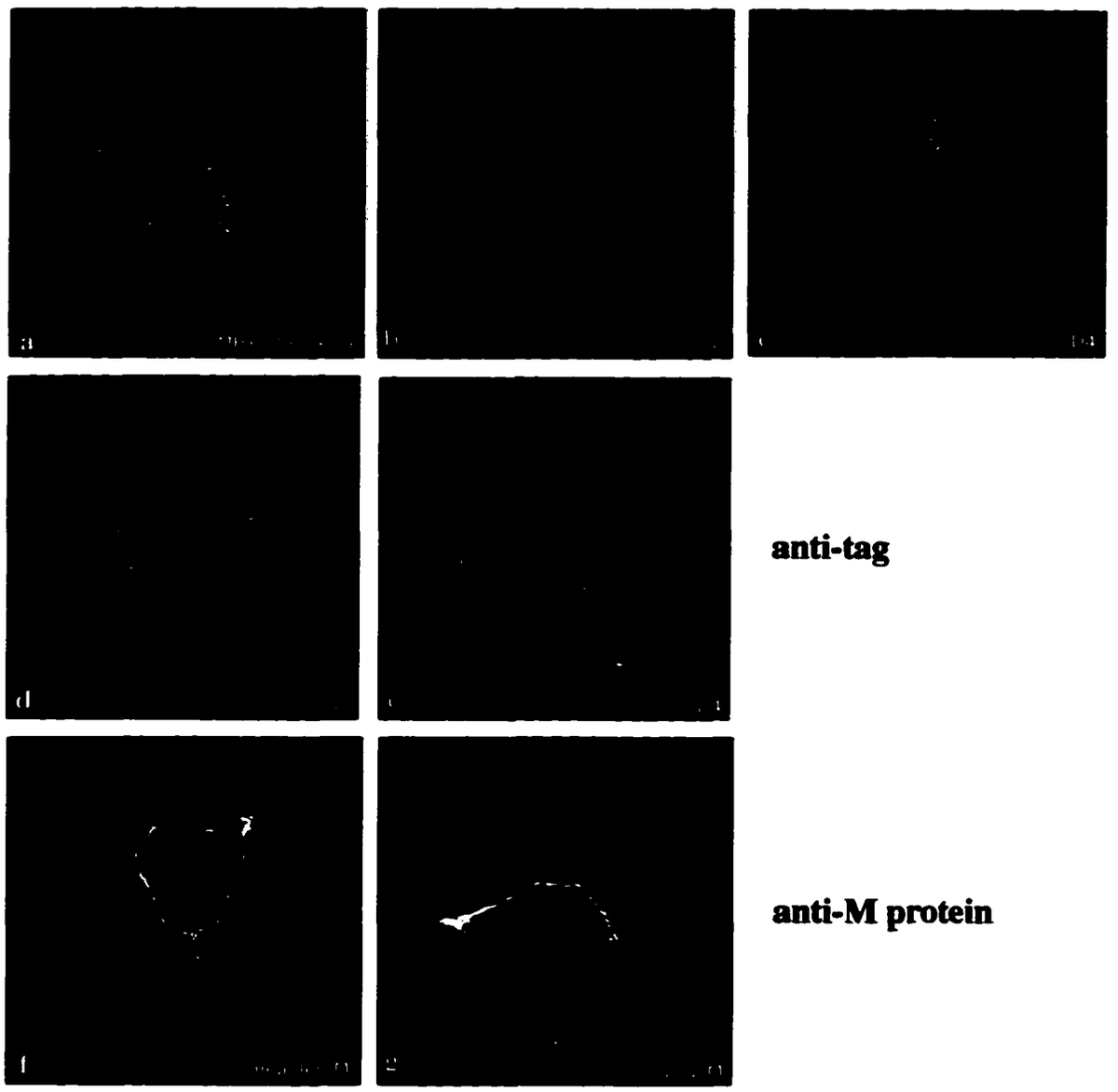

Figure 8. Immunofluorescent confocal microscopy of transfected Cos-7 cells. Cells transfected with pCMV-D2 and pCMV-D4 are in panels b, d and c, e respectively. Cells transfected with pCMV-MBP18.5 is in panel a, and cells expressing pCMV-MEA and pCMV-VSV are in panels f and g, respectively.

The D2 and the D4 minigene cDNAs were subcloned into the polycloning site of the CMV vector and then transiently transfected into Cos-7 cells by coprecipitation with calcium phosphate. The transfected cells were screened with the MBP antibody or with the

tag antibody (described in Chapter 4) which stained both the D2 and the D4 protein (Fig. 8a-c, d-e respectively). The mouse monoclonal anti-MBP antibody used here was obtained from Dr. R. Fritz (67) and recognizes an epitope in the peptide encoded by the first exon. Consequently, it not only reacts with the 18.5 kDa isoform of MBP (Fig. 8a) in the transfected cells but also with the D2 and D4 proteins (Fig. 8b,c respectively). Since the tag sequence was appended onto the COOH-terminal of each protein, staining with both antibodies confirmed that the encoded proteins were translated completely and in frame from the transcribed cDNA.

The staining pattern in the cells indicates that the D4 miniMBP is localized in the cell body, the nucleus and at the plasma membrane (Fig. 8c, e). Similarly, the D2 miniMBP is localized to the cytoplasm of all cells and to the nucleus in only a fraction of the cells. However, D2 does not accumulate at the plasma membrane (Fig. 8b, d), as does the 18.5 kDa MBP or D4 (Fig. 8a and c, e, respectively). Transfection and immunostaining of the 18.5 kDa isoform of MBP, revealed that the addition of exons 5 and 6 does not change the localization of MBP in Cos-7 cells, as the staining pattern resembles the staining of the D4 protein (compare Fig. 8a to c and d). Because these cells do not recapitulate the milieu of the oligodendrocytes nor the cellular influences in the CNS, these results are not indicative of the transgenic protein's behavior *in vivo* , but the similarity in cellular localization of the D4 and the 18 kDa isoform is interesting.

C. Generation of the transgenic mice and *in vivo* tg expression

The transgenes were excised from the carrier plasmid vector and microinjected into the pronuclei of fertilized eggs obtained from B6D2f1 mice at Mt. Sinai School of Medicine. This hybrid strain of mice generated by crossing two inbred strains of mice, C57BL x DBA2J, is used because it is more robust than either parent. The injected eggs were reimplanted into the uterus of a psuedopregnant SW mouse which gives rise to

potential transgenic founder mice. Mouse lines were generated only from founder mice able to pass the transgenes to their progeny.

Different variables can effect the level of transgene expression such as rearrangement of the transgene during integration, the insertion site, and the copy number of the integrated transgenes; consequently, it was necessary to obtain several lines for each transgene (summarized in Table 2). The lines with the highest expression of the correct cDNAs were chosen to cross onto the shiverer background.

TABLE 2: SUMMARY OF THE TG MOUSE LINES

GENE	EMBRYOS INJECTED	EMBRYOS TRANSFERRED	LIVE BIRTHS	# OF FOUNDERS	# LINES
D2	1191	915	71	3	3
D4	379	197	28	4	4
D5	N/A*	N/A	46	4	3
M'MP	N/A	N/A	34	4	N/A
M'VP	N/A	N/A	14	3	N/A

* N/A refers to data that was not available.

PCR and Southern analysis (Fig. 9) was used to determine which mice in a given litter carried the transgene. A 5' primer (AG037) which is a 25 base pair (bp) sense oligonucleotide to a region proximal to the transcription start site of the promoter of *mbp* and a 3' primer (DRP25), an antisense 25 bp oligonucleotide to the region just after the BamH1 in the PLP 3' UTR (Fig. 5) were used in PCR for this screening. Figure 9a is an example of a PCR using these primers on tail DNA from a litter of mice carrying the D4 tg. The top band is the 595 bp amplified fragment from the D4 transgene using primers DRP25 and AG037. The lower band represents the predicted 185 bp fragment amplified from the endogenous *mbp* gene to serve as an internal control for the reaction. A second set of primers, DRP31 and DRP32 which are sense and antisense 25 bp oligonuceotides to the

end of exon two and the beginning of intron two, were used to generate this control band. Other controls included reaction tubes containing either plasmid DNA of the appropriate cDNA(not shown here), known wild type DNA (Fig. 9a lane 7) or no DNA (Fig. 9a lane 8).

Southern blot analysis with subsequent phosphoimaging was used to determine zygosity (Fig. 9b) and copy number for each of the transgenes (data not shown) on the transgenic littermates determined from the PCR screen. For these purposes, a BglII/BspMII fragment of the *mbp* promoter was used to probe Southern blots of Nsi 1 digested tail DNA. Since the probe spans the first Nsi 1 site (Fig. 5), three bands appear in the lanes of transgenic DNA. The top band represents the transgene to the next Nsi 1 site in the 5' upstream region at the insertion site and the second, more intense band represents the predicted size transgene fragment that is from the first to the second Nsi 1 site (in the

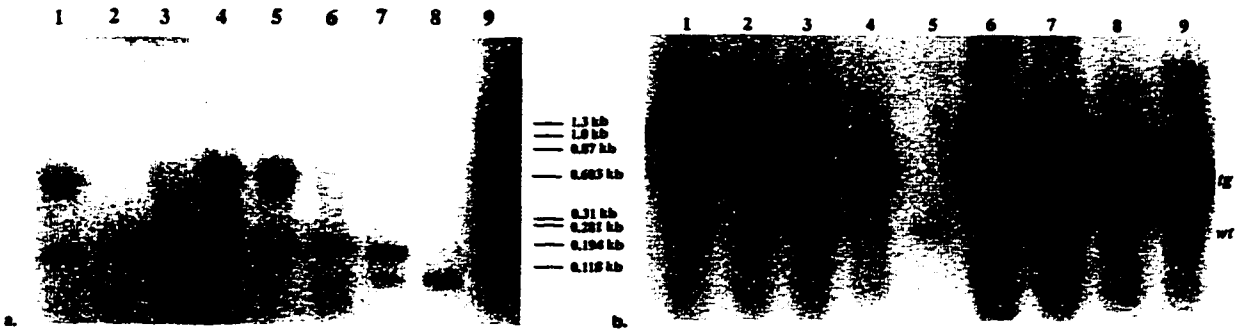

Figure 9. PCR (a) and Southern blot (b) determination of the genotype of a litter from tg parents. Panel A is an example of the a PCR screen of tail DNA from a f1 litter of 7 pups using primers DRP25 and AG037 (in this case, mice carrying the D4 tg). Lanes 1, 4, and 5 represent different tg pups (595 bp fragment). The smaller band is the internal control. Panel B is a Southern blot of Nsi 1 digested tail DNA from the pups of a f2 litter from D4 heterozygous parents. Mice represented in lanes 1-4, and 6-9 are tg, with the mouse represented in lane 5 is wild type. Mice in lanes 1, 4, 7, 8, and 9 are homozygous for the D4 transgene, and mice in lanes 2, 3, and 6 are heterozygous (quantitated using phosphoimaging analysis).

case of D4, a 4.5 kb band). The lowest band represents the endogenous *mbp* gene which yields a 2.3 kb band. The D2, and D5 transgenes yields a fragment of about 4.3 kb and 4.53 kb, respectively. In the Figure 9b, the second band is the 4.5 kb Nsi1 fragment corresponding to the D4 transgene DNA, and the bottom band corresponds to the 2.3 kb Nsi1 endogenous *mbp* gene fragment used as a control for loading. All phosphoimaging analysis was based on the ratio of tg/*mbp* DNA band labeling.

The transgenic lines to be used for the rescue experiments must have transgene RNA and protein levels high enough to provide adequate amounts to function in the myelin sheath. RNase protection assays were employed to determine the level of transgenic message. To efficiently compare RNA levels from sample to sample and between different experiments, the data was normalized to the signal obtained from the endogenous MBP mRNA, in the same reaction samples. I generated an anti-sense and sense radioactive transcripts for each transgene and hybridized them together to serve as a size marker for the experimental samples. These latter reactions employed only the antisense radioactive transcript of the cDNA minigenes to probe 1 μg of total brain RNA purified from a 1 month old transgenic mouse, and from a nontransgenic littermate, as a control. After hybridization of the probe and the brain RNA, the reactions were digested with RNases, purified and separated electrophoretically. The resulting bands represent either the transgene message or the endogenous *mbp* message, since each cDNA contains endogenous exonic sequence.

Since the size of the protected fragments will be the same size as the region of total hybridization, the entire 416 bp coding region of the D4 transgene is protected as well as a 327 bp fragment corresponding to the *mbp* mRNA protected fragment of exons one, three, and four, (the most abundant band with the D4 antisense probe, Fig. 10b). The same scheme was followed to quantitate the D2 and D5 transgenic message levels relative to *mbp* message (Fig. 10a, c). Phosphoimaging analysis of the protected bands provided a quantitative measure of the amount of transgene message relative to endogenous *mbp*

mRNA levels. All three lines of D2 express the transgene very abundantly and at similar levels (Fig.10a). Quantitative analysis of these lines reveal a 10 fold higher expression of the D2 transgene compared to MBP. Line D4.4 and D4.7 are the highest expressing lines of the four D4 tg lines (Fig. 10b), with a 2 fold more tg mRNA compared to *mbp* mRNA. D5, encoding the natural 14 kDa form of MBP had the lowest amount of tg message in all three lines tested (Fig. 10c, d). The line with the highest level of expression accumulated tg mRNA equal, in amount, to the *mbp* mRNA, and the poorest expressing line accumulated only 50% of that level.

Figure 11 is a semi-quantitative Northern blot analysis of the six transgenic lines of the D2 and D4 genes using two oligonucleotide probes, specific for tg mRNA, the other specific for the endogenous *mbp* mRNA. The probes were of the same length and same G/C content and were labeled to the same specific activity. These results not only quantitatively verified the data in Figure 10, but allowed for the comparison of the levels of tg message between the different lines. RNA loading was normalized to *mbp* mRNA. Again, the D2 message level, of all three lines, is far more abundant that the tg message levels in the other tg mice. The amount of overexpression of the transgenes here agreed with the transgene levels determined by the RNase protection assays (Fig.10a). Kimura et al. was able to rescue the shiverer mutant with a transgene that was expressed at only 3% of the endogenous *mbp* level (8). Readhead observed compact myelin in the CNS of mice expressing the tg at only 1-2% the level of endogenous MBP (21). Thus, it appears that there is sufficient amounts of tg mRNA in the highest expressing lines of the three transgenes to putatively rescue the shiverer mutant.

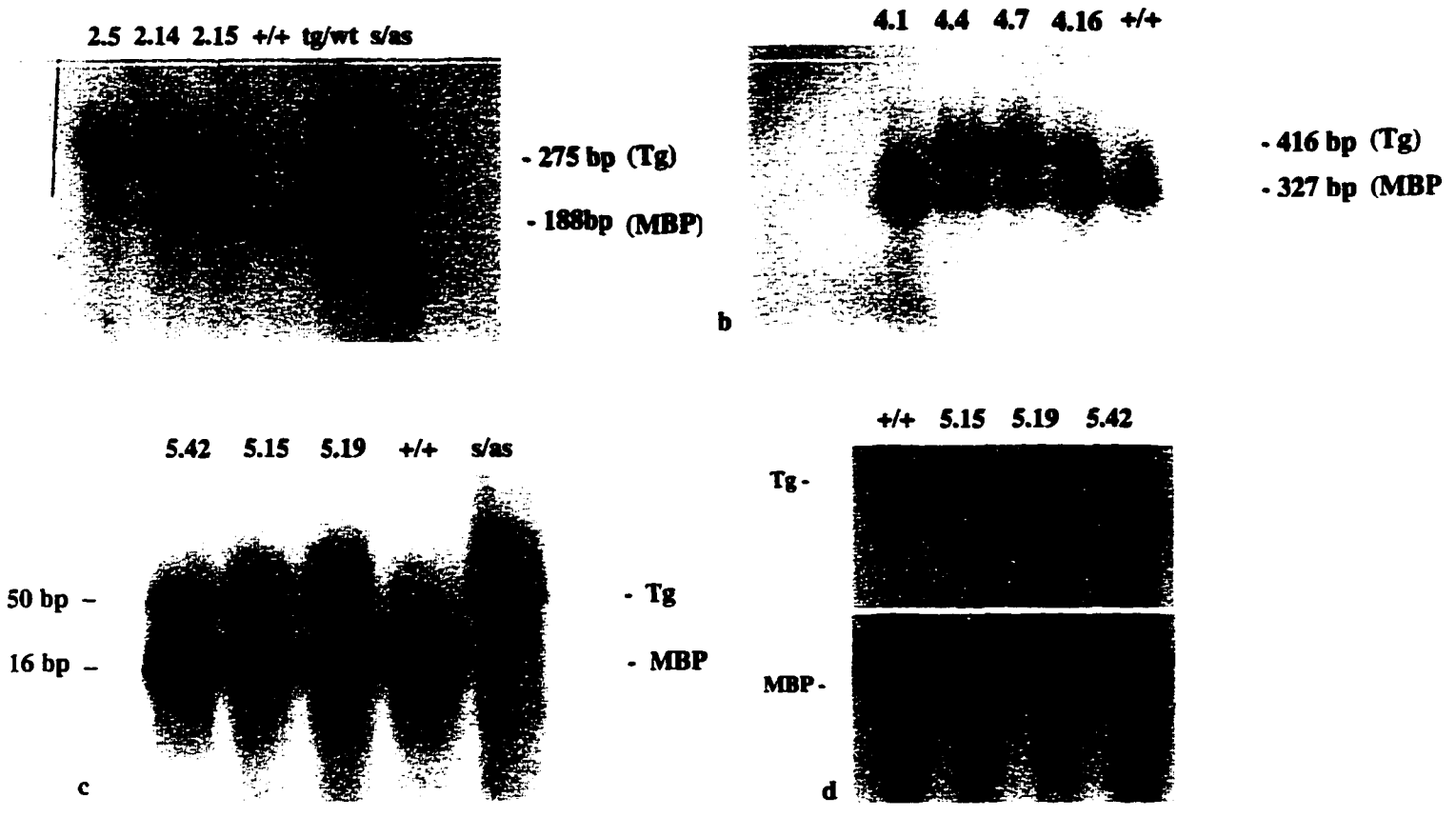

Fig. 10 RNase protection assay on equivalent amount of RNA from one month old mice from the three lines of D2 tg/wt (a) or D4 tg/wt mice. RNA from a wild type littermate (+/+). Equal amounts of wt RNA was mixed with tg RNA to be assayed separately to determine if the reduction in wild type signal is a function of down regulation by the transgene (lane tg/wt). Sense probe and antisense probe were hybridized together and digested with the RNases to serve a size marker for the protected tg message (a/s). Panels c and d are RNase protection and Northern assay (respectively) of the D5 tg/wt lines.

Though it seems transgene expression is quite high, these experiments do not reveal any information of the amount of tg protein in the CNS. To investigate the expression at the level of the protein, I performed Western blot analysis. In Figure 12, the proteins of myelin and brain extracts from the different transgenic lines were separated by SDS-PAGE, transferred and immobilized to a polyvinylidene fluoride (PVDF) microporous membrane. Immuno-blotting, using the same antibodies that were used in the immunostaining of the transfected cells to probe the membrane, recognized both the endogenous MBP and the

tagged miniMBPs. I used an alkaline phosphotase conjugated secondary antibody against the specific primary antibodies. Traditional NBT/BCIP reagents or an enzymatic

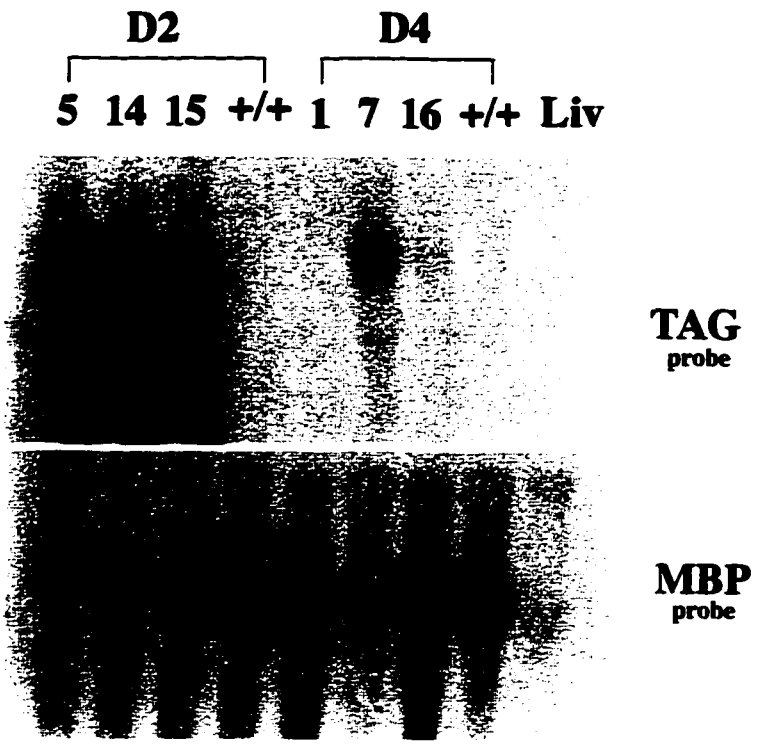

Figure 11. Semi-quantitative Northern Blot analysis of transgenic lines with the D2 and D4 transgenes. Equal amount of RNA was used in each lane and probed with either a TAG specific oligonucleotide or a MBP specific oligonucleotide.

chemiluminescence (ECL) assay system (Amersham) was used to generate bands for the transgenic proteins which then could be relatively quantitated against endogenous MBP (see Chapter 4. Material and Methods).

D2's predicted size is 9.4 kDa, which is significantly smaller than the smallest, endogenous isoform of MBP (14 kDa), thus, the transgenic band migrates at a different position by SDS-PAGE. Using the MBP antibody, I was able to quantitate the amount of D2 protein relative to MBP by Western blot analysis and subsequent illumination of the proteins (Fig. 12a). Using to tag antibody, I was able to quantitate the level of D2 protein

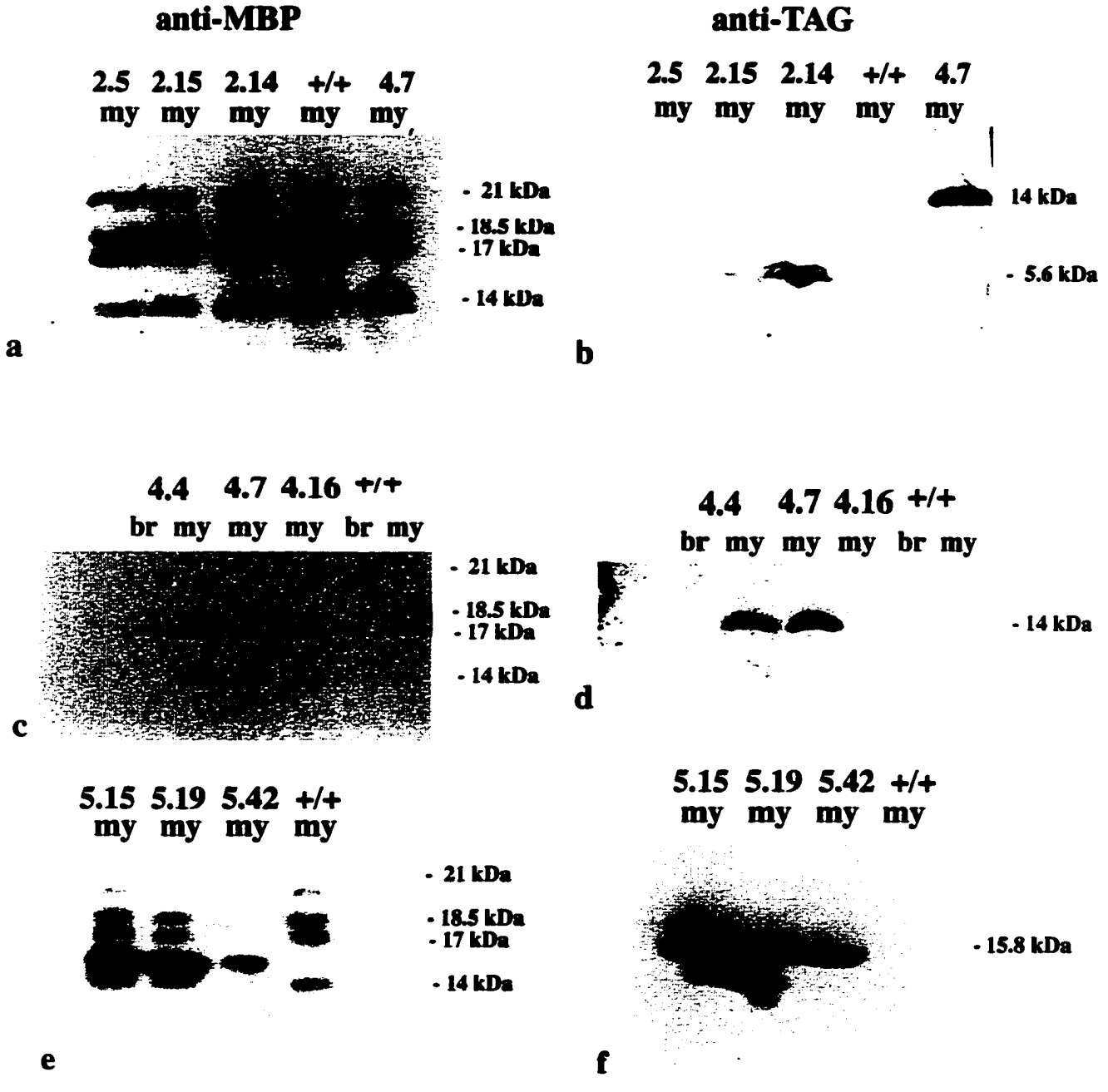

Fig. 12 Western blot analysis of brain and myelin extracts from all three D2 tg/wt lines (panels a-b) or three of the D4 tg/wt lines (panels c-d). Equal amounts of protein were loaded in a and b; c and d; and analyzed by SDS-PAGE. Membranes were either blotted with the MBP antibody (a, c and e) or the tag antibody (b, d and f). Proteins were illuminated with either alkaline phosphotase/BCIP-NBT (a-d) or an enzymatic chemiluminescence (e, f) reaction assays.

between the different D2 tg mouse lines (Fig. 12b). Although all three mouse lines had similar levels of transgene specific message, line D2.14 (Fig. 12a, b) had the highest level

of myelin enriched protein, (10% of endogenous MBP) of the D2. Consistent with the mRNA data, Western blots of the 4 D4 lines (Fig. 12c, d) revealed D4.4 and D4.7 as the higher protein expressing lines, producing 25% of the net MBP level. Like the D2 protein, the D5 protein migrates at a different place than endogenous MBP using SDS-PAGE analysis (molecular weight of D5 is 15.8 kDa). Semiquantitative western blot analysis of the three D5 tg/wt mouse lines showed that the D5.19 line had the highest level of expression of tg protein, exceeding the relative level of its mRNA (Fig. 12e, f). The D5.19 transgenic protein is expressed 5 fold over the amount of endogenous MBP. The other two D5 tg/wt mouse lines (D5.15 and D5.42) also expressed higher levels of the transgenic protein relative to endogenous MBP.

Interestingly, one representative line from each transgene (D2.5, D4.7 and D5.19) developed a pathology in the CNS. Except for D2.5, these lines expressed the respective transgene at the highest level relative to the other transgenic mouse lines. The pathology will be described later in Chapter 7, however, it should be noted here that the D2.5 tg/wt mice displayed a more severe pathological phenotype, dying around postnatal day 25, earlier than the D4.7 or D5.19 mouse lines that also developed a similar myelin pathology. Western blot analysis detected very little D2 protein at the time of death (Fig. 12) or earlier, so documentation of protein overexpression in this tg mouse line could not be verified.

D. Localization of the miniMBPs in mouse CNS

Initial expression experiments in cell culture verified that the encoded proteins are translated properly, and the anti-tag monoclonal antibody recognizes the epitope at the COOH- terminal of each protein. The 14 kDa MBP-tag protein (D5) localizes in the oligodendrocyte's cell body, processes, and in the myelin sheath both on a wild type background (tg/wt) and in the shiverer mice (tg/shi), as predicted from published data (Fig. 20, ref. 8), which served as an appropriate control for the tag epitope.

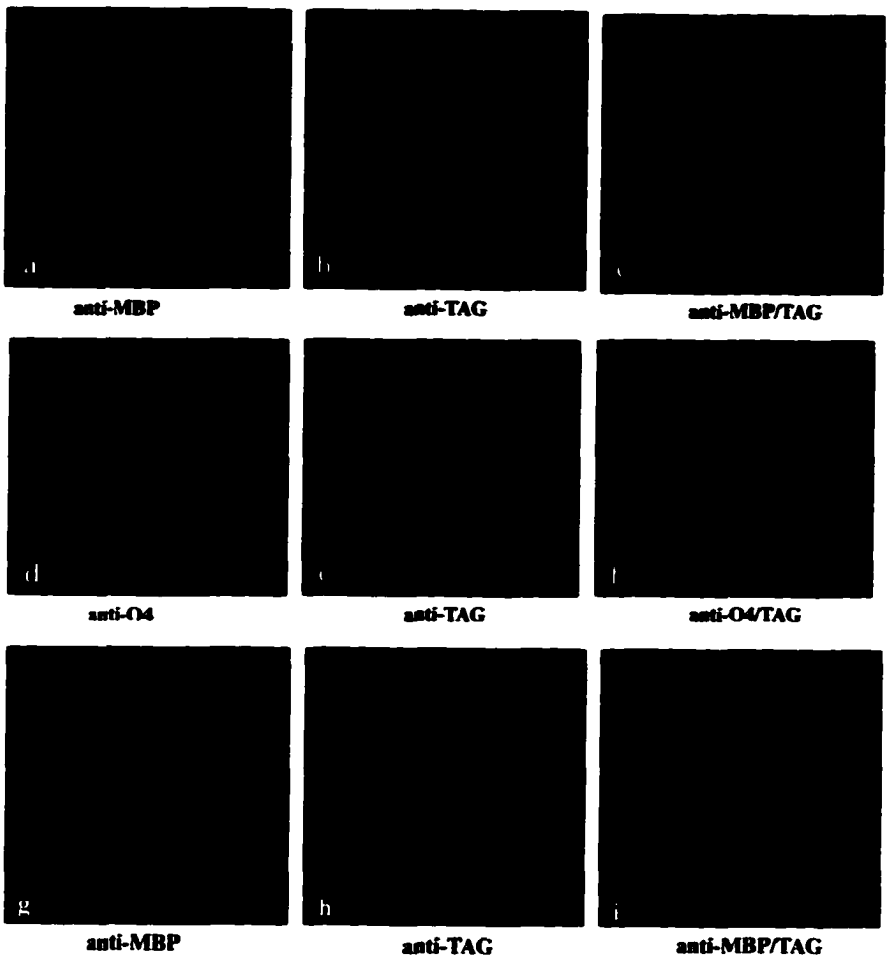

Figure 13 Confocal images of serial cryostat sections from D2 tg/wt spinal cord are panels a-c, oligodendrocyte in d-f and striatum in g-i (at lower magnification). Staining with the MBP antibody (green) is shown in panels a, d and g: with the tag antibody (red) is shown in panels b, e and h; and superimposition of the green and red images, respectively is shown in panels c, f and i.

Cryostat sections from a one month old D2 transgenic mice were stained with both MBP or O4 (a marker for oligodendrocytes) antibodies and tag antibodies to show the localization of the D2 protein relative to MBP in different CNS regions. The D2 protein was observed throughout the CNS in every observed oligodendrocyte that was labeled with the MBP antibody. High magnification confocal images of a cross section area of the spinal cord (Fig. 13, a-c), an oligodendrocyte (Fig. 13, d-f), and lower magnification images of caudate putamen (Fig. 13, g-i) shows the distribution of the D2 protein (Fig. 13b, e, h), MBP (Fig. 13 a, g) and O4 (Fig. 13d). The juxtaposition of these proteins is demonstrated by superimposing two images of the same field (Fig. 13c, f, i). The low magnification confocal images of the caudate putamen from the same animal illustrates the wide distribution of the transgenic protein (Fig. 13h) relative to MBP (Fig. 13g) and the

close association of both proteins (Fig. 13i). It is clear that the D2 protein is not only abundantly present in the cell body and processes of the oligodendrocytes, but is found with MBP in the myelin sheaths (Fig. 13c, f, and i). It is interesting though, that the juxtaposition of MBP and the D2 protein is seen in only a fraction of the axons of the spinal cord. It appears that the D2 protein is only found in the myelin around axons that have a smaller to medium size caliber.

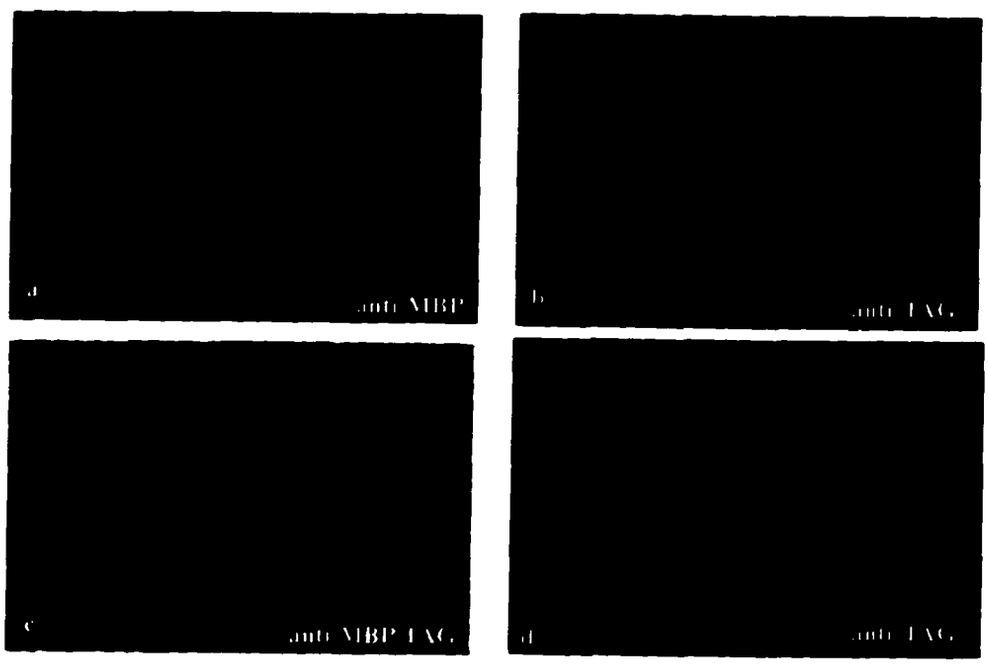

Figure 14 Confocal images of serial cryostat sections from D4 tg/wt spinal cord panels a-c, oligodendrocyte in d. Staining with the tag antibody (green) is shown in panels a; with the MBP antibody (red) is shown in panels b; and superimposition of the green and red images, respectively is shown in panels c.

Figure 14 panels a-d are confocal images of the spinal cord from a one month old D4 transgenic mouse similarly immunostained as in Fig. 13. Like D2, D4 is found in great abundance throughout the CNS of the tg animals specifically in oligodendrocyte cell bodies, processes, and around axons in the vicinity of myelin sheaths. However, different from finding D2 in the myelin around small-medium caliber axons, D4 consistently is present in the myelin sheath, with MBP, around all sized diametered axons. In panel c, the myelin sheath around every axon stains yellow, which the result of superimposing the

tagged epitope red image (panel b) with anti-MBP green image (panel a). This suggests a close juxtaposition of the two proteins.

F. Summary

It seems for all three miniMBP transgenes, there are mouse lines that express the transgenes at the appropriate levels and the encoded polypeptides are targeted to the myelin sheath. Lines D2.14, D4.4 and D5.15 express the transgenes (when heterozygous for the tg) at levels far above the level of the other expressed transgenes that successfully rescued the shiverer phenotype (8, 21), and do not result in myelin pathology, and so were chosen to be used in the shiverer backdoors experiments. In the next chapter, I discuss the behavior of these proteins in the absence of endogenous MBP, and show that one of the smaller MBP proteins can, in fact, function in myelin compaction.

CHAPTER 6: *SHIVERER MUTANT RESCUE: WHAT PART OF MBP IS NECESSARY FOR MYELIN COMPACTION?*

A. Crossing the transgenes onto the shiverer background

If the smallest isoform of MBP is sufficient to function in compaction in lieu of the complement of the other isoforms, then perhaps even a smaller, unnatural form of MBP would suffice. I have demonstrated, in Chapter 5, that several of my transgenic mouse lines have RNA and proteins levels that are comparable to the levels reported in the previous rescue experiments (8, 21). Thus, mouse lines D2.14, D4.4, and D5.15 were chosen to be crossed with shiverer mice.

Litters from shi/shi x tg/- mice were screened to determine which progeny pups carried both the transgene and the shiverer mutation. Figure 16 is a pedigree chart of a backcross of a D4 heterozygous transgenic mouse to a shiverer mouse and the successive interbreeding of the f1 generation. The backcross eventually incorporates the particular tg into the shiverer genome, and consequently is expressed on a MBP null background. The D2 and D5 transgenes were genetically crossed to the shiverer background in the same manner.

For the purpose of screening, I developed different sets of primers for PCR that will strategically identify the pups that have the specific alleles of interest (see Material and Methods). For the *mbp* locus, I developed primers that could distinguish the wild type MBP allele from the mutant allele since the deletions sites of the shiverer mutation were cloned and the flanking regions sequenced (Fig. 15, ref. 77). To screen for the transgene, I used the set of primers that were described in Chapter 5 and shown in Figure 5.

An example of the PCR products obtained from progeny tail DNA from a litter of pups from an f1 generation mating (Fig. 15) between mice heterozygous for both the D4 tg and the *shi* mutation is shown in Figure 16. In Figure 15, D4.4 pups numbered 1,4, 5, 7 and 8 are tg for D4, and pups D4.4.1, 3, 7, and 8 are shiverer (shi), thus pups D4.4.1, 7,

and 8 are transgenic/shiverer (tg/shi). Southern blot and phosphoimage analyses of DNA from these mice were done to determine the zygosity of the transgene.

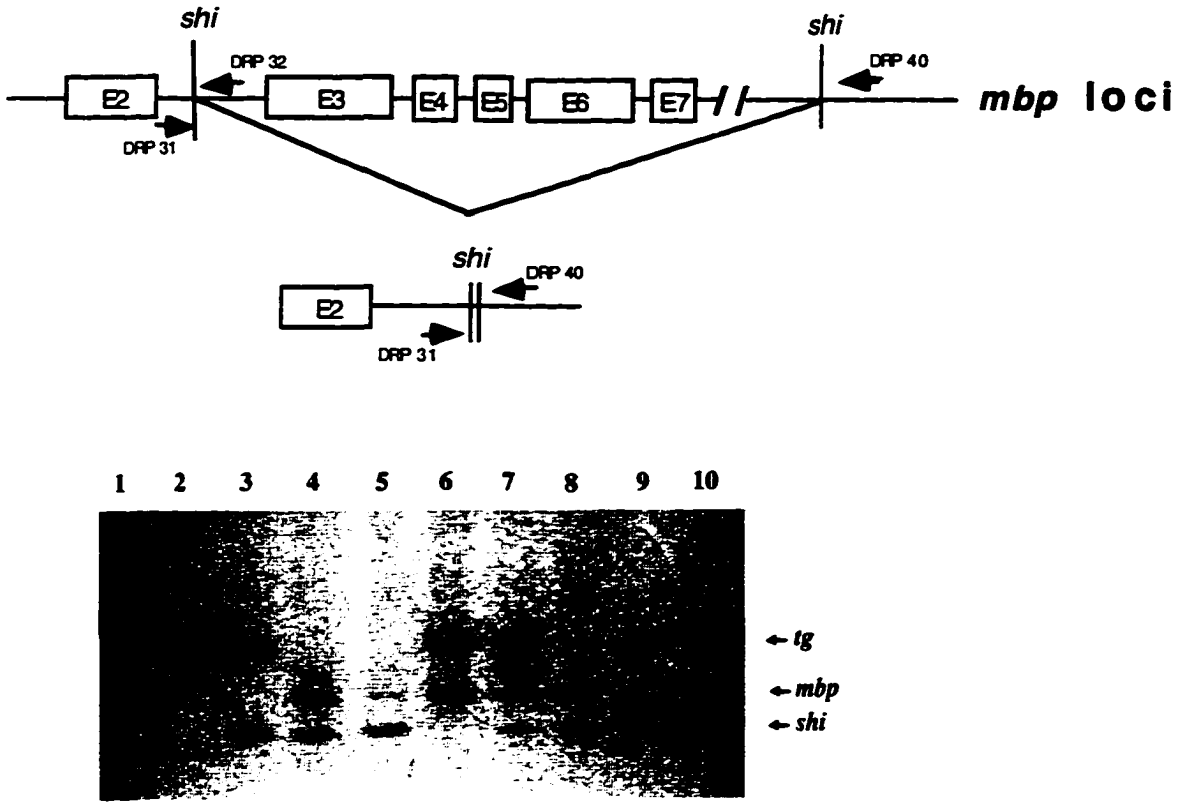

Figure 15. The top panel is a schematic of the partial *mbp* locus in chromosome 18 of mice. This cartoon depicts the gene from exon 2 (E2) including the rest of the exons (E3-E7) and the relative position of the shiverer deletion points (*shi*). Arrowheads show the position of the primers used in the PCR screen for the *mbp* and shiverer alleles (top and bottom cartoons, respectively). Primer set, DRP31 and DRP40 were used to amplify a fragment spanning the breakpoint in the shiverer allele, and primer set DRP31 and DRP32 were used to amplify fragment specific for the wild type *mbp* allele. The bottom panel is a PCR of tail DNA from a litter of D4 tg/shi mice using different combinations of primers to screen for the different alleles from the *mbp* locus , and the tg allele. Lane 1 is phiX174 markers (NEB), the sizes of each band are listed in Figure 8. Lane 2 is D4 plasmid DNA used as a control in this experiment. The genotypes (tg allele is listed first with the mbp locus listed second) in lanes 3-10 are as follows: 3 is tg/shi/shi; 4 is wt/shi/+; 5 is wt/shi/+; 6 is tg/wt; 7 is tg/shi/+; 8 is wt/shi/+; 9 is tg/shi/shi; 10 is tg/shi/shi.

B. Analyses of gene expression in the absence of endogenous MBP

It has been observed previously, that *plp* gene expression is reduced by 50% in oligodendrocytes of shiverer mice (12) suggesting the presence of a feedback loop that regulates the availability of myelin proteins. I wanted to determine if other genes have altered expression in the shiverer mice and if the presence of the transgenic proteins might influence any of them.

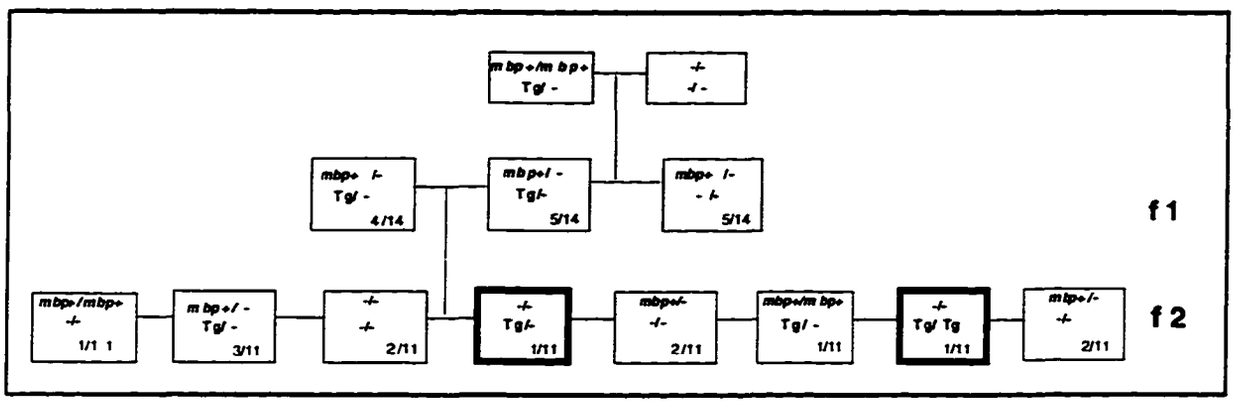

Figure 16. Family tree showing two generations of the D4 line after crossing with a shiverer mouse. A heterozygous transgenic male was used for the initial mating with a shiverer female. The f1 siblings that carry both the transgene and the *shi* allele were mated together to produce mice that were transgenic/shiverer (bold boxes in the f2 generation). The fraction in the boxes represent the number of mice out of the litter carrying that genotype.

First, I determined if transgene expression in the tg/*shi* mice changed in the absence of the endogenous MBP. Northern analyses was employed to determine the level of transgene expression in the absence of endogenous MBP (Fig. 17). Quantitative phosphoimaging revealed no change in transgene expression of D4, however there was a minor reduction in D2 expression in the absence of MBP. Figure 17b shows the message levels of PLP in the different transgenic lines, either in the presence (tg/wt) or absence (tg/*shi*) of endogenous MBP. GAPDH message was probed as a control for the amount of RNA in each lane. Phosphoimaging analysis consistently revealed approximately 1/2 the amount of PLP mRNA in two month old shiverer mice compared to their wild type littermates, consistent with previous data (12). In the D2 transgenic line, PLP mRNA followed the same pattern between tg/*shi* compared to tg/wt littermates, however, in the

case of D4, there was no change in PLP gene expression, possibly revealing a difference between the two transgenes.

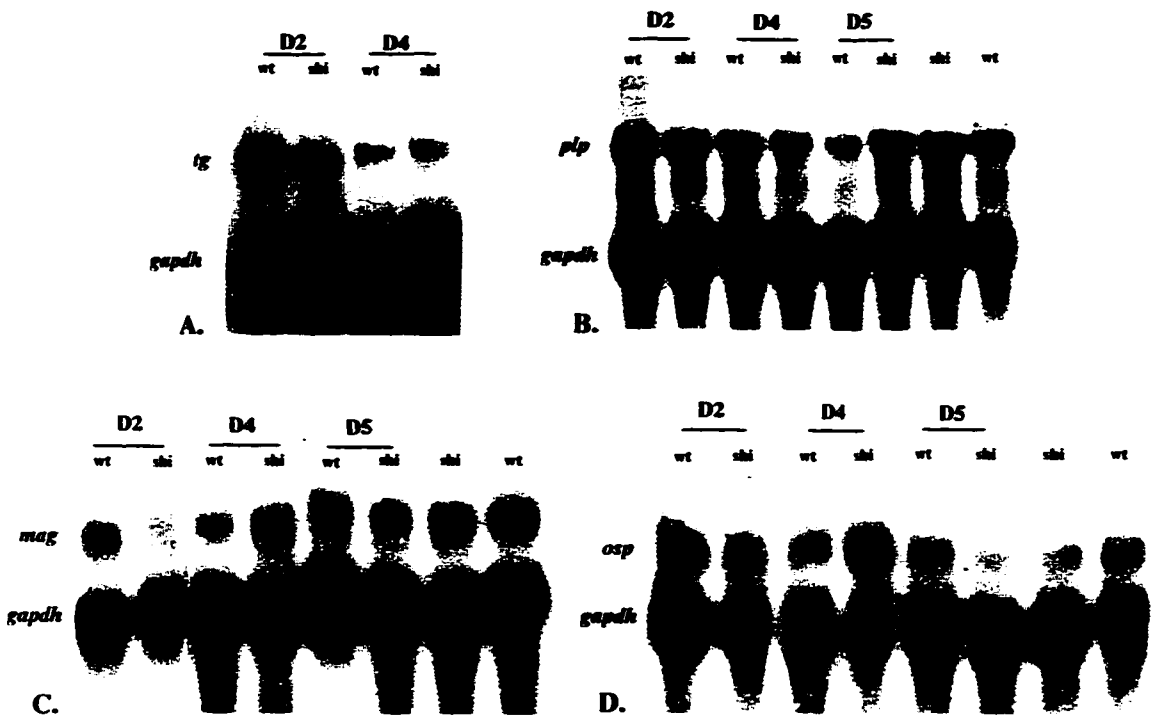

Figure 17. Northern analysis of tg expression (a) and other myelin genes (*plp*, b, *mag*, c, and *osp*, d) in the presence (wt) and absence (shi) of endogenous MBP.

Other oligodendrocyte genes were assayed for their expression in the tg/wt or tg/*shi* lines of mice. MAG and OSP expression were only minorly affected in the D4 tg/*shi* mice versus the D2 tg/*shi*, mice which seemed to be the case for their expression in shiverer mice (Fig. 17c, d).

C. Localization of transgene products in the absence of endogenous MBP

In Chapter 5, it was demonstrated that D2 and D4 proteins (Figs. 12 and 13) localize to the oligodendrocyte cell body and processes, but more importantly, to the myelin sheaths. Using double label immunocytochemical analysis of cryostat sections of brain and spinal cord, I determined that the localization of all of the transgenic proteins was unchanged by the presence or absence of endogenous MBP. Figures 18 and 19 shows the localization of the D2 and D4 proteins in the CNS of a tg/*shi* mouse, respectively. Confocal images were collected of double immunolabled cryostat sections of the striatum

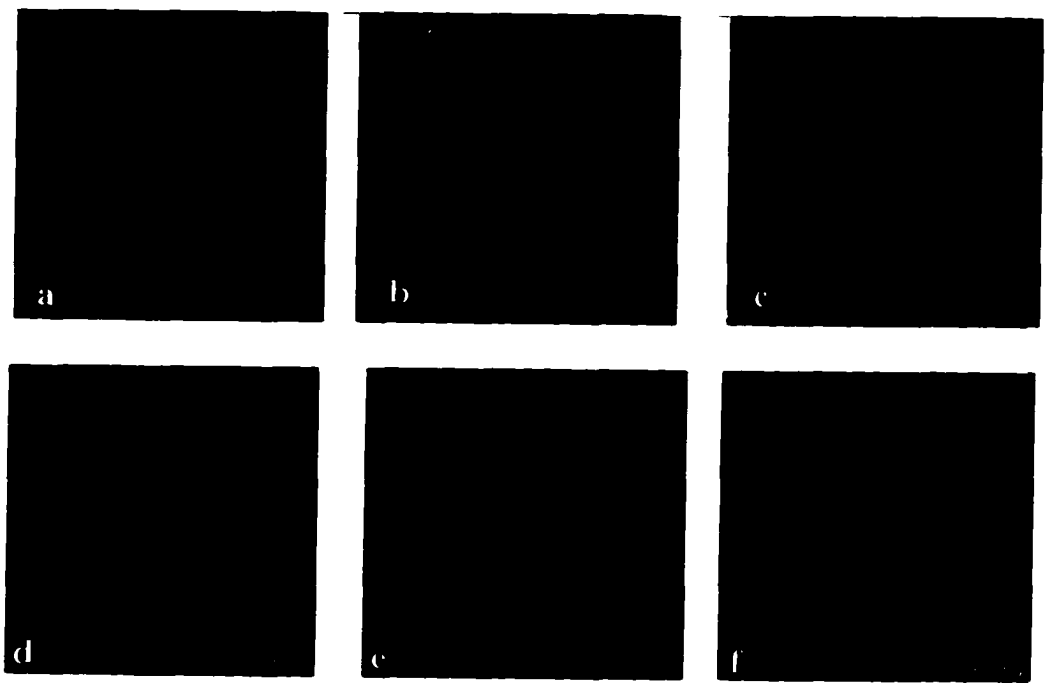

Figure. 18 Confocal images of serial cryostat sections from D2 tg/*shi* CNS are panels a-f Fluorescein (green) conjugated antibody staining PLP is shown in panels a, d; rhodamine (red) conjugated antibody staining for the D2 antigen is shown in panels b, e; and superimposition of the green and red images showing the juxtaposition (yellow) of PLP and tagged D2 protein (panels c, f respectively).

and spinal cord using both, the tag antibody shown in Figure 18b, e and in Figure 19b, d, and the PLP antibody shown in Figure 18a, d and in Figure 19a. Figure 20 shows the localization of the D5 transgene in the shiverer CNS, demonstrating also, that the

localization of the tg protein is not affected by the absence of endogenous MBP isoforms. Since both miniMBPs localized to the myelin wrappings around the axons and expressed at appropriate levels, they both can potentially rescue the mutant phenotype.

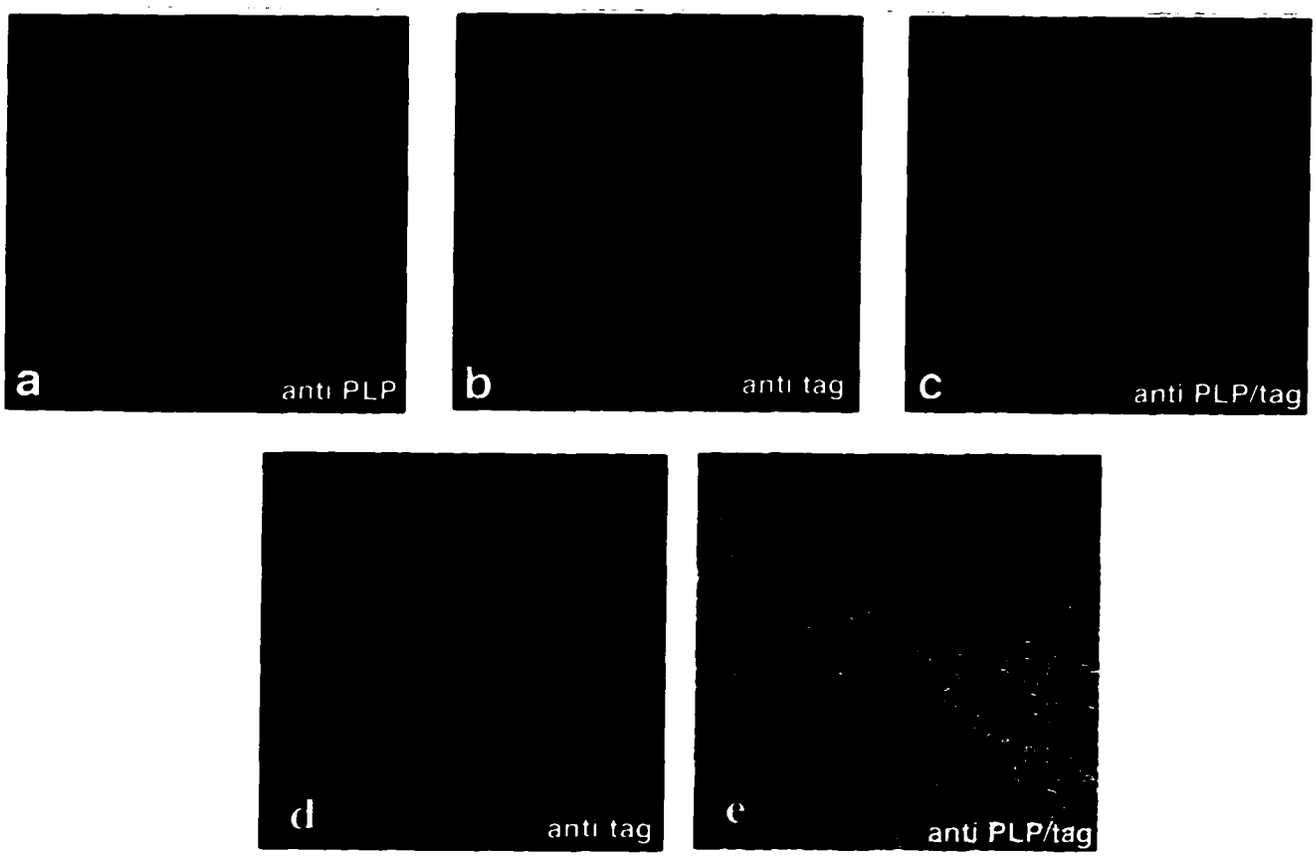

Figure. 19 Confocal images of serial cryostat sections from CNS of D4 tg/*shi* mice (a-e). Staining with the PLP antibody (green) is shown in panel a and with the tag antibody (red) is shown in panels b, d; and superimposition of the green and red images is shown in panels c, e respectively.

Histochemical experiments were carried out to determine if any of the transgene products are involved in myelination. To examine the state of the myelin sheaths in the tg/shi mice, samples from the spinal cords of these mice were examined with thin section electron microscopy (EM). In preparing the tissue for EM, 1μm sections were made and

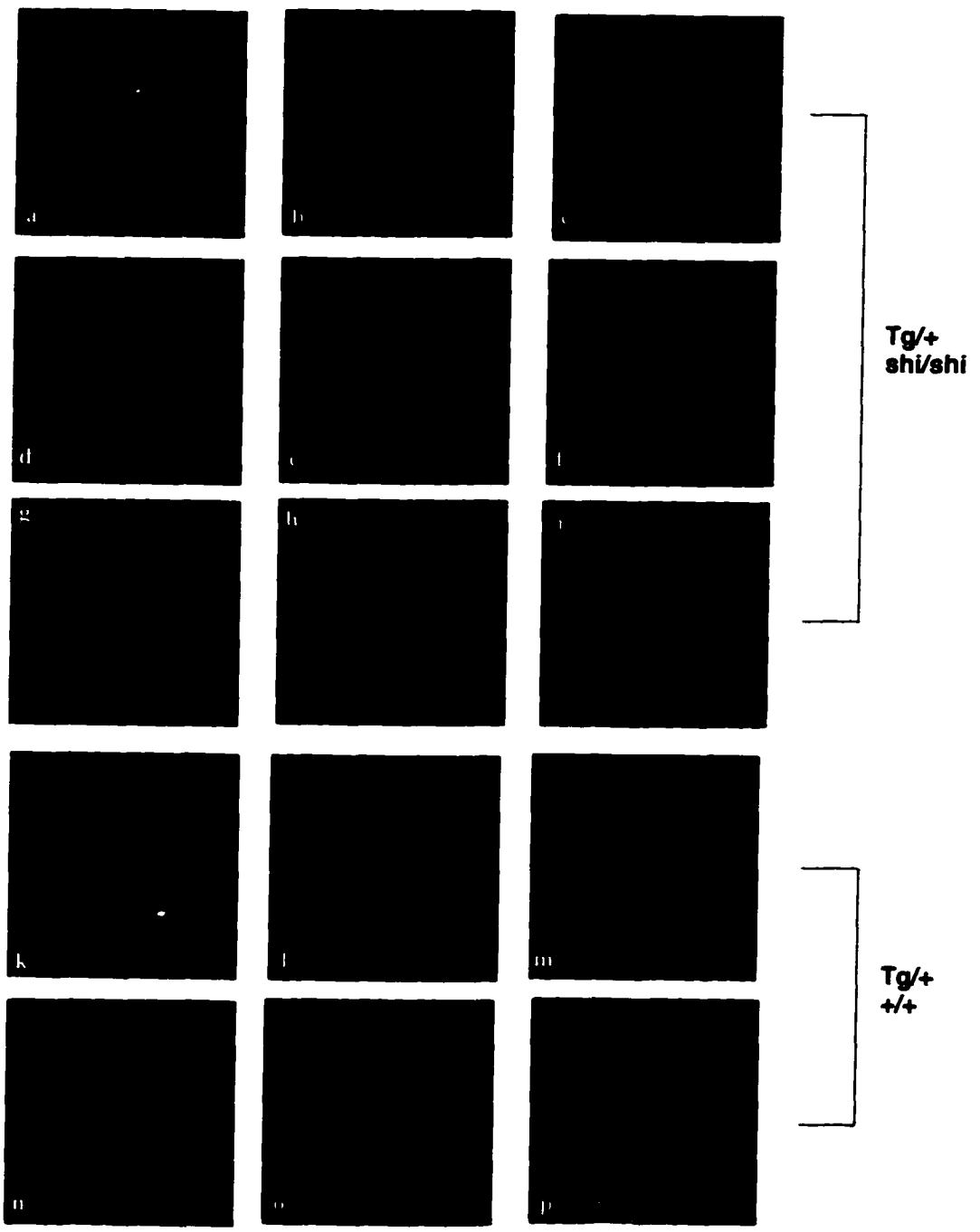

Fig. 20 Confocal images of serial cryostat sections from transgenic/shiverer mice. Staining with the PLP antibody (green) is shown in panels a, d, g, k and n, and with the tag antibody (red) is shown in panels b, e, h, l and o. The superimposed green and red images for each row is respectively, shown in panels c, f, i, m and p. Staining of the D5 tg/*shi* are panels a-in and tg/wt in panels k-p.

stained with Toluidine Blue to check the integrity of the tissue. Toluidine Blue (TB) readily stains myelin blue or purple and thus gives an overview of the amount of myelin in the field.

Figure 21 is TB stained spinal cord sections from two month old shiverer (*shi*), D4 tg/shi, and D2 tg/shi mice. In the spinal cord sample from a shi animal (Fig. 21a), one can appreciate the severe hypomyelination or lack of myelin. Most of the axons are naked with only a few thin myelin rings around some of the axons. In the D4 tg/shi, however, there is clearly more myelin (Fig. 21b). Although the spinal cord from this animal has many naked axons resembling the shiverer mouse, there are more axons myelinated with thicker sheaths. The D2 tg/shi (Fig. 21c), on the other hand, more closely resembles the mutant spinal cord (Fig. 21a). The sheaths that are present are very thin and only around the smaller diameter axons, reminiscent of the tag-stained spinal cord confocal images of the D2 tg/wt and tg/*shi*. (Figs 13 and 18). These observations are verified by low magnification (1.6K X) electron microscopy (Fig. 22). In this figure, it is evident that there are more myelinated axons in the D4 tg/shi spinal cord than in the D2 tg/shi spinal cord; however, the point of this dissertation is to determine if smaller MBP proteins can function in compaction of myelin. Although it is clear that the D4 tg/shi mice can produce thicker and more myelin-like sheaths, this magnification does not shed any light on the state of compaction.

Figure 23 is a set of high magnification electron micrographs (100K X) of the myelin produced in the D2 and D4 tg/shi mice compared to the semicompact myelin produced in shiverer mice (Fig. 23a). Clearly the myelin that is produced in the D4 tg/shi mouse (Fig. 23b) is compacting like the myelin in wt mice (Fig. 2). The MDL forms in every wrap of the oligodendrocyte. In the myelin produced by the D2 tg/shi mice (Fig. 23c), the MDL is unable to form leaving cytoplasmic channels in the semicompact myelin.

In fact, the D2 tg/shi mice produces similar semicompact myelin that is seen in the nontransgenic shiverer mouse.

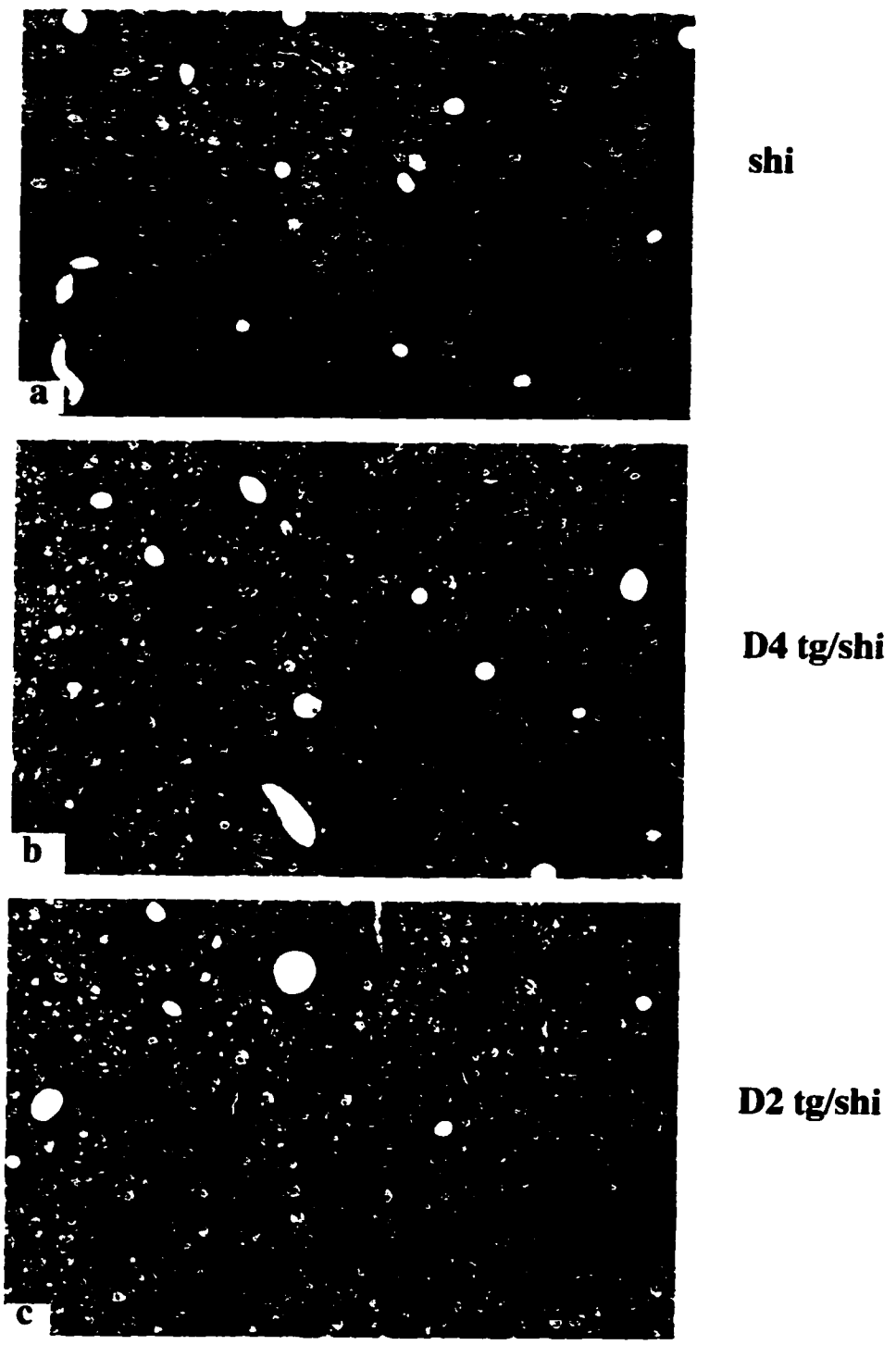

Figure 21. Toluidine Blue stained 1μm spinal cord sections from shi (a), D4 tg/shi (b) and D2 tg/shi (c) 2 month old mice, at approximately the same region in the lateral funiculus of the cervical spinal cord are shown in each panel.

Although immunoflourescence confocal images demonstrated that the D4 protein is found in the myelin sheaths in the tg/shi mice, immunoEM was done on the spinal cord samples to verify the localization of the D4 protein in the compact myelin (fig. 24). The concentration of gold particles over the compact myelin of these images provides strong evidence that the D4 miniMBP is functioning in the compaction of shiverer CNS myelin.

It is clear from the EM studies, that the D4 and not the D2 protein, functions in myelin compaction around axons in the shiverer CNS. Although the compact myelin in D4 tg/*shi* CNS looks like wt myelin (Fig 2, p.5), measurements of the lamellar spacing or myelin period is one parameter that tests how close to normal the D4 tg/*shi* oligodendrocytes can myelinate. In high magnification (100K X) micrographs (Fig. 25), I measured the interlamellar spacing the compact myelin in the D4 tg/shi mice and compared it to that measured in wild type mice of the same age. These results, summarized in Table 3, show no substantial difference in the lamellar spacing between D4 transgenic (10.6 nm) and wild type (10.3 nm; Table 3). The difference amounting to only 3% of the control value, was not significantly significant ($p = 0.1967$; unpaired t-test).

E. Summary

So, it appears that the D4 protein can function in place for the endogenous forms of MBP in the compaction of myelin. Not only is more myelin formed in the D4 tg/shi mice than in the shi or in the D2 tg/shi, but the sheaths are properly wrapping around axons multiple times (i.e. no redundant loops of myelin, Fig. 26), compacting and creating interlamellar spacing identical to that seen in wild type mice. Specializations such as radial components, which was discussed in Chapter 2 as another hallmark of wild type myelin, are also formed in the myelin in the D4 tg/shi mice (Figs. 23, 26). Thus, these experiments demonstrate that exons one, three, four and seven encode a form of MBP that facilitates normal compaction of myelin.

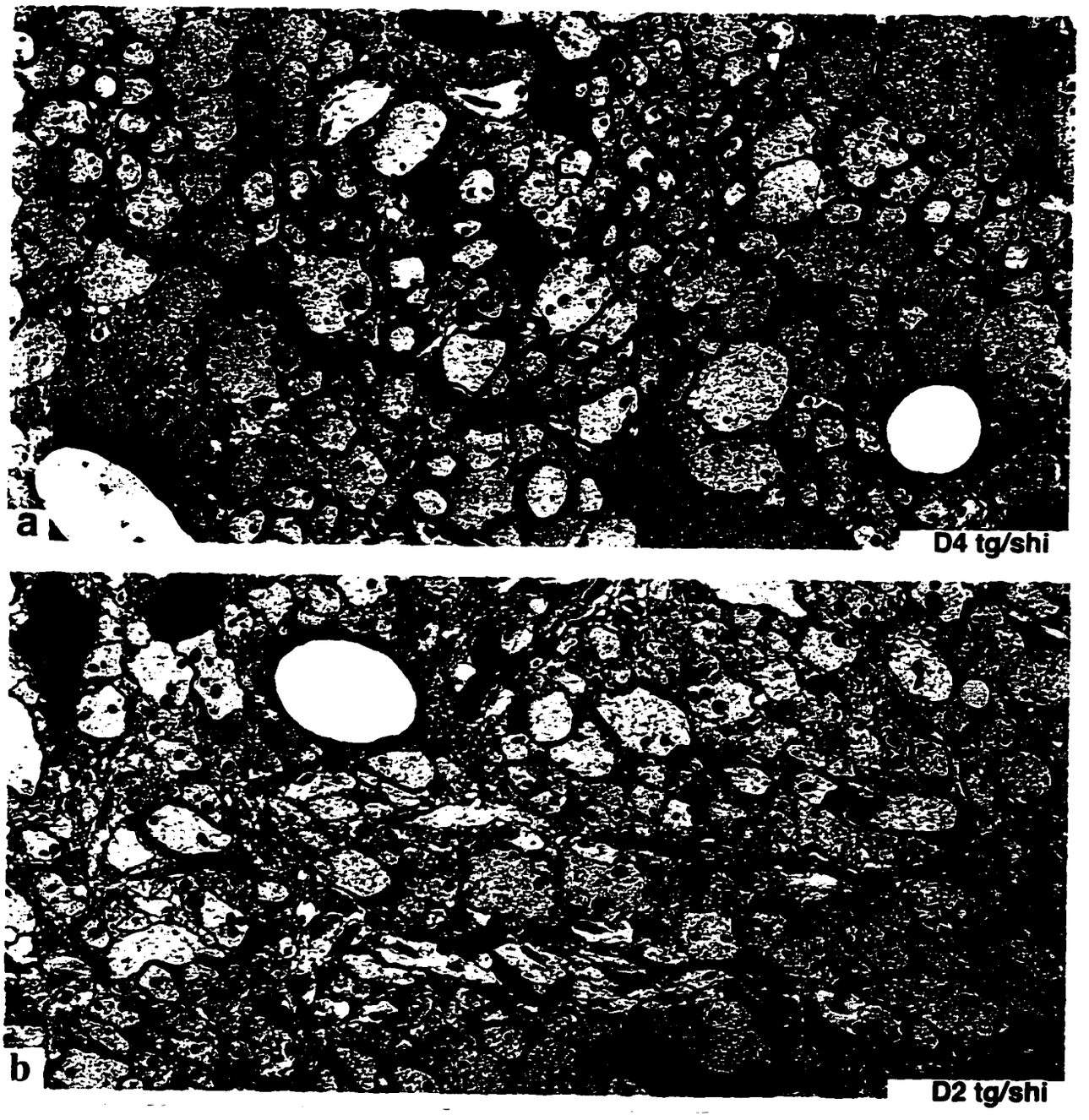

Figure 22. Low magnification (1.6K X) EM of thin sections from lateral funiculus of cervical spinal cord from 2 month old D4 tg/shi (a) and D2 tg/shi (b) mice. An example of a cross section view of an unmyelinated axon is seen at the arrow in the midst of many myelinated axons in a and other unmyelinated axons in b.

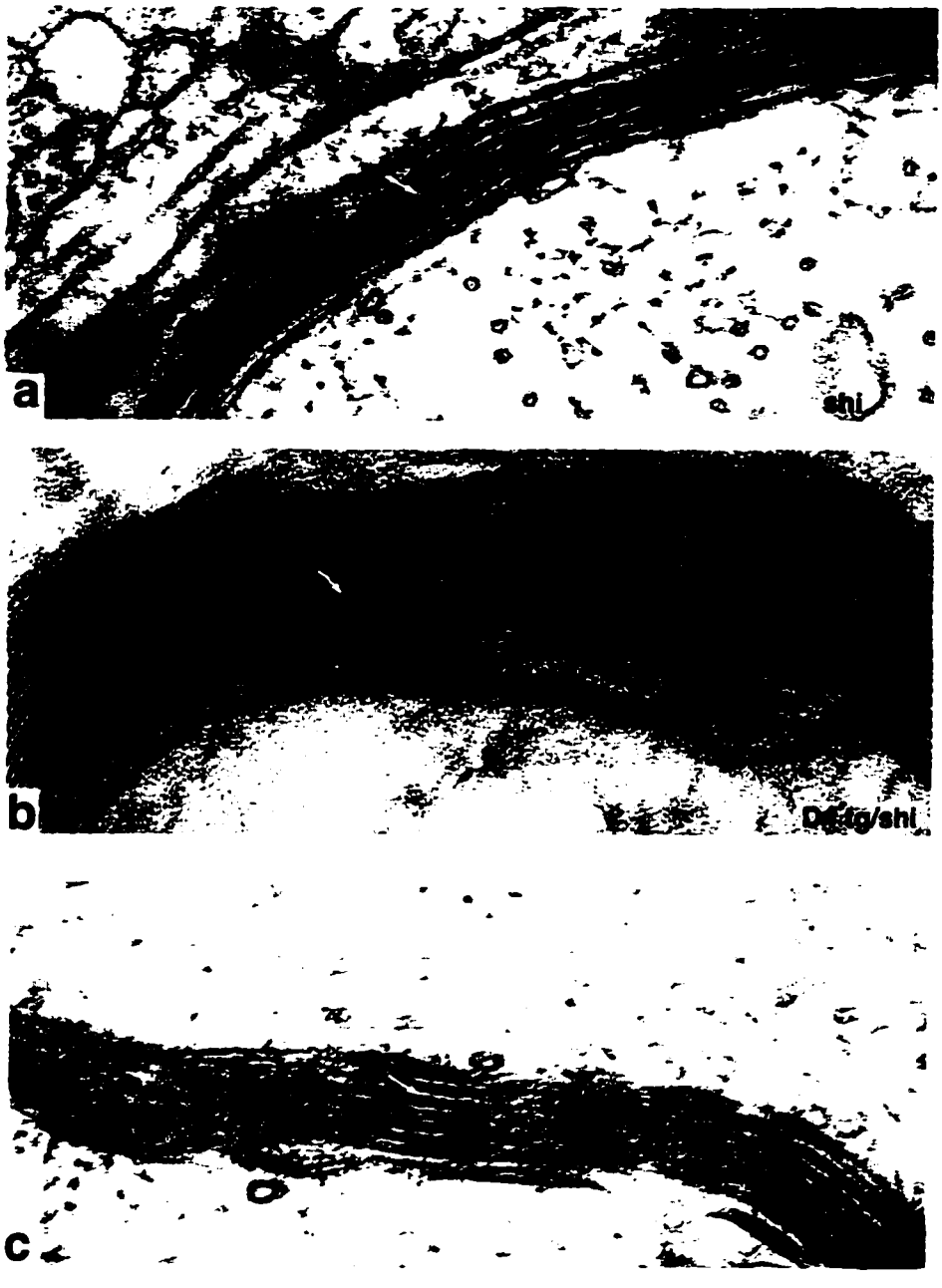

Figure 23. High magnification (100K X) electron micrographs of myelin sheaths from 2 month old shi (a), D4 tg/shi (b), and D2 tg/shi (c) mice. These are representative sheaths that were observed in the spinal cord (same regions as in Figure 22). Note the cytoplasmic channels in the sheaths from the shi and the D2 tg/shi mice (arrow) where the MDL should form, and the presence of the MDLs in the sheaths from the D4 tg/shi mouse (arrow).

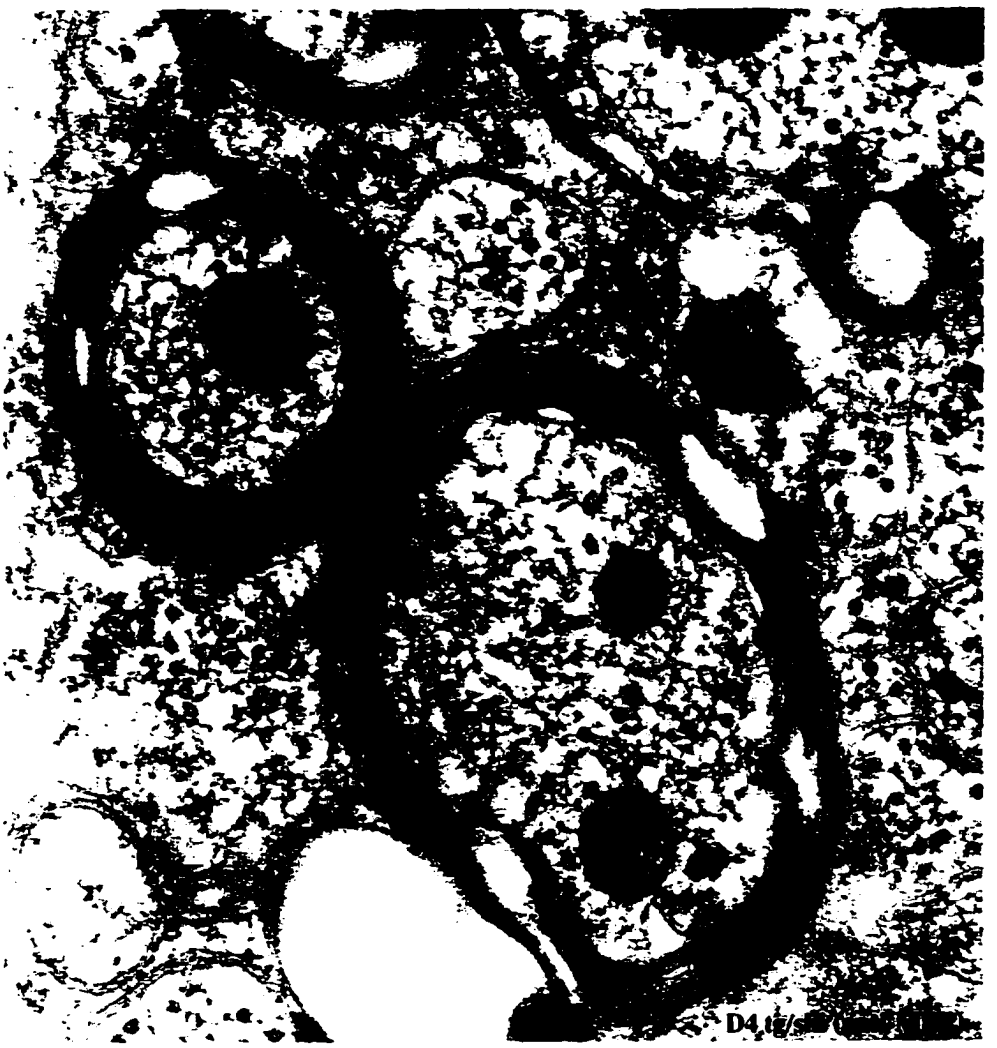

Figure 24. Immuno-electron micrograph of a myelin sheath from spinal cord of a two month old D4 tg/shi mouse. Tissue was label 12-nm gold particles conjugated to antibodies against the MBP antibody label the D4 protein in the compact myelin (arrows).

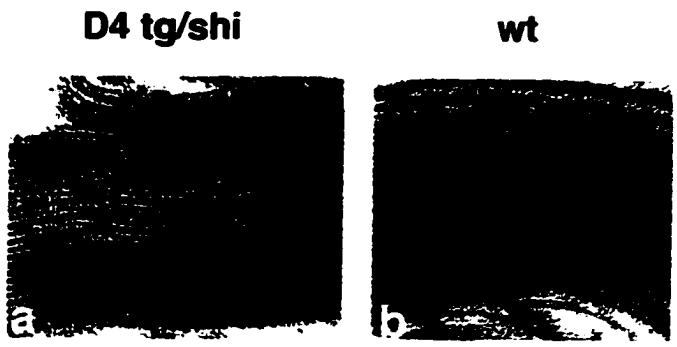

TABLE 3: MEASURE OF THE MYELIN PERIOD (D4 vs. wt)

gene	no. of prints meas.	no. of meas.	ρ (nm)	stdev.
D4	12	30	10.57	0.75
MBP	8	15	10.31	0.34

Figure 25. Representative compact myelin from D4 tg/shi (a) and wt (b) mice used to determine the periodicity (ρ). Table 5 is a summery of the measurements made that were used to determine the mean periodicity of the myelin. Mean periodicity from a number of measurements from original prints with negative magnification and print magnification considered ($p = 0.1967$; unpaired t-test).

Figure 26. Electron micrograph (50K X) of a myelinated axon of the cervical spinal cord from a 2 month old D4 tg/shi mouse. The axon was ensheathed and compacted properly by the oligodendrocyte process. This section shows a cytoplasmic channel and radial components (striations in the bottom right part of the myelin sheath), which are features of wild type myelin. Note the continuity of the properly compacted myelin around the entire circumference of the axon.

CHAPTER 7: *OVEREXPRESSION OF DIFFERENT DOMAINS OF MBP RESULTS IN DIFFERING PATHOLOGIES*

A. Background information

As the oligodendrocyte precursors differentiate, they express numerous genes at different stages of the maturation process. Until recently, the delicate regulation of these genes and the impact of the accumulation of the resulting protein products, had not been well studied. The results of independent investigations have shown that myelinogenesis can tolerate only a narrow window of myelin protein concentration. The overexpression of different myelin genes in the oligodendrocyte leads to a series of symptoms of myelin pathology and mostly premature death (52, 83, 84, 85). In this chapter I show that the overexpression of the different domains of MBP in the transgenic mice produced for this dissertation, also leads to a multiplicity of severe pathological symptoms and premature early death.

Two separate studies demonstrate that a tight control over the expression of the *plp* gene is necessary to ensure normal myelinogenesis (83, 84). Nave and coworkers demonstrated that 1.5 to 2.0 fold PLP overexpression in mice results in hypomyelination and astrocytosis of the CNS. Behaviorally, these mice initially display mild tremors that progress to tonic convulsion, seizures, ataxia and early death. Large axonal swellings were also observed in the demyelinated areas. The myelin deficit first appears in the dorsal column of the spinal cord at one month of age with affected areas having thinner (by 40 - 50%) myelin sheaths and a few naked axons particularly with larger diameter axons. Later, at two months of age, most of the axons of the ventral column and all of the axons of the dorsal column of the spinal cord were completely devoid of myelin. Compaction was not affected as the observed myelin contained major and minor dense lines. As the animal nears death, the number of both vacuolated sheaths and redundant myelin loops increased.

It was also reported that there was a two fold increase in the number of oligodendrocytes, they appeared morphologically normal (apart from the occasional swollen Golgi) (84).

Independently, Mikoshiba and colleagues reported similar findings when they, too, overexpressed the wild type *plp* gene in mice (83). They observed that the same range of PLP overexpression produced similar phenotypic behavior, including ataxia, intentional tremors, tonic convulsions and premature death at around 30 days postnatal (P30). However, unlike what was observed in Nave's experiments, oligodendrocytes appeared morphologically abnormal from the presence of vacuolar structures within the cell body and swollen Golgi, as early as P14, with a few thinner or denuded sheaths. The severity of the pathology increased with age and level of gene overexpression. For instance, by P20, the majority of the axons in the CNS of affected mice were either naked or ensheathed by proportionately thinner myelin. The CNS of affected mice were riddled with redundant loops and debris from myelin. Degenerating axons and vacuolization were also prevalent. Again , the compaction of myelin was not affected in the pathological mice (83).

Overexpression of DM-20, an isoform of PLP expressed proportionately higher in the developing CNS of mice, can also result in a demyelinating phenotype (85). Many of the symptoms reported in the PLP overexpressing mice, were also observed, in the DM-20 tg mice generated by Moscarello and coworkers. The time of onset for the pathology was much later than the PLP overexpressing mice. Moscarello observed tg mice with a 3-4 fold increase of the DM-20 message develop a "wobbling gait, with tremors and seizures" after 8-10 months of age. These mice displayed wide vacuolization throughout the CNS, redundant myelin sheaths, myelin debris, with regional thinning of the myelin sheaths, in this case, around axons of smaller diameter. Astrogliosis was also reported throughout the CNS by the abundance of GFAP positive stained cells. This group explained the lengthy time of onset of disease (8-10 months) by arguing that mice of this age had a "persistence of immature myelin " in the adult CNS. Different regions of the tg CNS appeared quite normal (e.g. the of presence thick, unaffected sheaths) at three months of age (85).

CNP, a nonstructural myelin protein and a marker for the initial myelinogenesis (86), also alters oligodendrocyte development producing a pathological phenotype when overexpressed transgenically (52). At P30, transgenic mice had 3 to 3.5 times higher CNP mRNA levels and 6.4 times higher CNPase activity than wild type mice. Although a behavioral phenotype was not immediately apparent, histochemical analysis and EM of 90 day old tg mice revealed many of the myelinating abnormalities observed in the PLP overexpressing mice, including a 30% reduction in the amount of myelin compared to wild type mice. The CNS of these mice contained many vacuoles that were surrounded by CNP and PLP positively stained membranes. These membranes were multilamellar and with occasional redundant myelin sheaths similar to the other overexpressing transgenic mice described above.

Strikingly, however, at higher magnification it was noted that the myelin membranes were not fully compacted, as indicated by the absence of the MDL. Unlike the tg mice overexpressing other myelin genes, these mice were unable to form wild-type like compact myelin. This was an unexpected finding since it is believed that CNP is not involved the compaction process, and it is not even localized to that particular myelin compartment (86).

Thus, the oligodendrocyte is a delicate cell and has a seemingly stringent criteria for the toleration of protein accumulation to function normally in myelination. In the present experiments, oligodendrocytes in the transgenic nonshiverer mice were exposed to higher than normal levels of particular domains of MBP. This is the first demonstration of CNS abnormalities arising from the overexpression of different domains of MBP.

Because each of the transgenes were initially expressed in wild type mice, I was able to follow the behavior of the mini-MBPs in the presence of the endogenous isoforms. Most of the tg mice expressed tg mRNA at very high levels (higher than *mbp* mRNA in most cases) and as a result one representative line for each tg induced a myelinating pathology in the founder lines that, for the most part, had the highest level of transgene

expression (lines: D2.5, D4.7, and D5.19). Although the time of disease onset differs for each for each of these lines, they displayed similar CNS abnormalities and behavioral phenotypes, reminiscent of the PLP overexpressing mice (83, 84). The MBP overexpressing mice display many of the same aspects of the diseased CNS observed previously (52, 83, 84, 85), but only a few of the symptoms were common to all. A few of these common CNS white matter abnormalities are described below.

B. Common myelin abnormalities associated with miniMBP overexpression

1. Hypomyelination

One of the unifying myelin abnormalities from the studies described above and the MBP overexpressing mice described in this thesis is a lowered amount of compact myelin or hypomyelination in the white matter of the CNS. Hypomyelination can be defined by the absence and/or thinning of the myelin sheaths and is not found under wild type conditions in the white matter of the CNS. As mentioned previously, shiverer mice also are hypomyelinated, in that most of the axons that would normally be myelinated are naked or surrounded by semicompact myelin.

One representative line from the D2 (D2.5) and D5 (D5.19) tg/wt mice are grossly hypomyelinated, whereas the D4 tg/wt line (D4.7) is myelinated normally. Naked axons and thinner sheaths are most obviously noticed in the cerebellum of TB stained sections and in low magnification electron micrographs of spinal cord (Fig. 27 and 28, respectively). In Figure 27, there is a noticeable difference in the amount of hypomyelination between the tg mice and wt, from normal myelination seen in the D4 tg/wt (Fig. 27c) to the most severe hypomyelination seen in the D5 tg/wt (Fig. 27 d and Fig. 28b). This difference is thought to be a direct result to the different levels of expression between the lines that showed a CNS pathology.

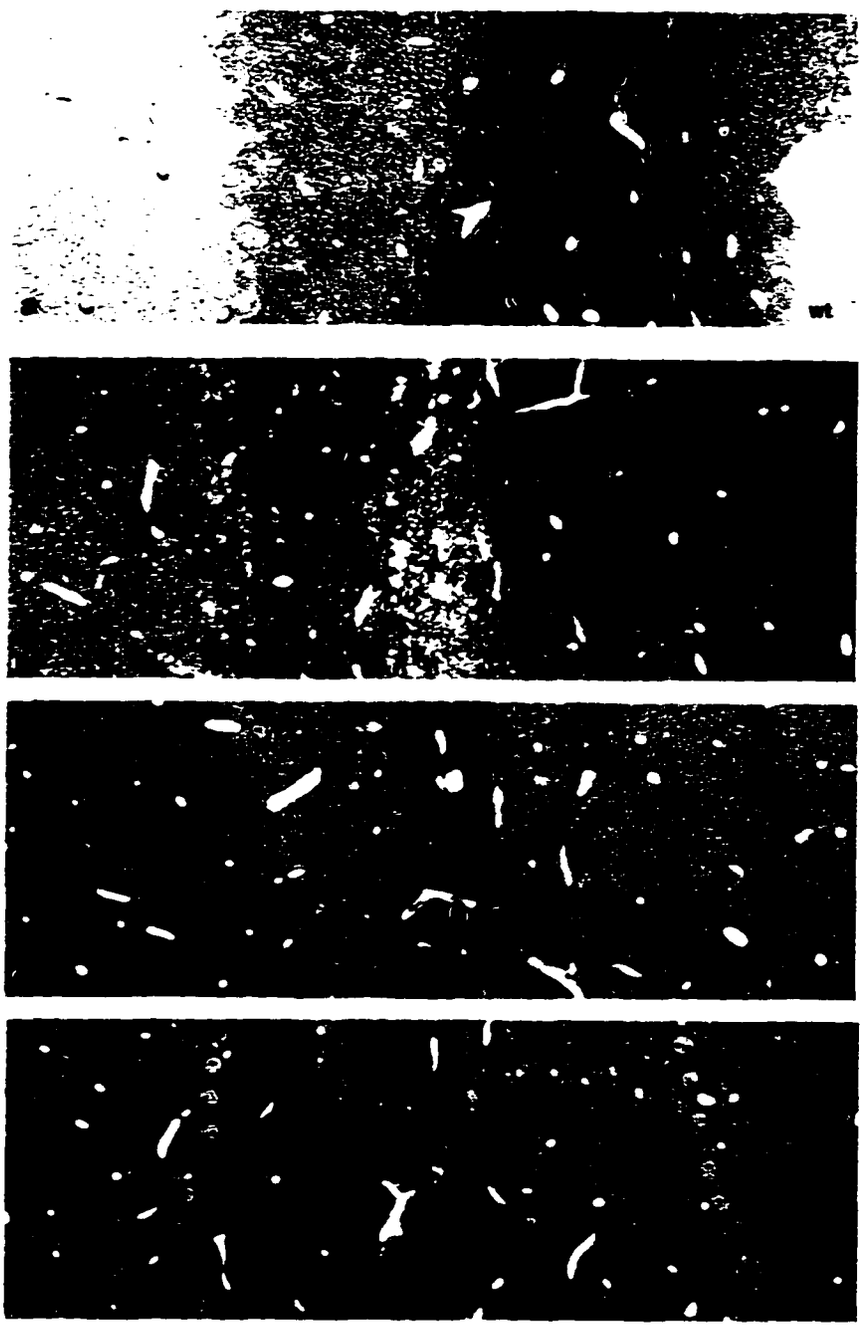

Figure 27, Sections of Toluidine Blue stained cerebellar cortex and white matter from P25 wt (a), P 25 D2 tg/wt (b), P60 D4 tg/wt (c) and P60 D5 tg/wt (d) mice. Note the lighter stained white matter tracts (less myelin) in the white matter of D2 tg/wt((b) and of D5 tg/wt (d), verses darkly stained myelin in wt (a) and in D4 tg/wt (c).

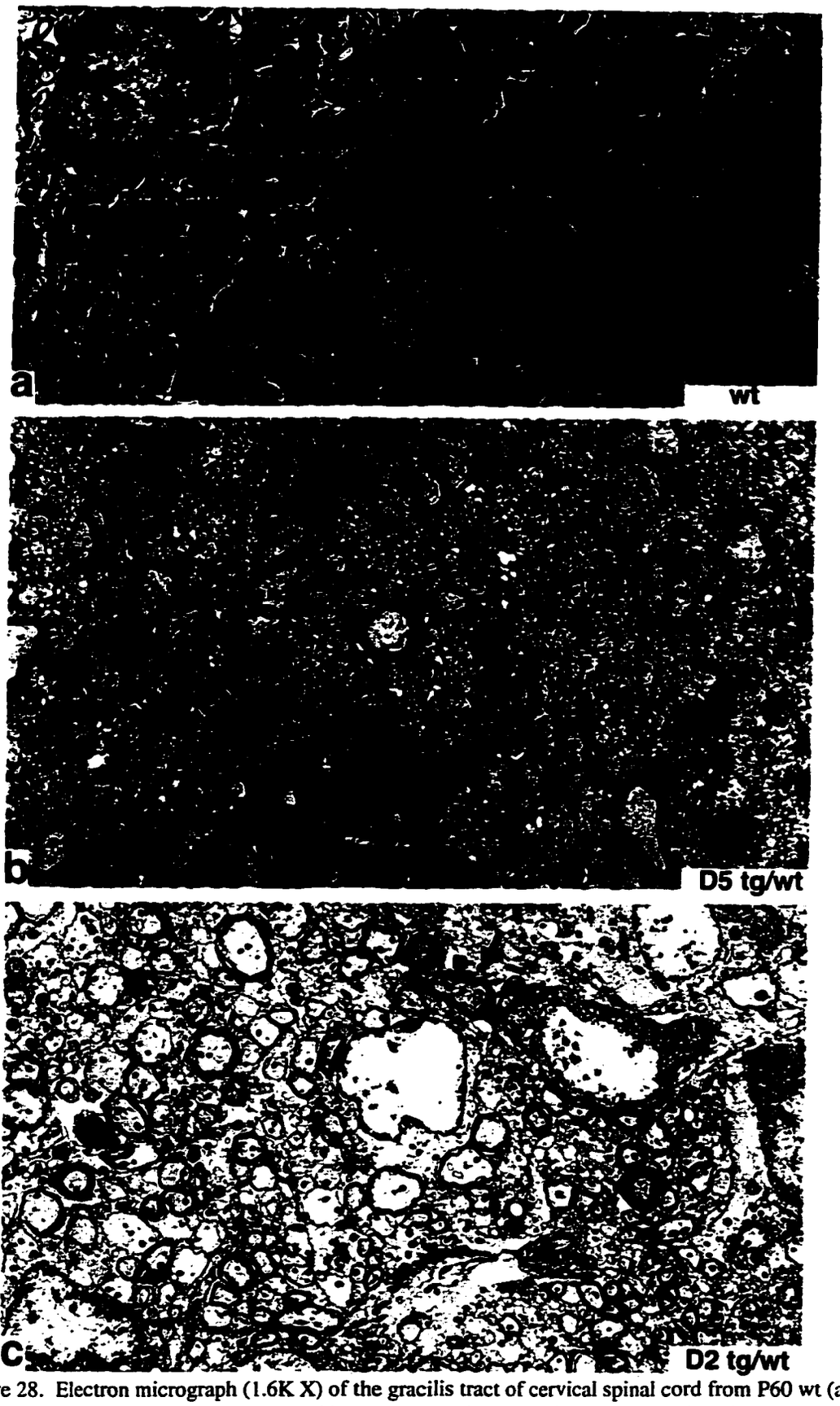

Figure 28. Electron micrograph (1.6K X) of the gracilis tract of cervical spinal cord from P60 wt (a), P60 D5 tg/wt (b) and P25 D2 tg/wt (c) mice. Note the severe hypomyelination in b and c with many naked axons and the redundant myelin sheaths (arrows).

2. Vacuolization

The presence of vacuoles and vacuolated myelin sheaths are one of the most common myelin abnormalities observed CNS pathological conditions in mice overexpressing myelin genes (Table 4). The pathogenesis of the parenchyma is unclear but can appear in the middle of myelin lamellae or unensheathed in the parychema of the CNS white matter. Although the miniMBP tg mice presented in this dissertation display differing symptoms at differing degrees, vacuolization is the only condition that appears consistent between all of the tg/wt lines showing pathology. Figure 29 is an electron micrograph from the spinal cord of a 25 day old D2.5 showing a large, representative vacuole containing myelin debris. This type of vacuolization was observed in those D5 and D4 lines of mice that showed pathology, though at a later onset. Some of the vacuoles that were myelinated (Fig. 30a,c) stained positive for MBP and the tag epitope (Fig. 31).

TABLE 4: PATHOLOGY OBSERVED BY OVEREXPRESSING MYELIN GENES

	PLP*	DM-20**	CNP***	D2	D4	D5
Oligo. abnormality	++	-	-	++	-	-
Change in Oligo. #	+	-	+	-	-	-
Hypomyelination	++	++	-	++	-	++
Vacuolization	++	++	++	++	+	+
Myelin Debris	++	++	-	++	-	++
Redundant Sheaths	++	++	++	++	++	++
Behavioral Phenotype	++	+	-	++	+	+
Norm. compaction	++	++	-	++	++	++
Astrogliosis	++	++	++	++	n/a	n/a
Neuronal dystrophy	+	-	-	++	+	+

* references 83 and 84
** reference 85
*** reference 52

Figure 29. Electron micrograph (10K X) from the lateral funiculus of the cervical spinal cord from a P25 D2 tg/wt mouse. Note the large, myelin debris filled vacuole (*), and the myelinated axon with an abnormally large cytoplasmic filled wrap (**). Arrow indicates one of the unmyelinated axons in this field.

3. Redundant myelin sheaths

Redundant myelin sheaths exist, though very rarely, in wild type mice suggesting that the ensheathing and wrapping processes of the oligodendrocyte can sometimes go awry. Redundant sheaths are formed by an inappropriate wrap during myelination, where an oligodendrocyte process strays from the axon is myelinating and begins to ensheath either neighboring axons or more likely, itself. The latter phenomena is a quintessential occurrence in shiverer CNS. These redundant sheaths increase in frequency in pathological conditions (52, 83, 84, 85) and are numerous in the MBP overexpressing mice described here. Figure 30 (panel c) shows a degenerated myelinated axon within an oligodendrocyte process which looped out and myelinated another oligodendrocyte process nearby. Variations of this abnormal ensheathing is seen throughout the white matter in the CNS D2 and D5 tg/wt overexpressing mice (Fig. 28). The D4 overexpressing mice showed normal myelination. Although the overexpression of transgene (D2, D4 and D5) caused a pathological condition which manifested by numerous myelin abnormalities, there are differences between each line of mice that are discussed below.

C. Overview of the specific pathologies observed for each transgene

1. D2

Heterozygous (tg/-) D2.5 mice displayed an abnormal gait and mild tremors at P12 (postnatal day 12) similar to behavioral phenotype seen in shiverer mice of the same age. As these animals age, this behavioral phenotype becomes progressively worse displaying severe seizures, tonic convulsions, constant tremors and escalating to premature death at around P25. Using immunofluorescent confocal microscopy, some of the MBP/tag positive oligodendrocyte cell bodies appear abnormally large, while the spinal cord has a reduced amount of MBP stained myelin sheaths. Astrogliosis (by GFAP staining) was also noticed throughout the CNS of the tg mice, which is common in other pathological

conditions of the CNS (84). Vacuolization, one of the most common observations seen in the other overexpressing mice, is also observed throughout the CNS of affected tg mice with many of the vacuoles surrounded by MBP and tag positive membranes.

Toluidine Blue stained semithin spinal cord sections from D2.5 spinal cord reveals that the reduction of MBP staining seen in the spinal cord is due to both an absence and overall thinning of the myelin sheaths (Fig. 24). This hypomyelination was regionally localized to certain areas of the CNS specifically affecting smaller to medium diameter axons. For the most part, naked axons were restricted to the ventral white matter tracts of the spinal cord with a few affected sheaths around axons in the cerebellum. The sheaths in the other regions of the CNS were myelinated with thinner than normal sheaths. Many of the swollen oligodendrocyte cell bodies that were observed with the confocal microscope, were found to be localized to the white matter of the CNS.

Electron microscopy (EM) of the above mentioned regions of the CNS proved the most informative in characterizing these initial observations. EM of P25 CNS confirmed the presence of the different sized debris filled vacuoles and thinly myelinated or naked axons (Fig. 25). The myelin that was seen had both the MDL and the intraperiod line, suggesting that compaction proceeded normally, However, myelin debris and redundant loops of myelin membrane were prevalent throughout the CNS. One explanation is that the myelin of these mice were able to compact normally, but failed to stabilize during the maturation of the ensheathment. Since the pathology in these mice follows the same time course as normal myelination, the thin or naked sheaths are probably a result of improper myelinogenesis, versus a dysmyelination phenomenon occurring after the cessation of myelination. One unexplainable observation in these mice is the appearance of the dystrophic neurons since the transgenes are specifically expressed in oligodendrocytes. Axonal swellings were also observed in the spinal cord and cerebellum of D2.5 mice.

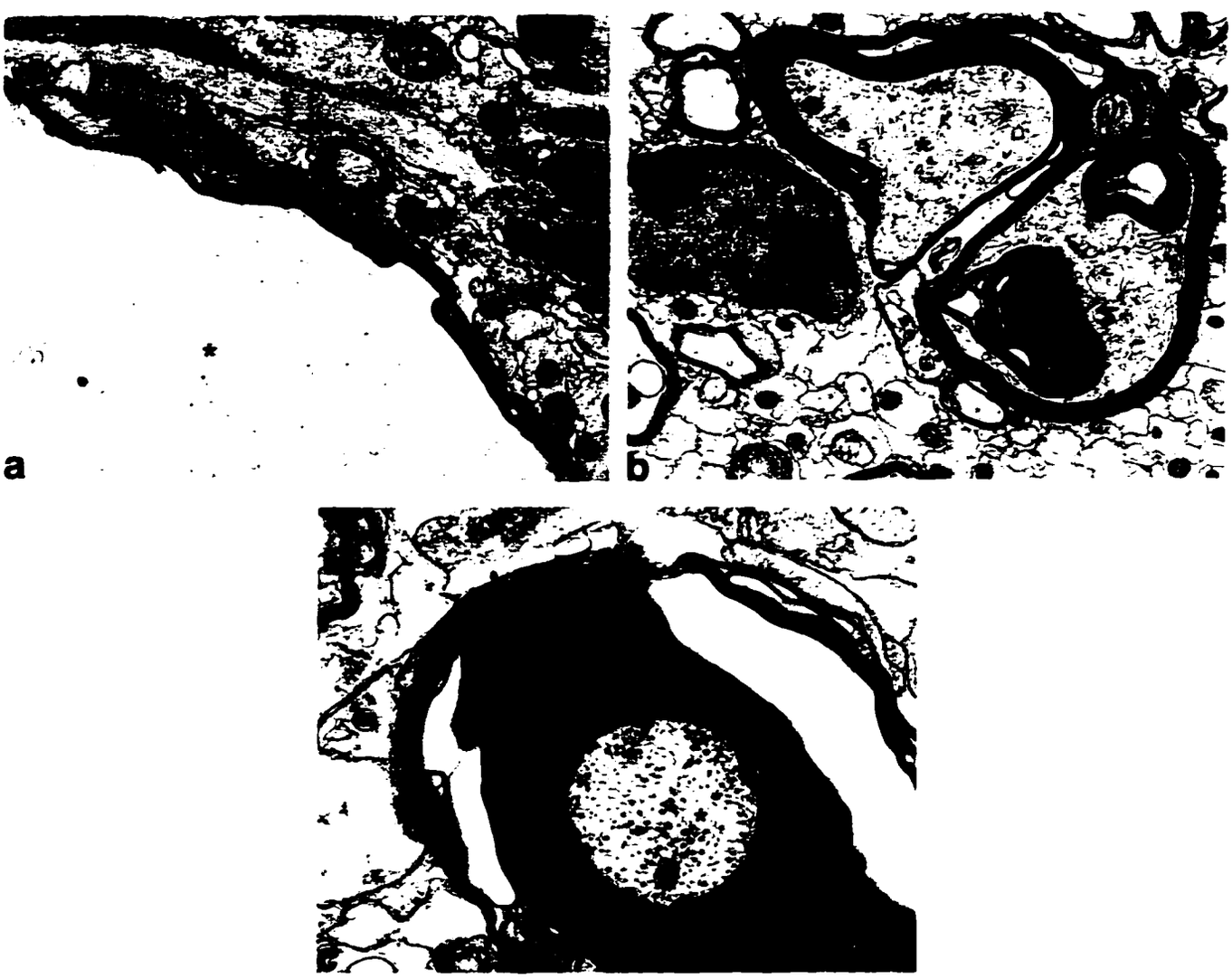

Figure 30. Electron micrographs from spinal cord sections from either a P60 D5 tg/wt mouse (a and c) or a P25 D2 tg/wt (b) mouse. Panel a (10K X), shows a myelinated vacuole (*) with a bit of myelin debris. Panel b (8K X) shows a degenerated myelinated axon (arrow), in which the myelin sheath has looped around on itself as well as ensheathing a nearby oligodendrocyte process (*). Panel c (20K X) shows an improperly myelinated axon (*) with an abnormally large inner mesaxon and vacuoles in-between myelin lamellae.

2. D4

Mice expressing the D4 protein resulted in a pathology similar that seen in the D2.5 tg line, with a few differences. The mice in the D4.7 tg line had a similar behavioral phenotype to that observed with the D2.5 mice, but beginning later at around P60. Like the D2.5, mice heterozygous for the tg (tg/-) displayed mild tremors and ataxia, progressing to tonic convulsion and an early death at around P90. The time of onset and longevity was decreased when the mice were bred to homozygosity (tg/tg).

Immunofluorescent confocal microscopy anti-MBP and anti-tag stained sagittal sections from P90 tg/- D4.7 mice demonstrated that like the D2.5 mice, abundant MBP and tag positive vacuoles were throughout the CNS (Fig. 26). However, unlike the D2.5 mice, there seemed to no lack of stained myelin sheaths in the brain or in the spinal cord, which was verified by TB staining of the same regions (Fig. 24).

Although these mice were not hypomyelinated, EM pictures of the CNS showed redundant myelin sheaths around some of the axons in the spinal cord with deposits of myelin debris (Fig. 27). Myelinated vacuoles were better appreciated at this level and ranged in size similar to the vacuoles seen in the D2.5 mice. These vacuoles were surrounded by myelin membrane that were MBP and D4 positive (Fig. 28). High magnification of the sheaths revealed that the myelin had compacted normally and the thickness was not affected. Neuronal dystrophy was also observed in the CNS of affected mice, with similar axonal swelling and membrane stacks in the axons of the spinal cord and cerebellum. GFAP staining revealed that astrogliosis accompanied the disease process in these mice, but there seemed to be no macrophage infiltration or breakdown of the blood brain barrier.

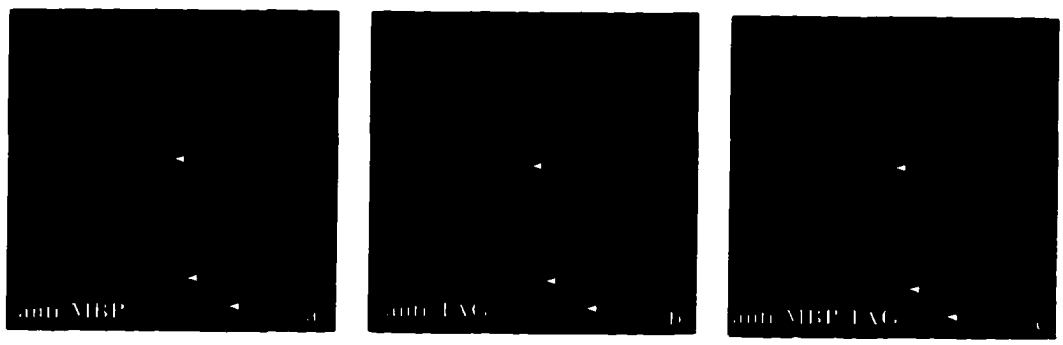

Figure 31. Cryostat section of the cerebral cortex from a late stage D4 overexpressing mouse stained with anti-tag and anti-MBP antibodies conjugated to fluorescein and Texas Red, respectively. Confocal images were generated to demonstrate the wide vacuolization. Panels a-c are confocal images of the same field of view stained with MBP (a) and TAG (b) antibodies and the superimposition of the two images (c). Arrowheads point to a few of the myelinated MBP/TAG positive vacuoles.

3. D5

Overexpressing the 14 kDa isoform of MBP, in the presence of the other endogenous isoforms, lead to the same pathology observed in the D2.5 and the D4.7 mice. Mice expressing the 14 kDa isoform in 2-fold excess of the other isoforms, experienced mild ataxia, tremors, tonic convulsions and early death at P90-P120. The onset of this behavior mimicked the time of onset in the D4.7 mice (P60).

EM analysis demonstrated that the heavily hypomyelinated regions were restricted to the dorsal funiculus of the spinal cord, mostly affecting the gracilis and cortical spinal tracts (Fig. 28). Thus, like the D2.5 mice, medium to smaller diametered axons were affected more than larger diametered axons. Vacuolization was prevalent throughout the CNS which harbored only a few dystrophic axons. The vacuoles were, at times surrounded by tag and MBP positively stained myelin-like membranes, and though smaller in number, similar to those seen in the D2.5 and D4.7 mice. Often, these vacuoles were filled with cellular material while others were essentially devoid of any debris. Normal

myelin compaction was observed with higher magnification EM micrographs, with an occasional redundant myelin sheath and deposits of myelin debris (Fig. 28).

D. Summary

In conclusion, vacuolization, myelin debris and redundant loops, and a behavioral phenotype, were common features in all of the tg mice that displayed a pathology. There was also no apparent change in oligodendrocyte number in the mice at the time of death, and only in the D2.5 mice did oligodendrocyte appeared morphologically abnormal. In some of the lines the sheaths were thinner or absent, but in all cases myelin compacted normally, as scored by the presence of the MDL and the intraperiod line. Neuronal dystrophy was observed throughout the CNS of affected animals. The reason for this is unknown due to the fact that neuronal expression of the transgenes in any of the lines was never demonstrated. In double labeling experiments, staining the CNS of these mice with anti-tag antibodies never colocalized in within the neuron with neurofilament (NF) antibodies (data not shown). So the effects of the transgene overexpression in the experiments presented here are also seen when other myelin genes are overexpressed and are not specific to MBP, but reflects an imbalance in protein production within the oligodendrocytes. The differences between the mouse lines most likely result from differing levels of protein production rather than site-specific mutations.

CHAPTER 8: *DISCUSSION*

This dissertation determined the minimal domains of MBP that are necessary for its role in myelin compaction. I linked together different exons of *mbp* creating nonnatural MBP cDNAs to be expressed in the MBP null mutant mouse, shiverer. This experimental paradigm enabled me to manipulate the number of domains of the protein and determine which of these domains can rescue the mutant (i.e. function for MBP in the compaction of CNS myelin). The M'P expression cassette that was used to express the miniMBP cDNAs afforded abundant expression in oligodendrocytes as reported previously (44) in mice with or without endogenous MBP. The levels of transgenic expression were above the amounts reported by others as necessary for the rescue of shiverer mice (8, 21). Preliminary transgenic expression in wild type mice demonstrated that these truncated MBPs were colocalized with the endogenous MBP in the oligodendrocyte and more importantly, in the myelin sheaths.

A. Localization of the transgenic proteins

A myelinating oligodendrocyte is mostly composed of lipid. Since many of the myelin proteins are highly charged there must be a controlled mechanism that allows for the proper incorporation of the polypeptides into the myelin compartment of the oligodendrocyte and the exclusion of other cellular proteins. Colman et al., examined the synthesis and incorporation of the two major structural polypeptides of CNS myelin , MBP and PLP (4). It was concluded that both proteins incorporate, with different kinetics, into the myelin compartment as it is forming. They found that newly synthesized PLP gets incorporated into the myelin sheath after a lag in time. It was reasoned that this period of time is accounted for by the time it takes PLP to be processed through the secretory pathway, including addition of covalently attached fatty acid molecules, which would occur in the Golgi apparatus. PLP could be targeted to the newly forming myelin sheath through a couple of possible mechanisms. Possibly, the PLP polypeptide/budded Golgi vesicle

fuses with the oligodendrocyte's plasma membrane and then laterly diffuse to the myelin compartment selectively retaining PLP during compaction, or the PLP-vesicles could actively be targeted to the myelinating processes (4). This presumably would be dictated by specific modifications of the PLP peptide and/or the vesicle which contains it, which would allow specific integration and retention of a particular polypeptide into the myelin compartment.

Evidence of specific exclusion of a membrane protein from the compact myelin membrane comes from the analysis of another myelin transmembrane protein, MAG. This protein has been immunolocalized to the myelin sheath but not colocalized with PLP in the compact lamellae, but rather in the noncompact periaxonal channels (114). So, given the different localization between PLP and MAG, there must be a gating process specifying the incorporation of certain peptides into the different oligodendrocyte compartments.

Similarly, since MBP is extremely basic and thus has the potential to aggregate with any lipid containing oligodendrocyte cellular component, there must also exist a mechanism that allows the MBPs to bypass interactions with these components and localize to the regions in which they function. I have already mentioned elsewhere that the mRNA of MBP is translocated to the myelin compartment as an MBP RNA-granule where it is translated and incorporated into the myelinating process (111). Likewise, it has been suggested that exon-2 containing isoforms of MBP are actively targeted to the nucleus in an energy, temperature, and cell growth dependent fashion (107).

From these data, it seems that the myelin membrane proteins are not randomly incorporated into the membrane but rather are targeted specifically to compartments in which they function. It is this compartmentalization of the myelin membrane and the specific interactions with the membrane proteins that keeps myelin from being a "sink" to all of the plasma membrane proteins of the oligodendrocyte.

I have demonstrated that the protein encoded by exons one, three, four and seven of *mbp* (D4) is located, with endogenous MBP, in the myelin sheaths throughout the CNS of

tg/wt mice. Surprisingly however, the D2 protein is localized (both in the tg/wt and the tg/shi mice) only in the myelin sheaths around medium to smaller diameter axons (Fig. 32). The difference in localization between the two proteins is difficult to reconcile because of scant information concerning the effects of axon caliber on myelination. One pivotal study reported that the amount of myelin per internode was in linear relation with the product of axon circumference and the length of the ensheathed axon segment (3). A simple, straightforward analysis of this relationship is not possible because large axons are myelinated earlier in CNS development than the smaller ones (45, 75). Thus, the differences in miniMBP localization in the D2 and D4 lines might be attributed to the differences in the timing of transgenic expression despite the fact that the same expression vector was employed in both transgenes. Nonetheless, one could speculate that the site of transgene insertion into the mouse chromosome may affect the timing of transgene expression.

A second, less likely explanation for this difference might be that different subpopulations of oligodendrocytes exist which myelinate different size classes of axons. If the D2 protein were poorly expressed in the subpopulation of the oligodendrocytes that myelinate larger diameter axons, the observed distribution would be obtained. However, D2 is immunolocalized with MBP in all MBP positive oligodendrocytes examined. Furthermore, there is no direct evidence for subpopulations of oligodendrocytes in the CNS that preferentially myelinate certain sized axons.

Uniquely, the rescued myelin sheaths in the D4 tg/shi mice and the hypomyelination seen in the D2 and D5 overexpressing mice were also restricted to medium to smaller diameter axons. Although it is clear that larger diameter axons are myelinated first in the developing CNS (45, 75), smaller diameter axons require less material from the oligodendrocyte to be fully ensheathed. Certainly, in the D4 tg/shi rescue mice, the smaller diameter axons may preferentially be myelinated because of the higher protein/membrane demand of the larger diameter axons. However, in the experiment by Readhead (21), it

was noted that the few compact myelin sheaths that were observed in the transgenic shiverer mice were around larger diameter axons. The exons that are excluded in the D4 miniMBP may ensure the ensheathment of larger diameter axons.

B. Myelin compaction

Kimura showed that the 14 kDa isoform of MBP alone can form compact myelin, suggesting an ambiguous role of the other isoforms in compaction (8). The experiments presented here reiterate this point by demonstrating that even a smaller, nonnatural form of MBP can allow the compaction of CNS myelin. Oligodendrocytes in the D4 tg/shi mice were able to ensheath, wrap multiple times, and compact around axons forming major and minor dense lines, the hallmarks of compact myelin. Immuno-EM data verified that the D4 protein is localized to the compact myelin and the lamellar spacing of the compact myelin or periodicity in the D4 tg/shi mice mimics the spacing observed in wild type myelin.

The semicompact myelin that is observed in electron micrographs of D2 tg/shi mice resembles the myelin sheaths observed in the shiverer CNS (Fig. 23). While it is apparent that the outer leaflets of the oligodendrocyte's bilayer can come together forming the intraperiod line, the cytoplasmic leaflets remain apart leaving a cytoplasmic gap in the myelin where the major dense line would normally form. Although immuno-EM data is not available for the D2 tg/shi mice, confocal immunoflourescent microscopy of spinal cord from these mice localize the D2 protein (with PLP) in the semicompact sheaths around smaller axons (Figs. 18 and 32), resembling the staining pattern in the D4 tg/shi confocal images (Fig. 19). This suggests that the polypeptide encoded by exons one and seven is found in the myelin sheaths but does not allow for their compaction and the subsequent formation of the MDL. In fact, the CNS of the D2 tg/shi mice looks remarkably like the CNS of nontransgenic shiverer mice. Therefore, exons one, three, four and seven of *mbp* specifies a miniMBP that facilitates myelin compaction, while the protein encoded by exons

one and seven alone cannot. It remains to be determined whether all of the information in exons one, three, four and seven are required for this activity or whether even simpler miniMBPs could be fashioned which would facilitate compaction.

Since the basic and acidic amino acids of MBP are located uniformly throughout its amino acid sequence (Fig. 4), any combination of the different exons will encode proteins that have roughly the same pI. So, if MBP functions only to neutralize the anionic headgroups of the phospholipid bilayer during compaction, it follows that any truncated form of MBP or other basic protein of similar size and isoelectric point as MBP may be sufficient to function in the compaction of myelin. Mateu demonstrated that different basic proteins in an aqueous solution with the acidic fraction of lipids extracted from myelin will cause spontaneous lamellar formations with a regular periodicity similar to that of CNS myelin (40). These experiments seem to support the idea that charge neutralization is the important feature of the protein. However, these experiments are complex and their interpretation is based on the following unsupported assumptions: 1) Protein interactions with lipid fractions are a reasonable model for the myelin membrane. The membranes of the myelin sheath contain a variety of phospholipid organized asymmetrically into two leaflets. Cholesterol, which constitutes about 25% of the myelin lipids (28) is not present in the experimentally produced lamellar structure. The inclusion of 20% cholesterol in the lipid fraction of these experiments actually prevents formation of the lamellar structures (40). 2) The molecular conformation of the protein is unchanged by its milieu. In fact, in these experiments, the basic proteins used were in an aqueous environment which does not reproduce the lipid rich environment of the oligodendrocyte, and will affect their folding and therefore, the surface charge (28, 105, 106).

In the experiments described in this dissertation, the charge neutralization hypothesis was directly tested without the complications and assumptions of an *in vitro* system. The availability of the MBP null, shiverer mutant allowed me to directly test whether different basic proteins can compact myelin membrane. I have deduced from

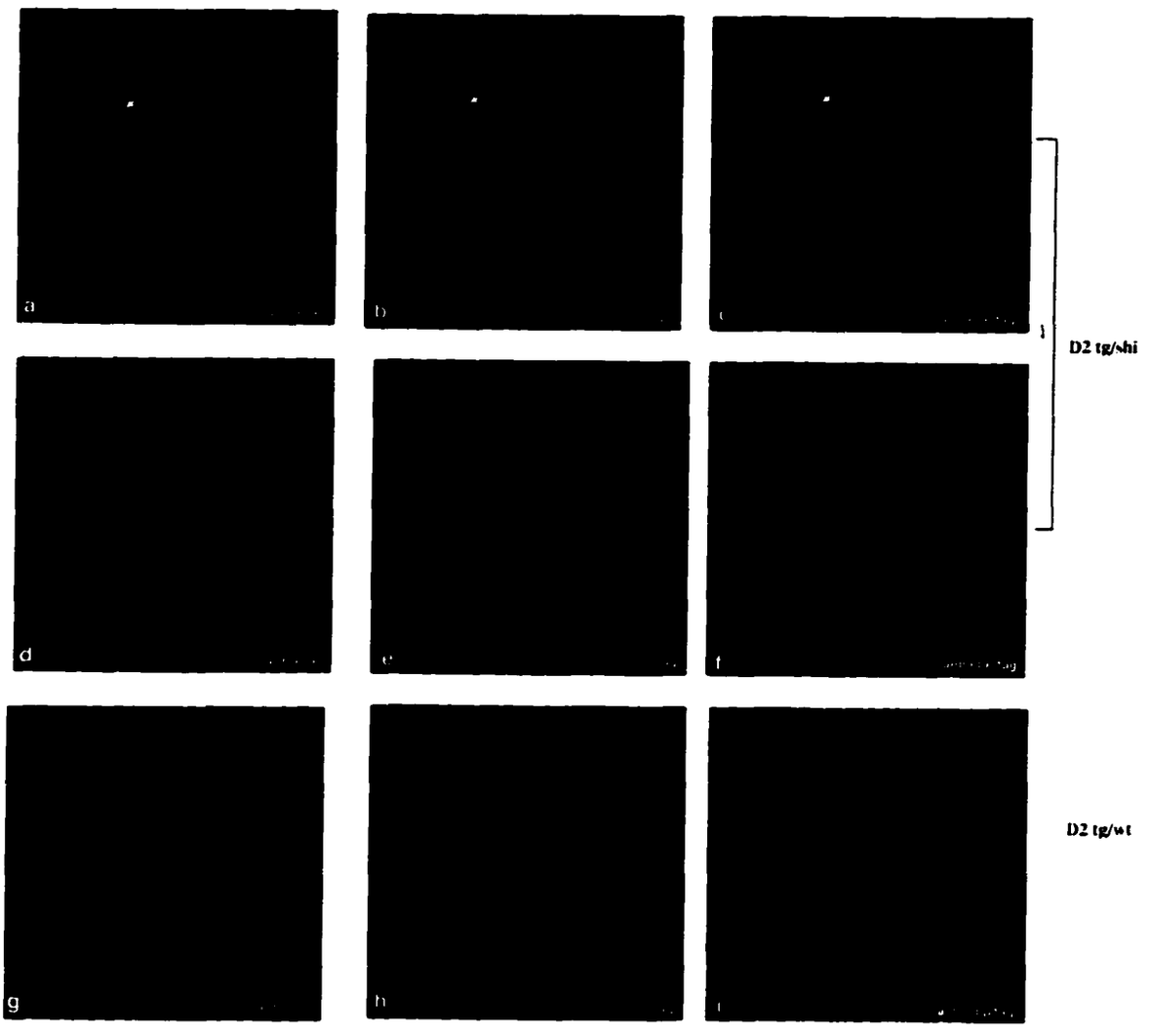

Figure 32. Immunofluorescent confocal images of both D2 tg/shi (a-f) and D2 tg/wt (g-i) sections stained with anti-tag/MBP and with anti-tag/PLP serum, respectively. Cross section images of the ventral column of the spinal cord (d-i) show the localization of D2 in the myelin and semicompact myelin of the tg/shi and tg/wt mice. A single oligodendrocyte (a-c) from D2 tg/shi shows the juxtaposition of D2 and PLP in the oligodendrocyte process (arrow).

these experiments that MBP cannot be simply neutralizing the anionic phospholipid headgroups of the lipid bilayer of the oligodendrocyte's processes. If this were the case then any small, basic polypeptide would be able to allow for the compaction of CNS myelin in the shiverer mouse. D2 is smaller than any of endogenous MBP isoforms, has an isoelectric point of 12.4 (as high as any of the natural isoforms), and is localized to the

semicompact myelin sheaths (Fig. 32). It is unable, however, to allow for the compaction of myelin sheaths. If D2 was able to function in the compaction of shiverer myelin, then other heterologous proteins of the same molecular weight and isoelectric point as MBP might also suffice. Initially, viral matrix proteins were cloned into the M'P expression cassette to be expressed in the oligodendrocytes of the shiverer mouse. Viral matrix (M) proteins from VSV and Measles virus are peripheral membrane proteins that are roughly the same size and share a high pI with MBP; and they function as a link between heavily charged molecules. However, since D2 was unable to rescue the dysmyelinating mutant, myelin compaction must be dependent on unique properties in the domains encoded by exons one, three, four, and seven. Thus MBP must not be functioning to simply neutralization the acidic phospholipid headgroups of the oligodendrocyte lipid bilayer in compaction.

One possibility is that exons one, three, four, and seven of *mbp* encode a polypeptide that folds into a "core" conformation that is needed for compaction and the other domains of MBP afford the protein other functions needed for complete myelination of the CNS. Since the amino acid sequence of MBP has remained fairly the same throughout evolution, it is reasonable to suggest that there might be essential domains of the protein that are strictly needed for myelin compaction.

However, the structure of MBP remains elusive and has yet to be established. Computer algorithms have been used by Stoner and colleagues to predict an ordered conformation of the native MBP polypeptide (50). This model suggests a secondary structure consisting of five anti-parallel beta-pleated sheets separated by loops of amino acid stretches, some forming alpha helices (5 and 50). This analysis also predicts a planar conformation, dimensions that would fit the hypothesis that MBP is localized to the 0.4 nm space in between the cytoplasmic surfaces of compact myelin. Another model has been recently proposed by Haruaz and colleagues based on electron microscopic three-dimensional reconstruction, but relies on the premise of a conserved consensus β–sheet

backbone (57). As yet, MBP has not been crystallized (82) and so any structural theory about the protein remains unverified.

Hydropathy plots of the shark and murine MBP amino acid sequence reveal alternating hydrophilic and hydrophobic regions spaced at regular intervals and completely conserved between species. This data together with the documented conservation of the primary amino acid sequence throughout evolution, suggest that MBP may have a core conformation composed of the polypeptide encoded by the four exons conserved in all of the isoforms and thus the exons in D4 (38). The other exons might serve to form "variable" loops inserted at the flexible boundaries of a particular exon or domain. With these different structural properties, MBP can possibly be viewed as a *modular* protein that is composed of individual domains. The deleted exons or domains may be independent from each other and structurally neutral in terms of a general protein's core topology. While these variable domains might not play any part in MBP's general role in compaction, the inserted loops or domains might confer other, unexplored functions of MBP in oligodendrocytes. Certainly, total and complete myelination was never achieved in the D4/shiverer rescue or the other reported rescue experiments (8, 21).

In a 1987 study by Popko et al., it was shown that an increase in MBP expression correlated well with an increase in myelin formation (9). The subsequent studies of Shine and Sidman, in 1992 (79), provided further evidence of this correlation and extended the correlation of MBP mRNA level with the amount of myelination. They found that as MBP message level increases, the number of myelinated axons, as well as the myelin thickness around individual axons increase proportionally (79). Like the shiverer/14kDa rescued mouse (8), the CNS of the D4 tg/shi mice is not fully myelinated. Not only are the larger diameter axons devoid of myelin, but much of the myelin that is present around smaller to medium diameter axons is thinner than in wild type CNS. These results suggest that the other isoforms may play other roles in the oligodendrocyte biology.

For instance, it has been demonstrated that the isoforms of MBP are developmentally regulated and exon-2 containing isoforms may function in other aspects of the oligodendrocyte. As mentioned earlier, these isoforms are proportionately more abundant in the developing mouse CNS and are specifically enriched in the radial components of mature myelin (1, 64). Colman and other groups have demonstrated that exon-2 containing isoforms may act by shuttling the other isoforms of MBP into the nucleus (17, 56, 107, 113). Pedraza et al. reported that there is a close similarity in two regions of the peptide encoded by exon two of *mbp* with known nuclear localization signal peptide sequences in the nuclear proteins nucleoplasmin and SV-40 T-antigen (107). Whether these regions of the peptide sequence of MBP are necessary for the targeting of the MBPs to the nucleus remains to be investigated, but these data do suggest that MBP may function in aspects in the oligodendrocyte other than in myelin compaction. Therefore, the domains of MBP that are excluded in the D4 protein may be important in the highly orchestrated process involving the initiation, thickening, and cessation of myelin production in the CNS of mice, which is separate from the role in membrane apposition or compaction.

C. Pathology from MBP overexpression

Pathology of demyelinating diseases have recently been the focus of much study. Overexpressing many of the myelin genes results in a severe demyelinating disease manifested in a variety of myelin abnormalities (52, 83, 84, 85). In the results presented here, I have shown that similar pathology arises when different domains of MBP are overexpressed. From this, it appears that oligodendrocyte biology and myelination are not as plastic as other systems in the nervous system, and are vulnerable to the slightest alteration.

The pathology observed in our experiments closely resembled what is observed in other myelin gene overexpression experiments, displaying different subsets of symptoms

depending on the different transgenes. A few common symptoms (Table 7) such as vacuolization and redundant myelin sheaths are shared between the transgenic lines. Another common feature of the three overexpressing mouse lines is that myelin is formed compacts normally. Although the CNS from D2.5 tg/wt and D5.19 tg/wt mice are hypomyelinated, the myelin that is present (including the myelin seen around the vacuoles), compacts normally, forming MDLs and intraperiod lines. However, the abnormalities observed in all three lines of transgenic mice are also observed in animals that overexpress other myelin genes suggesting that the pathological features listed in Table 7 may be the direct result of an imbalance between myelin components.

Each tg line (D2.5, D4.7 and D5.19) had a different levels of transgene expression. Among the various lines of mice carrying the transgene (D2, D4 or D5) the line showing the highest level of tg expression developed pathology. In some cases, animals that were heterozygous for the transgene were normal but animals homozygous for the same transgene developed pathology. For instance, mouse lines D5.15 and D2.14 developed a behavioral phenotype when bred to transgenic homozygosity. So it appears that there is a threshold effect for the transgene encoded proteins. The D2 and D4 proteins are truncated nonnatural versions of endogenous isoforms which could interact in a toxic manner. However, the D5 tg encodes a normal isoform of MBP (14 kDa) but nonetheless, causes a pathology. At this juncture it seems reasonable to speculate that the differences in pathology are a direct result of the expression levels of the transgenes instead of a specific effect by the specific domains of MBP. Each of the transgenes contains the tag epitope that enabled me to follow the localization of the tg proteins in the presence of the MBP isoforms in the tg/wt mice, and it is formally possible that the tag sequence causes the observed pathologies. We do not believe that this is the case because of the demonstration by others that perturbing the balance of myelin components is, by itself, sufficient to cause a similar dysmyelination in mice (52, 83-85).

D. Future Directions

In this dissertation I have demonstrated that a smaller, nonnatural form of MBP can substitute for the endogenous forms in the compaction of CNS myelin. However, there are a few implications that arise from the observations from these experiments. One issue deals with the different localization of D2 and D4 in the myelin sheath between different caliber size axons. Since the exact timing of transgene expression for each tg line of mice relative to each other and to endogenous *mbp* is not presently known, one can analyze onset of expression levels using the same probes and RNase protection assay that were used in the experiments described in this dissertation. Since the probes that were employed hybridize and protect both transgene and *mbp* mRNA, this type of assay, if carried out with RNA extracted from different aged transgenic animals, would give insight to the onset of gene expression. *In situ* hybridization assays using an antisense oligonucleotide sequence against the tag sequence would provide further information on the localization of the transgene mRNA in the oligodendrocytes in which they are expressed. For example, a difference in mRNA localization between D4 and D2 message could account for the different localization patterns of the protein in the tg/wt mice. Immuno-EM of D2 tg/wt and tg/shi CNS sections would also provide information about the differences seen in the localization between the two proteins.

Another line of experiments that stem from these data deals with the determination of D2's inability to facilitate the compaction of myelin. For instance, D2 may be selectively excluded from the compartment in the oligodendrocyte's process that would normally form compact myelin. Although confocal imaging data reveals that D2 is juxtaposed with MBP and PLP in the D2 tg/wt and tg/shi mice, respectively, it cannot resolve the ultrastructural localization of D2 in the myelin sheath which is further information that immuno-EM would provide. If D2, for instance, is found in the compact myelin in the tg/wt CNS and in the cytoplasmic channels where the MDL would normally form in the tg/shi CNS, then this type of data would demonstrate that D2 is located in the regions to be compacted in the

tg/shi mice but does not contain the necessary information to facilitate compaction. On the other hand, if this data reveals that D2 is found in the cytoplasmic channels (inner and outer mesaxon) in the tg/wt mice, and not in the compact myelin compartment of the myelin sheath, it follows that D2 is selectively excluded from the membrane regions involved in compact myelin. The staining patterns of the D2 protein relative to MBP and PLP suggest that the latter possibility is unlikely, but immuno-EM data of D2 tg/wt and tg/shi CNS would provide stronger interpretable evidence. It is possible that D2 cannot facilitate the compaction of myelin in the tg/shi mice because of size limitation of the protein. D4 is about 14 kDa whereas D2 is about 9 kDa. If size is the important factor for D2's inability to function in compaction, then a transgene expressing a concatamer of D2 or one that contains innocuous "filler" sequence between exons one and seven, expressed in shiverer mice would test this possibility.

The sequence of amino acids encoded by the four exons in D4 must contain important information regarding MBP's function in myelin compaction. It follows that the essential information may be encoded in exons three and/or four that affords MBP its ability to facilitate compaction. Even though D4 is sufficient to function in the formation of the MDL, there might be a subset of the exons in D4 that would also suffice. Exons three and four of *mbp* are excluded in D2 and are the only sequence difference between the two miniMBPs. One could create other transgenes to be expressed in shiverer mice that contain a different combination of the exons in D4 and ones that contain either both or one of exons three and four of *mbp*. If a protein encoded by the same number of exons in D4 but in different combinations was able to facilitate compaction of shiverer CNS myelin then one can conclude that the exons in D4 provide individual domains that act independently from the context of the other exons (here I refer to "exon" as the polypeptide unit encoded by the genomic exon). If this is the case then possibly a transgene containing exons three and/or four of *mbp* might facilitate the compaction of myelin when expressed in shiverer oligodendrocytes. If the proteins encoded by the different combinations of D4 exons

cannot facilitate myelin compaction, it would suggest that the context of the four exons relative to each other must be maintained. Hence, D4 may contain a "core" conformation that affords it (and MBP) the ability to function in the compaction of myelin.

The experiments suggested here would address some of the implications and issues that remain unanswered by this dissertation. While it is clear that further analysis would arise from the results from the data generated, these proposed experiments are plausible directions to take from the conclusions of the data presented above.

REFERENCES

1. Barbarese E., Carson J. H., and Braun P. E., (1978) *Accumulation of the Four Myelin Basic Proteins in the Mouse Brain During Development.* J. Neurochem. **31**, 779-782.

2. Campagnoni C., Carey G., and Campagnoni A. T., (1978) *Synthesis of Myelin Basic Proteins in the Developing Mouse Brain.* Arch. Biochem. Biophys. **190**, 118-25.

3. Friede, R., and Bischhausen, R. (1982) *How are Sheath Dimensions affected by Axon Caliber and Internode Length?* Brain Research. **235**, 335-350.

4. Colman D. R., Kreibich G., Frey A., and Sabatini D. (1982) *Synthesis and Incorporation of Myelin Polypeptides into CNS Myelin.* J. Cell Biol. **95**, 598-608.

5. deFerra F., Engh H., Hudson L., Kamholz J., Puckett C., Molineaux S., and Lazzrarini R. A. (1985) *Alternative Splicing Accounts for the Four Forms of Myelin Basic Protein.* Cell **43**, 721-27.

6. Kamholz., Toffenetti J., and Lazzarini R.A., (1988) *Organization and Expression of the Human Myelin Basic Protein Gene.* J. Neurosci. Res. **21**, 62-70

7. Katsuki M., Masahiro S., Kimura M., Yokoyama M., Kobayashi K., and Nomura T. (1988) *Conversion of Normal Behavior to Shiverer by Myelin Basic Protein Antisense cDNA in Transgenic Mice.* Science **241**, 593-95.

8. Kimura M., Sato M., Akatsuka A., Nozawa-Kimura S., Takahashi R., Yokoyama M., Nomura T., Katsuki M. (1989) *Restoration of Myelin Formation by a Single Type of Myelin Basic Protein In Transgenic Shiverer Mice.* Proc. Nat. Acad. Sci. USA **86**, 5661-65.

9. Popko B., Puckett C., Lai E., Shine D., Readhead C., Takahashi N., Hunt III, S., Sidman R., and Hood L. (1987) *Myelin Deficient Mice: Expression of Myelin Basic Protein and Generation of Mice with Varying Levels of Myelin.* Cell **48**, 713-721.

10. Macklin W., Gardinier M.V., Obeso Z.O., King K.D., Wight P.A., (1991) *Structure and Expression of the Myelin Proteolipid Protein Gene Expression In Jimpy and Jimpy^{msd} Mice* . J. Neurochem. **56**, 436-445.

11. Waehneldt T. (1990) *Phylogeny of Myelin Proteins.* Ann. N.Y. Acad. Sc. **605**, 15-27.

12. Campagnoni A. T. (1988) *Molecular Biology of Myelin Proteins from the Central Nervous System.* J. Neurochem. **51**, 1-14.

13. Hudson L. D. (1990) *Molecular Biology of Myelin Proteins in the Central and Peripheral Nervous Systems.* Seminars in the Neurosciences **2**, 483-496.

14. Campagnoni A., Verdi J., Verity A., Amur-Umarjee S., and Byravan S. (1990): *Posttranscritional Regulation of Myelin Protein Gene Expression.* Ann N.Y. Acad Sci. **605**, 270-79.

15. Devine-Beach K., Lashgari M., and Khalili K. (1990) *Myelin Basic Protein Gene Transcription* J. Bio. Chem. **265**, 13830-35.

16. Amiquet, P., Gardineir, M., Zanetta J-P., and Matthieu, M. (1992) *Purification and Partial Strucural and Functional Characterization of Mouse Myelin/Oligodendrocyte Glycoprotein.* J. Neurochem. **58**, 1676-80.

17. Hardy, R., Lazzarini R.A., Colman, D.R., and Friedrich, V. (1996) *Cytoplasmic and Nuclear Localization of MBPs Reveal Heterogeneity Among Oligodendrocytes.* J. Neurosci. Res. **46**, 246-57.

18. Wiktoromwicz M., and Roach A. (1991) *Regulation of Myelin Basic Protein Gene Transcription in Normal and* Shiverer *Mutant Mice* Dev. Neurosci. **13**, 143-150.

19. Sidman R., Conover C., and Carson J. (1985) *Shiverer Gene Maps Near the Distal End of Chromosome 18 in the House Mouse* Cytogenet. Cell Genet. **39**, 241-245.

20. Karthigasan, J., Inouye, H., and Kirschner, D. (1995) *Implications of the Sequence Similarities Between Tau and MBP.* Medical Hypothesis **45**, 235-40.

21. Readhead C., Popko B., Takahashi N., Shine H. D., Saavedra R., Sidman R., and Hood L. (1987) *Expression of Myelin Basic Protein Gene in Transgenic Shiverer Mice: Correction of the Dysmyelinating Phenotype.* Cell **48**, 703-12.

22. Roach A., Takahashi N., Pravtcheva D., Ruddle F., and Hood L. (1985) *Chromosomal Mapping of Mouse Myelin Basic Protein Gene and Structure and Transcription of the Partially Deleted Gene in Shiverer Mutant Mice* Cell **42**, 149-55.

23. Macklin W., Campagnoni C., Deininger P., and Gardinier M. (1987) *Structure and Expression of the Mouse Myelin Proteolipid Protein.* J. Neurosci. Res. **18**, 383-94.

24. Mikol D., Wrabetz L., Marton L., and Stefansson K. (1988) *A Phosphatidylinositol-Linked Peanut Agglutinin-Binding Glycoprotein in the CNS Myelin and on Oligodendrocytes* J. Cell Biol. **106**, 1273-79.

25. Mikol D., Gulcher J., and Stefansson K., (1990) *The Oligodendrocyte-Myelin Glycoprotein Belongs to a Distinct Family of Proteins and Contains the HNK-1 Carbohydrate.* J. Cell Biol. **110**, 471-479.

26. Takahashi N., Roach A., Teplow D., Prusiner SA., and Hood L. (1985) *Cloning and Characterization of the Myelin Basic Protein Gene from Mouse: One Gene Can Encode Both 14 kd and 18 kd MBP's by Alternative use of Exons.* Cell **42**, 139-148.

27. Lemke G. (1988) *Molecular Biology of the Major Myelin Genes.* Neuron **1**, 533-543.

28. Morell P. ed., (1984) Myelin, second edition (New York: Plenum Press).

29. Tamura T., Sumita K., Hirose S., and Mikoshiba K. (1990) *Core Promoter of the Mouse Myelin Basic Protein Gene Governs Brain-Specific Transcription in vitro.* EMBO **9**, 3101-08.

30. Tamura T., and Mikoshiba K. (1991) *Demonstration of a Transcription Element in vitro Between the Capping Site and Translation Inititation Site of the Mouse Myelin Basic Protein Gene.* FEBS Letters **280**, 75-8.

31. Campagnoni A.T., Carey G., and Yu Y. (1980) *In vitro Synthesis of the Myelin Basic Proteins: Subcellular Site of Synthesis* J. of Neurochem. **34**, 677-86.

32. Newman S., Kitamura K., and Campagnoni A. (1987) *Identification of a cDNA Coding for a Fifth Form of Myelin Basic Protein in Mouse.* Proc. Nat. Acad. Sci. USA **84**, 886-90.

33. Colman D., Staugaitis S., D'Urso D., Sinoway M., Allinquant, B., Bernier L., Mentaberry A., Stempak J., and Brophy P., (1990) *Physiologic Properties of Myelin Proteins Revealed by Their Expression in Nonglial Cells.* Ann. N. Y. Acad. Sci. **605**, 294-301.

34. Newman S., Kitamura K., Roth H., Kronquist K., Kcrlero de Rosbo N., Crandall, B., and Campagnoni A. (1987) *Differential Expression of the Myelin Basic Protein Genes in Mouse and Human.* (abst) J. Neurochem. **48**, (suppl) 527.

35. Rosenbluth J. (1980) *Central Myelin in the Mouse Mutant Shiverer.* J. Comp. Neurol. **194**, 639-48.

36. Edwards, A., Ross, N., Ulmer, J., and Braun, P. (1989) *Interaction of Myelin Basic Protein and Proteolipid Protein.* J. Neurosci. Res. **22**, 97-102.

37. Omlin F., Webster H., Palkovitz G., and Cohen S. (1982) *Immunocytochemical Localization of the Basic Protein in the Major Dense Line Regions of Central and Peripheral Myelin.* J. Cell Biol. **95**, 242-248.

38. Martenson, R. ed., (1992) Myelin: Biology and Chemistry (CRC press).

39. Kandel E., Schwartz J., Jessell T. ed., (1991) Principles of Neural Science, third edition (Elsevier).

40. Mateu L., Luzzati V., London Y., Gould R., Vosseberg F., and Olive J., (1973) *X-Ray Diffraction and Electron Microscope Study of the Interaction Of Myelin Components: the Structure of a Lamellar Phase With a 150 Angstrom Repeat Distance Containing Basic Proteins and Acidic Lipids.* J. Mol. Biol. **75**, 697-709.

41. Tamura T., Miura M., Ikenaka K., and Mikoshiba K. (1988) *Analysis of Transcription Control Elements of the Mouse Myelin Basic Protein Gene in HeLa Cell Extracts: Demonstration of a Strong NFI-binding Motif in the Upstream Region.* Nucl. Acids Res. **16**, 11441-11459.

42. Popot J., Dinh D., and Dautigny A., (1991) *Major Myelin Proteolipid : The 4 alpha-helix Topology* J. Membr. Biol. **120**, 233-46.

43. Zeller, N., Hunkeler, M., Campagnoni, A., Sprague, A., and Lazzarini, R. (1984) *Characterization of Mouse Myelin Basic Protein messenger RNAs with Myelin Basic Protein cDNA Clone.* Proc. Nat. Acad. Sci. USA **81**, 18-22.

44. Gow A., Freidrich V., Lazzarini R., (1992) *Myelin Basic Protein Gene Contains Separate Enhancers for Oligodendrocyte and Schwann Cell Expression.* J. Cell Biol. **119**, (3) 605-616.

45. Jacobson S., (1963) *Sequence of Myelination in the Brain of the Albino Rat* J. Comp. Neur. **121**, 5-29.

46. Sambrook, J., Fritsch, E., and Maniatis, T. (1989) Molecular Cloning, A Laboratory Manual, 2nd Ed. Cold Spring Harbor Laboratory Press.

47. Ausubel, F., Brent, R., Kingston, R., Moore., Smith, J., Seidman, J., and Struhl, K., ed. (1987) Current Protocols in Molecular Biology, Greene Publishing Associates and Wiley-Interscience.

48. Hogan B., Lacy E., and Costantini F. (1986) Manipulating the Mouse Embryo (Cold Spring Harbor Laboratory publ.)

49. Gardinier M.V., Amiguet P., Linington C., and Matthieu J.-M. (1992) *Myelin/Oligodendrocyte Glycoprotein is a Unique Member of the Immunoglobulin Superfamily* J. Neurosci. Res. **33,** 177-187.

50. Stoner G.L. (1984) *Predicting Folding of Beta-strands for Myelin Basic Protein* J. Neurochem. **43,** 433-47.

51. Spivack, W.D., Zhong, N., Salerno, S., Saavedra, R. A., and Gould, R.M. (1993) *Molecular Cloning of the Myelin Basic Proteins in the Shark,* Squalus Acanthias, *and the Ray,* Raja Erinacia. J. of Neurosci. Res. **35**, 577-84.

52. Gravel, M., Peterson, J., Yong, V.W., Kottis, V., Trapp, B., and Braun, P. (1996) *Overexpression of CNP in Transgenic Mice Alters Oligodendrocyte Development and Produces Aberrant Myelination.* Mol. Cell. Neurosci. **7,** 453-66.

53. Scherer, S., Braun, P., Grinspan, J., Collarini, E., Wang, D., and Kamholz. (1994) *Differential Regulation of the CNP Gene during Oligodendrocyte Development.* Neuron **12**, 1363-75

54. Shafer, M., Fruttiger, M., Montag, D., Schachner, M., and Martini, R. (1996) *Disruption of the Gene for the Myelin-Associated Glycoprotein Improves Axonal Regrowth along Myelin in C57BL/Wld-s Mice.* Neuron **16**, 1107-13.

55. Mukhopadhyay, G., Doherty, P., Walsh,W., Crocker, P., and Filbin, M. (1994) *A Novel Role for MAG as an Inhibitor of Axonal Regeneration.* Neuron **13**, 757-67.

56. Staugaitis, S., Smith, P.R., and Colman, D.R. (1990) *Expression of Myelin Basic Protein Isoforms in Nonglial Cells.* J Cell Biol. **110**, 1719-27.

57. Ridsdale, R., Beniac, D., Tompkins, T., Moscarello, M., and Harauz, G. (1997) *Three-dimensional Structure of Myelin Basic Protein.* J. Biol. Chem. **272**, 4261-75.

58. Goverman, J.,Woods, A., Larson, L., Hood, L., and Zaller, D. (1993) *Transgenic Mice that Express a Myelin Basic Protein T-cell receptor Develop Spontaneous Autoimmunity* Cell **72**, 551-60.

59. Nave, K. (1994) *Neurological Mouse Mutants and the Genes of Myelin.* J. Neurosci. Res. **38**, 607-12.

60. Yoshida, M., and Colman, D.R. (1996) *Parallel Evolution and Coexpression of the Proteolipid Proteins and Protein Zero in Vertebrate Myelin.* Neuron **16**, 1115-26.

61. Kitagawa, K., Sinoway, M., Yang, C., Gould, R., and Colman, D.R. (1993) *A PLP Gene Family: Expression in Sharks and Rays and Possible Evolution from an Ancestral Gene Encoding a Pore-forming Polypeptide.* Neuron **11**, 433-48.

62. Peters, A. (1961) *A Radial Component of Central Myelin Sheaths.* J. Biophys. and Bioch. Cytol. **11**, 733-35.

63. Kosaras, B., and Kirschner, D. (1990) *Radial Component of CNS Myelin: Junctional Subunit Structure and Supramolecular Assembly.* J. Neurocytol. **19**, 187-99.

64. Karthigasan J., Kosaras, B., Nguyen, J., and Kirschner D. (1994) *Protein and Lipid Composition of Radial Component-Enriched CNS Myelin.* J. Neurochem. **62**, 1203-13.

65. Steinman, L. (1992) *Multiple Sclerosis and Its Animal Models: the Role of the Major Histocompatibility complex and the T Cell Receptor Repertoire.* Springer Sem. in Immunopath. **14**, 79-93.

66. Gow, A., Gragerov, A., Gard, A., Colman, D., and Lazzarini, R.A. (1997) *Conservation of Topology, but not conformation, of the PLPs of the Myelin Sheath.* J. Neurosci. **17**, 181-89.

67. Fritz, R. and Chou, C.-H. (1983) *Epitopes of Peptide 43-88 of Guinea Pig Myelin Basic Protein: Localization with Monoclonal Antibodies.* J. Immunol. **130**, 2180-82.

68. Lutz-Freyermuth, C., Query, C. and Keene, J. (1990) *Quantitative Determination that One of Two Potential RNA-binding Domains of the A Protein Component of the U1 Small Nuclear Ribonucleoprotein Complex Binds with High Affinity to Stem-Loop II of U1RNA.* Proc. Natl. Acad. Sci. USA. **87**, 6393-97.

69. Cernoff, G.F. (1981) *Shiverer: An Autosomal Recessive Mutant Mouse with Myelin Deficiency.* J. Heredity. **72**, 128.

70. Hildebrand, C., and Muller, H. (1974) *Low Angle X-ray diffraction studies on the Period of Central Myelin Sheaths During Preparation for Electron Microscopy: Comparison Between Different Anatomical Areas.* Neurobiology **4**, 71-82.

71. Karthigasan J., Garvey, J., Ramamurthy, G., and Kirschner D. (1996) *Immunolocaliztion of 17 and 21.5 kDa MBP Isoforms in Compact Myelin and Radial Components.* J. Neurocytol. **25,** 1-7.

72. Chou, P., and Fasman, G. (1978) *Prediction of the Secondary Structure of Proteins from their Amino Acid Sequence.* Adv. Enzym. **47,** 45-58.

73. McAlpine, D., Lumsden, C., and Acheson, E. (1972) *Multiple Sclerosis, A Reppraisal,* Williams & Wilkins, Baltimore.

74. Kirschner, D., Ganser, A., and Caspar, D. *Diffraction Studies of Molecular Organization and Membrane interactions in Myelin.* Chapter 2 in reference 28.

75. Raines, C. *Morphology of Myelin and Myelination.* Chapter 1 in reference 28.

76. Hodgkin, A., and Huxley, A. (1952) *The Components of Membrane Conductance in the Giant Axon of Loligo.* J. Physiol. (London) **116,** 473.

77. Molineaux, S., Engh, H., DeFerra, F., Hudson, L., and Lazzarini, R. (1986) *Recombination Within the Myelin Basic Protein Gene Created the Dysmyelinating Shiverer Mouse Mutation.* PNAS **83,** 7542-46.

78. Giese K., Martini R., Lemke G., Soriano P., and Schachner M., (1992) *Mouse Po Gene Disruption Leads to Hypomyelination, Abnormal Expression of Recognition Molecules, and Degeneration of Myelin and Axons.* Cell **71,** 565-76.

79. Shine, D., Readhead, C., Popko, B., Hood, L., and Sidman, R. (1992) *Morphometric Analysis of Normal , Mutant, and Transgenic CNS: Correlation of MBP Expression to Myelinogenesis.* J. Neurochem. **58** (1), 342-49.

80. Gow, A. and Lazzarini, R. (1996)*A Cellular Mechanism Governing the Severity of Pelizaeus-Merzbacher Disease.* Nature Genetics **13,** 422-28.

81. Stoffel, W., Hillen, H., and Gierstiefen, H. (1984) *Structure and Molecular Arrangement of PLP of Central Nervous System.* Proc. Nat. Acad. Sci. USA **81,** 5012-16.

82. Sedzik, J. and Kirschner D. (1992) *Is MBP Crystallizable?* Neurochem. Res. **17,** 157-66.

83. Kagawa, T., Ikenaka, K., Inoue, Y., Kuriyama, S., Tsudjii, T., Nakao, J., Nakajima, K., Aruga, J., Okano, H., and Mikoshiba, K. (1994) *Glial Cell Degeneration and Hypomyelination Caused by Overexpression of Myelin Proteolipid Protein Gene.* Neuron **13,** 427-42.

84. Readhead, C., Schneider, A., Griffiths, I., and Nave, K. (1994) *Premature Arrest of Myelin Formation in Transgenic Mice with Proteolipid Protein Gene Dosage.* Neuron **12,** 1-20.

85. Mastronardi, F., Ackerly, C., Arsenault, L., Roots, B., and Moscarello, M. (1993) *Demyelination in Transgenic Mice: A Model for Multiple Sclerosis.* J. Neurosci. Res. **36,** 315-24.

86. Trapp, B., Bernier, L., Andrews, S., and Colman. D. (1988) *Cellular and Subcellular Distribution of CNP and Its mRNA in the Rat CNS.* J. Neurochem. **51**, 859-868.

87. Bronstein, J., Popper, P., Micevych, P., and Farber, D. (1996) *Isolation and Characterization of a Novel Oligodendrocyte-Specific Protein.* Neurology **47**, 772-78.

88. Deber, C., and Reynolds, S. (1991) *Central Nervous System Myelin: Structure, Function, and Pathology.* Clin. Biochem. **24**, 113-34.

89. Fujinami, R., and Oldstone, M. (1985) *Amino Acid Homology between the encephalitogenic site of MBP and virus: Mechanism for Autoimmunity.* Science **230**, 282-84.

90. Maugh, T. (1977) *The EAE Model: A Tentative Connection to Multiple Sclerosis.* Science **195**, 969-71.

91. Wood, P. and Bunge, R.(1986) *Myelination of Cultured Dorsal Root Ganglion Neurons by Oligodendrocytes Obtained from Adult Rat.* J. Neurol. Sci. **74**, 153-69.

92. Notterpek, L., Bullock, P., Malek-Hedayat, S. Fisher, R., and Rome, L. (1993) *Myelination in Cerebellar Slice Cultures: Development of a System Amenable to Biochemical Analysis.* J. Neurosci. Res. **36**(6), 621-34.

93. Lyman, W., Hatch, W., Pousada, E., Stephany, G., Rashbaum, W, Weidenheim, K. (1992) *Human Fetal Myelinated Organotypic Cultures.* Brain Res. **599**(1), 34-44.

94. Roth, G., Spada, V., Hamill, K., and Bornstein, M. (1995). *Insulin-like Growth Factor I Increases Myelination and Inhibits Demyelination in Cultured Organotypic Nerve Tissue.* Dev. Brain Res. **88** (1), 102-8.

95. DeFerra, F., Engh, H., Hudson, L., Kamholz, J., Puckett, C., Molineaux, S., and Lazzarini, R. (1986) *Alternative Splicing Accounts for the Four Forms of Myelin Basic Protein.* Cell **43**, 721-27.

96. Black, B. and Lyles, D. (1992) *Vesicular Stomatitis Virus Matrix Protein Inhibits Host Cell-Directed Transcription of Target Genes in vivo.* J. Virology **66**(7), 4058-64.

97. Coulon, P., Deutsch, V., LaFay, F., Martinet-Edelist, C., Wyers, F., Herman R., and Flamand, A. (1990).*Genetic Evidence for Multiple Functions of the M Protein of VSV.* J. Gen. Vir. **71**, 991-6.

98. Bohn, W., Ciampor, F., Rutter, R., and Mannweiler, K. (1990).*Localization of Nucleocapsid Associated Polypeptides in Measles Virus-infected Cells by Immunogold Labeling after Resin Embedding.* Arch.Virol. **114**, 53-64.

99. Zakowski J., Petri W., and Wagner R. (1981): *Role of Matrix Protein in Assembling the Membrane of Vesicular Stomatitis Virus: Reconstitution of Matrix Protein with Negatively Charged Phospholipid Vesicles.* Biochemistry **20**, 3902-07.

100. Ogden J., Pal R., and Wagner R. (1986) *Mapping Regions of the Matrix Protein of Vesicular Stomatatitis Virus Which Bind to Ribonucleocapsids, Liposomes, and Monoclonal Antibodies.* J. Virol. **58** (3), 860-68

101. Bergman J., and Fusco P. (1988)*The M Protein of Vesicular Stomatitis Virus Associates With the Basolateral Membranes of Polarized Epithelial Cells Independently of the G Protein.* J. Cell Biol. **107**, 1707-1715.

102. Newcomb W., and Brown J. (1981): *Role of the Vesicular Stomatitis Virus Matrix Protein in Maintaining the Viral Nucleocapsid in the Condensed Form Found in Native Virions.* J. Virol. **39**(1), 295-299.

103. Cuzner, M., and Davison, A. (1968) *The Lipid Composition of Rat Brain Myelin and Subcellular Fractions During Development.* Biochem. J. **106,** 29-33.

104. Denhardt, D. (1966) *A Membrane-filter Technique for the Detection of Complementary DNA.* Biochem. Biophys. Res. Commun. **23**, 641.

105. Mastronardi, F., Al-Sabbagh, A., Nelson., Rego, J., Roots, B., and Moscarello, M. (1996). *MBP in EAE is not Affected at the Posttranslational Level: Implications for Demyelinating Disease.* J. Neurosci. Res. **44**, 344-49.

106. Smith, R. (1977). *The Secondary Structure of MBP Extracted by Deoxycholate.* Biochim. Biophys. Acta. **491**, 581-90.

107. Pedraza, L., Fidler, L., Staugaitis, S., and Colman, D., (1997). *The Active Transport of MBP into the Nucleus Suggests a Regulatory Role in Myelination.* Neuron **18**, 579-89.

108. Bunge, R.P. (1970) *Structure and Function of Neuroglia : Some Recent Observations* . The Neurosciences: A Second Study Program (F.O.Schmitt, ed.)728-97. Rockefeller Press, New York.

109. Timsit, S. G., Bally Cuif, L., Colman, D. R. and Zalc, B. (1992) *DM-20 mRNA is Expressed During the Embryonic Development of the Nervous System of the Mouse.* J. Neurochem. **58**, 1172-75.

110. Saavedra, R., Fors, L., Aebersold, R., Arden, B., Horvath, S., Sanders, J. and Hood, L. (1989). *The Myelin Proteins of the Shark Brain are Similar to the Myelin proteins of the Mammalian Peripheral Nervous System.* J. Mol. Evol. **29**, 149-56.

111. Ainger, K., Avossa, D., Diana, A., Barry, C., Barbarese, E. and Carson, J. (1997) *Transport and Localization Elements in Myelin Basic Protein mRNA.* J. Cell Biol. **138**, 1077-87.

112. Barbarese, E., Koppel, D., Deutscher, M., Smith, C., Ainger, K., Morgan, F., and Carson, J. (1985) *Protein Translation Components are Colocalized in Granules in Oligodendrocytes* J. Cell Sci. **108**, 2781-90.

113. Allinquant, B., Staugaitis, S., D'Urso, D., and Colman, D. (1991) *The Ectopic Expression of Myelin Basic Protein Isoforms in Shiverer Oligodendrocytes: Implications for Myelinogenesis.* J. Cell Biol. **113**, 393-403.

114. Trapp, B., Andrews, S., Cootauco, C., Quarles, R., (1989) *The Myelin-Associated Glycoprotein is Enriched in Multiple Vesicular Bodies and Periaxonal Membranes of Actively Myelinating Oligodendrocytes.* J. Cell Biol. **109**, 2417-26.